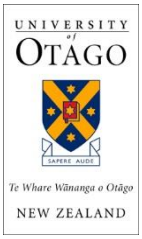

To Investigate and Fabricate Melt Processed Biomaterials Exhibiting Shape Recovery Properties

Keegan Riley Crake

A Thesis Submitted for the Degree of
Master of Science in Bioengineering
at the University of Otago,
Dunedin, New Zealand

March 2017

Abstract

The purpose of this research was to produce and characterise novel hybrid biomaterials. Currently, there is a research gap in the area of producing hybrid biomaterials with shape memory properties for use in the fields of bioengineering or biomedical devices. This research will provide the initial results for a novel hybrid biomaterial that could be further researched for use in a biomedical device. In this study, melt extrusion methods were applied to the hybrid polymers. Three characterisation methods were employed within this work: mechanical (tensile) testing, shape recovery, and *in vitro* (trypsin) degradation. Across the three characterisation methods, PCL:PLA 30:70WT% 20% PEG-200 plasticised hybrid fibres were found to outperform the other materials reported in this thesis. Three key findings resulted from this research. The melt extrusion method used proved to be successful. PCL:PLA hybrid fibres could be produced consistently. Both glycerol and PEG-200 plasticisers used within this work were found to improve the blend properties of the hybrids. A total of 65% of tested hybrid fibres exhibited shape recovery when tested at a temperature of 37.5°C. The overall results of this study indicate that the hybrid materials produced here need to undergo further testing prior to use in biomedical applications.

Acknowledgements

First, I want to thank my two supervisors, Dr. Azam Ali and A/P Sarah Wakes for their invaluable assistance in this project. Azam was indispensable in the trial and development of my experimental methods. As I had little prior experience in the field of bioengineering, this project could not have been completed, or even attempted without Azam's tireless assistance. Sarah was willing to answer all of the questions I had throughout the duration of this work. Sarah worked tirelessly to provide feedback on my seemingly endless iterations of graphs and figures. I also wish to thank Azam and Sarah for reading my preliminary drafts for this report.

I must also thank Tim Jowett for his assistance in determining the best methods for statistical analysis. While Tim was not involved in the experimental work of this project. However, Tim worked tirelessly to understand the scope of the project, and the experimental procedures involved. Tim's attitude meant I was able to receive invaluable statistical assistance from him. No statistical analysis could have been properly carried out on the data contained herein without the assistance of Tim Jowett. A number of additional staff members within the Centre for Materials Science and Technology provided invaluable technical assistance. Firstly, I must thank Dr. Bronwyn Lowe for here incredible patience in teaching me how to operate the Instron Universal Testing machine. Without Bronwyn's assistance, the acquisition of tensile data for my polymer fibres would not have been possible. Dr. Linda Dunn provided invaluable assistance in the imaging and description of my polymer fibres. For her endless technical assistance, I must thank Clare Nichols. Clare was responsible for the acquisition of many of the materials used within this project. Clare worked tirelessly to ensure that the resources I required were always available when they were required.

Without the assistance of the aforementioned people, this work would not have been possible; and for this, I thank you.

Nomenclature

Abbreviations

Abbreviation	Definition
ANOVA	Analysis of Variance
C	Carbon
CNT	Carbon Nanotubes
D.P.	Decimal Places (rounding)
DSC	Differential Scanning Calorimetry
EB	Elongation at Break
FDA	United States Food and Drug Administration
GLS	Generalised Least Squares
HCl	Hydrogen Chloride
LD_{50}	Lethal Dose in 50% of the sample
LSM	Least Squares Means
MWCNT	Multiwall Carbon Nanotubes
NaOH	Sodium Hydroxide
PA	Polyamide
PBS	Phosphate Buffered Saline
PCL	Polycaprolactone
PDLA	Poly-D-lactic Acid
PDLLA	Poly-D,L-lactic Acid
PEG	Polyethylene Glycol
PLA	Polylactic Acid
PLLA	Poly-L-lactic Acid
PP	Polypropylene
PVC	Polyvinyl Chloride
REML	Restricted Maximum Likelihood
SME	Shape Memory Effect
SMP	Shape Memory Polymer
SSE	Single Screw Melt Extruder

T_g	Glass Transition Temperature
TGA	Thermogravimetric Analysis
T_m	Melting Temperature
TS	Tensile Strength
WT%	Weight Percentage
YM	Young's Modulus
ø	Fibre Diameter

Units

Unit	Definition
mg/mL	Concentration (Enzyme)
%	Concentration (Plasticisers)
M	Concentration (Solutions)
WT%	Constituent Ratio
mm	Diameter, ø
mm	Dimensions
mm	Distance
%	Elongation at Break
lb force	Force (Fishing Line)
N	Force (Tensile Testing)
RH%	Humidity
g/mol	Molecular Weight
%	Strain
MPa	Stress
°C	Temperature
MPa	Tensile Strength
$Wm^{-1}K^{-1}$	Thermal Conductivity
s	Time (seconds)
N/m	Torque
mm/min	Velocity
mL	Volume
G	Weight
MPa	Yield Strength
MPa	Young's Modulus

Contents

Table of Figures

Table of Tables

Chapter 1 Introduction

1.1 Background

Polymers are large molecules that contain repeated subunits, referred to as monomers (Garni, Thamboo et al. 2017). Two broad categories of polymers exist: natural (biopolymers) and synthetic (Sionkowska 2011). Natural polymers are those which occur within organisms and nature, such as chitosan, keratin and collagen (Sionkowska 2011). Synthetic polymers are man-made, such as polyethylene glycol or polypropylene (Liang, Chen et al. 2015). It is common for polymers to be blended together (Sionkowska 2011). Natural and synthetic polymers are frequently blended to produce hybrid polymers; however, blends between only synthetic polymers are also used (Sionkowska 2011). This work will focus on synthetic polymers, referring to only these as polymers.

Polymers are of great importance in biomedical applications, such as in sutures or orthodontic retainers (Chabrier, Lloyd et al. 1999, Catanzano, Acierno et al. 2014). Polymers possess a variety of properties that make them suitable for biomedical applications (Lendlein and Kelch 2002). Polymers are typically much cheaper and easier to use than metallic devices (Lendlein and Kelch 2002). Suitable polymers for biomedical applications are biocompatible and typically biodegradable. A number of biomedical applications have been reported for polymeric materials and hybrids. These include (but are not limited to): synthetic muscle (Yeong, Sudarmadji et al. 2010); bone tissue regeneration (Costa, Puga et al. 2015); controlled drug release (Costa, Puga et al. 2015, Preis, Breitkreutz et al. 2015); and blood bags (Zhang, Chen et al. 2010, Pan, Trempont et al. 2016).

Polymers, like metallic alloys, can exhibit shape recovery properties (Lendlein and Kelch 2002, Behl and Lendlein 2007). The ability of polymers to undergo shape recovery is termed either, shape memory, or stimuli responsive (Meng and Hu 2009, Meng and Li 2013). The term stimuli responsive adequately describes shape recovery; a polymer's recovery is triggers by an external stimulus (Meng and Hu 2009, Meng and Li 2013). Shape memory polymers are of significant interest in biomedical applications, allowing a reduced initial loading on damaged tissue. The polymer will undergo shape recovery as it heats to the temperature of the implanted site, allowing the function to be fulfilled. Shape memory has been applied in medical sutures (Lendlein and Langer 2002). In this event, the sutures need not be pulled tight; as they heat to body temperature (37.5°C), they self-tighten (Lendlein and Langer 2002). The self-tightening of these sutures reduces tissue damage around the wound sites (Lendlein and Langer 2002).

1.2 Research Gap

There is a large scope for the application of shape memory polymers as components in biomedical devices (Lendlein and Kelch 2002). Several potential applications have been proposed for shape memory polymers: sensors, tools, sutures, and actuating materials (synthetic muscle) (Lendlein and Kelch 2002, Xie 2011, Moon, Choi et al. 2016). However, very few shape memory materials have been successfully applied in these applications. As such,

there is potential for new research to provide a useful contribution to the field of polymer science. Novel hybrid biomaterials have the potential to fulfil one, or more, biomedical applications.

1.3 Aims and Objectives

The aim of this work is to investigate and fabricate hybrid biomaterials exhibiting shape memory properties. The four research objectives to achieve the aims are to:

1. Investigate biocompatible polymers, and their fabrication techniques [Ch. 2,3,7]
2. Investigate shape memory polymers, their functionality and processing methods. [Ch. 2,5,7]
3. Investigate methods for analysing polymer hybrids [Ch. 2-8]
4. Define the ideal material properties. [Ch. 2-8]

1.4 Thesis Outline

Outlines of each chapter in the thesis are provided below.

Chapter 1: Introduction

This chapter introduces the main concepts of the research, the context in which it is to be undertaken, and defines the overall research aim and objectives.

Chapter 2: Literature Review

Chapter 2 provides a summary of published literature in relation to this field. The primary focus is on polymers, processing and testing. The materials used within the scope of this project are identified, and justified. Criteria for the ideal polymer hybrid is defined.

Chapter 3: Fibre Processing

Chapter 3 summarises the materials and methodologies employed to produce the polymeric fibres. An initial pilot study on the processing methods is reported within this chapter. The effects the processing conditions have on the materials are identified and discussed.

Chapter 4: Mechanical Testing

Chapter 4 provides the materials and methodologies required to undergo tensile testing of polymeric fibres. A pilot study carried out to determine the ideal tensile testing conditions is detailed. Further, the results of the mechanical tests are identified and explained.

Chapter 5: Shape Recovery

Chapter 5 summarises the materials and methods required to carry out shape recovery testing on polymeric fibres. The results are identified and explained.

Chapter 6: *in vitro* Trypsin Digestion

Chapter 6 identifies the materials and methods required to undergo trypsin digestion of polymer fibres. The results of this study are identified and discussed.

Chapter 7: Overall Discussion

Chapter 7 provides the overall discussion. The overall discussion compares the effects between the processing method(s) and properties – physical, mechanical, degradation and shape recovery. Further, the criteria defined for the best fibres is critiqued. The limitations to this study, and future work are discussed.

Chapter 8: Conclusion

Chapter 8 identifies the overall conclusions from this work.

Chapter 2 Literature Review

2.1 Introduction

This work primarily focuses on polymers and their characterisation. The issue of polymer biocompatibility is a central point for this work. As such, polymers that have been used in human related medical devices will be identified. However, it is common that polymers require additives. As such, these additives must be identified and discussed. A particular focus is placed on the ability of polymers to undergo shape recovery. This has significant benefits for a variety of human medical applications; such as sutures (Lendlein and Langer 2002). Polymers must first be processed into suitable forms; therefore, three common polymer processing methods are identified and discussed. Polymers must be characterised prior to use as medical devices. As such, a number of important polymer characterisation techniques are identified and discussed. This chapter concludes with a summary of what will be used in this project. Detailing why these materials and methods were chosen; and the criteria for what were considered the best fibre(s) are identified.

2.2 Polymers

By definition, a polymer is a molecular chain of repeated subunits (Garni, Thamboo et al. 2017). These subunits are typically referred to as monomers. However, two categories of polymer exist: those that have a single type of subunit, and those that have multiple. These are referred to as homopolymers (one type of monomer), and copolymers (more than one type of monomer) (Prud'homme 2016, Sedlak 2016, Huang and Turner 2017). A total of seven copolymer types have been identified (Huang and Turner 2017), see figure 2: 1 for pictorial representations:

1. Random: monomer types are randomly distributed.
2. Block: monomer types are in distinct, individual, groupings.
3. Graft: side chains are attached to the main monomer chain. These do not have to be singular monomers.
4. Alternating: the types of monomer alternate. This can be as either single monomers or groups.
5. Periodic: groupings of monomers randomly distributed.
6. Aperiodic copolymers: two (or more) aligned periodic chains.
7. Gradient: increases or decreases in monomer concentration across the polymer chain.

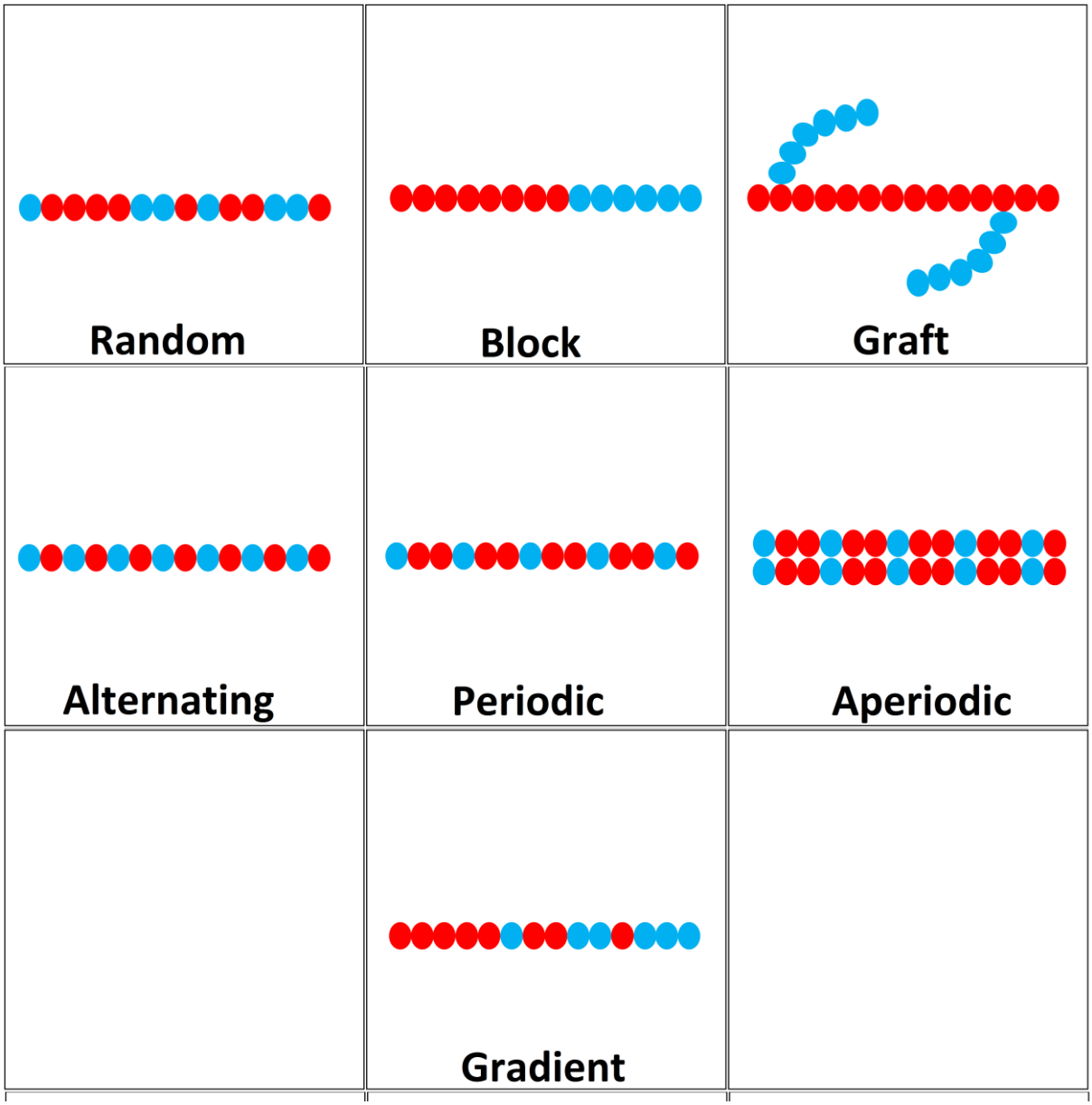

Figure 2: 1 Types of Copolymers. The red and blue circles are the two types of polymer used. Adapted from (Huang and Turner 2017).

The macrostructures of polymers are of vital importance. In this instance, macrostructure refers to the crystallinity of the polymer. In terms of polymer crystallinity, two phases are typically identified. Polymers are either termed semi-crystalline, or amorphous (little to no crystalline structure) (Middleton and Tipton 2000). There are several key distinction between semi-crystalline and amorphous polymers. The most important distinction relates to thermal transition points. Semi-crystalline polymers exhibit two distinct thermal transitions: glass transition and melting (Martin and Avérous 2001, Cadek, Coleman et al. 2002). However, amorphous polymers only exhibit glass transition; they cannot melt (Cadek, Coleman et al. 2002). Rather than melting, amorphous materials soften over a range of temperatures, increasing malleability (Sarode, Sandhu et al. 2013). Polycaprolactone (PCL) and polypropylene (PP) are typical semi-crystalline polymers (Middleton and Tipton 2000, Shi, Chen et al. 2010, Ostafinska, Fortelny et al. 2015, Urquijo, Guerrica-Echevarría et al. 2015), while polylactic acid (PLA) and Polyvinyl chloride (PVC) are amorphous (Middleton and Tipton 2000, Wei, Wu et al. 2014, Ostafinska, Fortelny et al. 2015, Urquijo, Guerrica-Echevarría et al. 2015, Mallakpour, Abdolmaleki et al. 2016). In the event that amorphous and semi-crystalline polymers are blended, they can produce varying degrees of crystallinity (Middleton and Tipton 2000). The crystallinity of the materials are vital for shape recovery. A higher crystallinity equates to a more rigid molecular structure (Yang, Li et al. 2015). A high crystallinity translates to a highly stable molecular matrix (Yang, Li et al. 2015). Shape recovery is to a degree, reliant on the ability of the polymer matrix to shift; therefore, a low crystallinity is preferable.

2.2.1 Polymer Processing and Properties

Many types of polymers exist, each with their own properties and optimal processing conditions. A polymer's thermal properties are of vital importance during processing. All traditional polymer processing methods first apply heat, to melt or soften the polymer. Without the knowledge of the specific polymers' thermal properties, this process becomes difficult and potentially damaging towards the equipment. Differential scanning calorimetry (DSC) and thermogravimetric analysis (TGA) methods (see section 2.6) are used to report the thermal properties of PCL, PLA, PP and PVC (table 2: 1). Three polymer processing techniques exist to process polymer powders and/or granules into usable fibres/products: melt extrusion, compression moulding and injection moulding (reviewed in section 2.5).

The particular processing technique used influences the properties of the materials produced (Chung 2017). During processing, it is common to blend a variety of polymers and additives to produce the desired composite material (Frketic, Dickens et al. 2017). When two or more polymers are blended into a composite, phase separation issues can arise (El-Hadi 2014). Two reasons are known for this, the primary one being the formation of two or more distinct glass transition temperatures (El-Hadi 2014). All polymer hybrids should have a single glass transition temperature, otherwise they produce sub-optimal mechanical properties. A further issue during polymer blending is that of phase miscibility (Chavalitpanya and Phattanarudee 2013). Phase miscibility issues occur when the surface properties of the polymers are incompatible: a gap forms between the polymer molecules (Chavalitpanya and Phattanarudee 2013). Additives are required to fix this problem. Plasticisers are materials that can be added to reduce the glass transition temperatures of a material, significantly reducing the probability of distinct glass transition zones along the material (El-Hadi 2014). Another additive, a compatabiliser, can be added to improve interfacial adhesion between the polymer molecules (El-Hadi 2014). Additives are further explained in section 2.3.

Polycaprolactone (PCL) is a semi-crystalline polyester homopolymer, typically with 50% crystallinity (Wan, Wu et al. 2008, Mallakpour and Nouruzi 2016). At room temperature (20°C), PCL fibres are highly elastic (Wan, Lu et al. 2009). This is a result of the low glass transition temperature of PCL (table 2: 1), approximately -60°C (Wan, Lu et al. 2009). However, while PCL is highly elastic, it is a relatively low strength polymer (table 2: 2), breaking easily under high load conditions (Monticelli, Calabrese et al. 2014). PCL's properties specified in table 2: 2 are for compression moulded bars (Monticelli, Calabrese et al. 2014). However, both melt extrusion (Ghosh, Ali et al. 2010, Bélard, Poncin-Epaillard et al. 2013, Catanzano, Acierno et al. 2014, Huo, Rojas et al. 2014, Wang, Langhe et al. 2014, Zhao and Zhao 2016) and injection moulding (Zhao and Zhao 2016) have been used to produce PCL products.

Polylactic acid (PLA) is an aliphatic (open chain) polyester, with carrying degrees of crystallinity: 1 – 37% (Middleton and Tipton 2000, Martin and Avérous 2001, Chavalitpanya and Phattanarudee 2013, Ostafinska, Fortelny et al. 2015). Further, PLA is hygroscopic in nature, meaning it readily absorbs ambient moisture (Jamshidian, Tehrany et al. 2010). As a result of PLA's crystallinity, it can be classified as an amorphous polymer, that is, it lacks a defined molecular structure (Guttman, DiMarzio et al. 1981). Variations in PLA's crystallinity are a result of its nature as a cyclic dimer (Middleton and Tipton 2000). Cyclic dimer molecules are those that can occur as multiple stereoisomers, that is, the materials atoms can appear in different spatial arrangements (Middleton and Tipton 2000). PLA is produced from lactic acid sugars (literally, many lactic acids); lactic acid sugars produce L and D stereoisomers, this is translated to the PLA molecule (Middleton and Tipton 2000). Typically, while both D and L isomers are apparent in sugars, the L isomer is considerably more common; this is reported in PLA molecules (Middleton and Tipton 2000). A synthetic, DL PLA molecule can be produced; this occurs when PDLA (D-isomer) and PLLA (L-isomer) are combined, and cannot happen naturally (Middleton and Tipton 2000). PLA has a high glass transition temperature, 60°C (table 2: 1), meaning it is rigid at room temperature (Ostafinska, Fortelny et al. 2015). PLA's amorphous nature results in softening at temperatures exceeding the glass transition (Sarode, Sandhu et al. 2013, Ostafinska, Fortelny et al. 2015). A variety of melting temperatures have been quoted for PLA (table 2: 1), ranging from 155 – 175°C, this is dependent on the crystallinity of the specific PLA (Middleton and Tipton 2000, Jamshidian, Tehrany et al. 2010, Khankrua, Pivsa-Art et al. 2014, Ostafinska, Fortelny et al. 2015, Urquijo, Guerrica-Echevarría et al. 2015). However, while PLA lacks elasticity, it has both a high strength and Young's modulus (table 2: 2) allowing it to withstand large loads and still undergo elastic deformation (Monticelli, Calabrese et al. 2014). The properties given for tensile testing in table 2: 2 are with compression moulded specimens (Monticelli, Calabrese et al. 2014). PLA can however be processed through thermal melt extrusion (Mosanenzadeh, Khalid et al. 2015) and injection moulding (Zhao and Zhao 2016).

Polypropylene (PP) is a commonly used semi-crystalline polymer (Liang, Chen et al. 2015). Several advantages exist for the use of PP: it is cheap, easy to work with, and it is recyclable; however, it produces mechanically weak materials (Liang, Chen et al. 2015). The glass transition temperature of PP, 12°C (table 2: 1) is such that it is rubbery at room temperature (Shi, Chen et al. 2010). PP reportedly has a max elongation of between 128 – 308% (table 2: 2) (Eslami-Farsani, Reza Khalili et al. 2014, Li, Zhang et al. 2014). The Young's modulus of PP is reported to be 523.42 MPa (table 2: 2), this suggest a low load is required for elongation (Eslami-Farsani, Reza Khalili et al. 2014). Several processing methods have been employed for PP within the literature: injection moulding (Suplicz, Szabo et al. 2013, Ameli, Kazemi et al.

2017), melt extrusion (Shi, Chen et al. 2010), and compression moulding (Goodship, Brzeski et al. 2014). Compression moulded sheets of polypropylene have been used in orthodontic vacuum formed retainers (Gardner, Dunn et al. 2003).

Polyvinyl chloride (PVC) is currently one of the most used polymers worldwide (Sterzyński, Tomaszewska et al. 2010). Several properties of PVC make it an ideal polymer: it is cheap, easy to process, and easy to, modify (Sterzyński, Tomaszewska et al. 2010). PVC is an amorphous polymer, lacking molecular structure (Cadek, Coleman et al. 2002, Wei, Wu et al. 2014). The glass transition temperature (69°C) of PVC means it is rigid, at room temperature (Sterzyński, Tomaszewska et al. 2010). PVC has a comparatively (to other polymers) high Young's modulus (table 2: 1), meaning it will show minimal elongation when a force is applied (Mallakpour, Abdolmaleki et al. 2016). Coupled with biocompatibility, the high Young's modulus makes PVC ideal for medical devices such as: medical tubing and blood bags (Ajili, Ebrahimi et al. 2003). Melt extrusion is frequently used to process PVC (producing piping) (Zhang, Chen et al. 2010, Pan, Trempont et al. 2016); compression moulding (Dan-asabe 2016) and injection moulding (Lladó and Sánchez 2008) are also used.

Large varieties of hybrid fibres have been produced with constituent materials that include at least on of: PCL, PP, PLA or PVC. Hybrid materials of PCL:PLA have been produced with ratios ranging from 10:90WT% – 80:20WT%; all of which are produced using twin-screw extrusion (Chavalitpanya and Phattanarudee 2013, Ostafinska, Fortelny et al. 2015, Urquijo, Guerrica-Echevarría et al. 2015, Malinowski 2016). PLA materials have been blended with polyamide (PA) materials to produce 70:30WT% hybrids through twin screw extrusion (Khankrua, Pivsa-Art et al. 2014). PP materials are frequently blended with multiwall carbon nanotubes (MWCNT) (Liang, Chen et al. 2015, Ameli, Kazemi et al. 2017). Injection moulded 90:10WT% – 95:5WT% PP:MWCNT hybrids have been successfully produced (Ameli, Kazemi et al. 2017). Further, twin-screw melt extruders have been used to process PP:MWCNT hybrids with 99:1WT% – 95:5WT% (Liang, Chen et al. 2015). There are reports of PVC materials being blended with both PEG and CNT (). A block copolymer between PEG-600 (600 g/mol) and PVC was produced through grafting (ratio unspecified) (Balakrishnan, Kumar et al. 2005). In a separate work, 70:30WT% PVC:PEG-400 (400 g/mol) hybrids were cast into moulds (Chen, Sheng et al. 2011). In both works, the addition of PEG to PVC improves the biocompatibility of the final materials, making them more suitable for biomedical applications (Balakrishnan, Kumar et al. 2005, Chen, Sheng et al. 2011). Ranges of PVC:MWCNT hybrids of 99.9:0.1WT% – 99.5:0.5WT% (Sterzyński, Tomaszewska et al. 2010).

Table 2: 1 Thermal Properties for Polycaprolactone (PCL), Polypropylene (PP), Polylactic acid (PLA) and Polyvinyl chloride (PVC)

Polymer	Molecular Weight	Crystal Structure	Melting Point	Glass Transition	Degradation Temperature	References
PCL	A variety exists for all.	Semi-crystalline	58 – 63	-65 – -60	358	(Koleske and Lundberg 1969, Middleton and Tipton 2000, Wan, Lu et al. 2009, Jamshidian, Tehrany et al. 2010, Zhao and Zhao 2016)
PP		Semi-crystalline	165 – 167	12	350-470	(Gómez-del Río and Rodríguez 2010, Shi, Chen et al. 2010)
PLA		Amorphous	155 (softens) 168 (softens) 175 (softens)	40 – 70	200°C and above	(Middleton and Tipton 2000, Jamshidian, Tehrany et al. 2010, Khankrua, Pivsa-Art et al. 2014, Ostafinska, Fortelny et al. 2015, Urquijo, Guerrica-Echevarría et al. 2015, Wu and Hakkarainen 2015)
PVC		Amorphous		69 – 70 91		(Sterzyński, Tomaszewska et al. 2010, Zhang, Chen et al. 2010)

Table 2: 2 Tensile Properties for Polycaprolactone (PCL), Polypropylene (PP), Polylactic acid (PLA) and Polyvinyl chloride (PVC). Details of the test conditions and specimens are provided, where reported.

Material (Product code)	Tensile Test Conditions	Test Specimen	Tensile Strength (MPa)	Elongation at break (%)	Young's (Elastic, Tensile) Modulus (MPa)	Reference
PCL (CAPA 6500)	Cross-head speed: 50 mm/min.	Rectangular bars. 10x25x0.5 mm	20±8	1200±400	220±10	(Monticelli, Calabrese et al. 2014)
PLA	Cross-head speed: 50 mm/min.	Rectangular bars. 10x25x0.5 mm	65±2	9±1	1200±40	(Monticelli, Calabrese et al. 2014)
			59.90±4.93	1.86±0.06	3990±420	(Pinto, Ramos et al. 2017)
PP	LC 25 kN 5 mm/min	Electrospun fibre membrane	5.14 19.76	128.19 307.64	Not Shown 523.42	(Li, Zhang et al. 2014)
		Injection moulded dumbbell, 3x13x165 mm (DxWxL)				(Eslami-Farsani, Reza Khalili et al. 2014)
PVC	ND.	Thin films. Size unspecified.	43.3	2.63	2060	(Mallakpour, Abdolmaleki et al. 2016)

2.3 Additives

An additive is any material processed with the polymer blend. Typically, these aim to improve either processing or mechanical properties of the final materials. Plasticisers function to increase molecular gaps, resulting in a decreased glass transition temperature; whereas compatabilisers function to improve interfacial adhesion (El-Hadi 2014).

2.3.1 Plasticisers

Plasticisers are small molecules that can be combined with a polymer. When added, the plasticiser acts to increase intermolecular space (Mekonnen, Mussone et al. 2013). Primarily, this provides a benefit to the system because the intermolecular forces are weakened (Mekonnen, Mussone et al. 2013). As the intermolecular forces decrease, the molecules relax and are able to move more freely (Mekonnen, Mussone et al. 2013). The overall effect of this is a reduction in polymer glass transition temperature (T_g) (Byun, Kim et al. 2010). Essentially, this functions to allow the polymer to soften at a lower temperature, allowing lower temperature processing (Douglas, Andrews et al. 2010). However, because the polymer chains are being separated, the mechanical properties are affected. The reduction in intermolecular forces allows the polymer molecules to be more mobile, allow better/faster alignment when placed under tension: the Young's modulus is reduced (Mekonnen, Mussone et al. 2013). Polymeric fibres that undergo tension elongate without breaking because their molecules move and realign (stretch) to stabilise the system. However, when the molecules can no longer elongate (effected by intermolecular forces) the material fractures. This means that with a reduction in intermolecular forces, a reduction in applied tensile load is required to achieve the same elongation. That is to say, a non-plasticised system could require 10 N force to elongate by 100 mm; however, a plasticised system may only require 8 N to elongate by 100 mm (Byun, Kim et al. 2010). An acceptable compromise must be found between the desired effect (T_g reduction) and undesired effects (mechanical property reductions). Two types of plasticiser exist: internal and external (Mekonnen, Mussone et al. 2013). The major difference between these is how they are introduced to the polymer system. Internal plasticisers require a chemical reaction to integrate into the polymer chain to act (Mekonnen, Mussone et al. 2013). Several issues are identified with the method: the plasticiser does not function over a large temperature range; the polymer is softened at a higher rate; and, the plasticiser side chains crystallise, reducing/negating their effect (Mekonnen, Mussone et al. 2013). Conversely, external plasticisers can act without a chemical reaction. Typically, external plasticisers require an increased processing temperature (when compared to internal plasticisers) to have an effect; however, this must be below the degradation temperature (Mekonnen, Mussone et al. 2013).

It has been reported that glycerol, sorbitol and poly(ethylene glycol) (PEG) are universally the most common plasticisers used in biomedical applications (Jung, Deng et al. 2016). Glycerol is a hygroscopic polyol molecule, meaning it readily takes up ambient moisture (Vieira, da Silva et al. 2011, Wu and Hakkarainen 2015). A search of ScienceDirect (www.sciencedirect.com, January 2017) did not provide any literature in support of glycerol plasticised PLA. Approximately 140 results were returned, for the most part, none of these used straight, unmodified glycerol. It has been suggested that PLA and glycerol are immiscible (Müller, Bere et al. 2016). Evidence for this exists from two DSC graph peaks, one at PLA's 60°C, the other at glycerol's -80°C (Müller, Bere et al. 2016). In the case of glycerol plasticised PVC, a search on

ScienceDirect yielded 26 results (www.sciencedirect.com, January 2017). It appears that glycerol acts as a wetting agent, when blended with PVC (Wang, Wang et al. 2014). A wetting agent is any material added to a blend that changes the floating behaviour of the polymer (Wang, Wang et al. 2014). No applications aside from as a wetting agent have been identified for blending glycerol with PVC. Based on similar searches of ScienceDirect (www.sciencedirect.com, January 2017) with sorbitol, this has rarely been used with PLA (4 results) or PVC (7 results). Both glycerol and sorbitol have been used in PLA to reduce the glass transition temperature (Wu and Hakkarainen 2015). Glycerol (10% solution) provided a 54.3°C temperature, while sorbitol provided a 59.3°C, both decreases in comparison to raw PLA, 61.8°C(table 2: 1) (Wu and Hakkarainen 2015).

PEG is a biocompatible United States Food and Drug Administration (FDA) approved water soluble polymer; it was claimed to be the most blood compatible plasticiser as of 2011 (Chen, Sheng et al. 2011, Cipolatti, Moreno-Pérez et al. 2015). Various molecular weight variants of PEG have been applied as plasticisers for PLA and PVC, ranging from 300 – 20,000 g/mol (Martin and Avérous 2001, Chen, Xie et al. 2006, Cao, Yang et al. 2009, Douglas, Andrews et al. 2010, Chen, Sheng et al. 2011, Hassouna, Raquez et al. 2011, Mekonnen, Mussone et al. 2013). In all instances, reductions to glass transition temperatures, tensile strengths and Young's moduli are observed; however, PEG-400 produces the most significant changes (Hassouna, Raquez et al. 2011, Mekonnen, Mussone et al. 2013). At a 90% PLA plasticised with 10% PEG-400, produced a glass transition of 34.3°C, and 80% PLA plasticised with 20% giving a 21.0 – 23.2°C glass transition (Hassouna, Raquez et al. 2011, Mekonnen, Mussone et al. 2013). Across a range of PEG molecular weights, trends are observed. When PLA is plasticised with a lower molecular weight PEG, a lower glass transition, and better elongation properties appear; conversely, when a higher molecular weight PEG is used, the opposite happens: a higher glass transition is observed, with a reduction to elastic properties (Cao, Yang et al. 2009). PVC polymers have also undergone PEG plasticisation (Balakrishnan, Kumar et al. 2005, Chen, Sheng et al. 2011). An increase in elongation is observed up to 40% PEG-400 loading, and a glass transition reduction is observed (Chen, Sheng et al. 2011).

2.3.2 Compatabilisers

Compatabilisers are essential in many hybrid materials, these act to reduce phase separation (Wu, Zhang et al. 2010). This is accomplished by a reduction in interfacial tension between the components in the hybrid polymer matrix (Wu and Hakkarainen 2015). Typically, anhydride based compatabilisers are used with biocompatible polymers (Carlson, Nie et al. 1999). Of the anhydride compatabilisers, maleic anhydride is the common (Carlson, Nie et al. 1999, Wu and Hakkarainen 2015).

Typically, one component in the hybrid undergoes reactive (melt) extrusion with maleic anhydride (Mekonnen, Mussone et al. 2013). PLA has undergone melt extrusion with maleic anhydride (Carlson, Nie et al. 1999, Hassouna, Raquez et al. 2011, Wu and Hakkarainen 2015). This process increases hydrogen bonding, lowering chain mobility and improves the overall intramolecular stability (Mekonnen, Mussone et al. 2013). An increase in glass transition and ductility was reported with the addition of maleic anhydride to PLA (Hassouna, Raquez et al. 2011, Hassouna, Raquez et al. 2012, Mekonnen, Mussone et al. 2013). In terms of hybrids, PLA-polypropylene carbonate (PPC) blends have been trialled with and without maleic anhydride compatabiliser (Yao, Deng et al. 2011). Without the compatabiliser, the blends

showed comparatively low elongation (82%); however, with the addition of 1.5WT% maleic anhydride, this increased to 243% elongation, an almost 300% increase (Yao, Deng et al. 2011).

2.4 Shape Recovery

Shape memory polymers (SMPs) are a class of polymer that exhibit shape memory effects (SMEs). It has been established that SMEs are not an innate property of polymers, rather, it has to be induced (Behl and Lendlein 2007). Essentially, this is a result of stimuli induced molecular interactions. In all cases, a transfer of energy triggers SME. All SMEs exhibit three key stages. The as produced (permanent) shape, the deformed shape, and the recovered shape (Behl and Lendlein 2007). In an ideal situation, the recovered and permanent shapes will be identical: there is usually a small degree of difference between them (Behl and Lendlein 2007). Five separate stimuli to trigger shape recovery have been identified: temperature (2.4.1), light (2.4.2), pH (2.4.3), electric (2.4.4) and magnetic (2.4.5) fields.

2.4.1 Thermal

Thermal shape memory polymers use heat changes to trigger recovery (Behl and Lendlein 2007). Amorphous polymers are typically most appropriate for thermal shape recovery (Lei, Yu et al. 2017). Following formation of a thermoplastic material, a shape is maintained – the permanent shape (Behl and Lendlein 2007). To maintain any material shape, the polymer chains (molecules) undergo thermally induced cross-linking (Moon, Cui et al. 2015). These cross-linked bonds ensure the molecules stay in one position; however, these bonds can be removed, or repositioned. The alteration to molecular cross-linking is the basis for thermal shape memory polymers (Behl and Lendlein 2007). If a given SMP is heated above what is termed the transition temperature (this is different to the glass transition temperature), the material can be deformed; further, the deformed polymer can be rapidly cooled and the new shape 'stored' – this is called the programed shape (Behl and Lendlein 2007). Thermal SMPs can return to their permanent shape upon the addition of heat (stimuli) (Behl and Lendlein 2007). In terms of medical devices, the ability for a polymer to recover its shape is of significance. Medical sutures have been produced from shape memory materials and used in wound management applications (Lendlein and Langer 2002). Shape memory sutures allow less force to be applied during wound closure: as the sutures heat to body temperature, they tighten, completely sealing the wound (Lendlein and Langer 2002).

2.4.2 Light

Light induced (photo induction) SMPs use photochemical modifications to trigger shape changes (Chatani, Kloxin et al. 2014). However, photosensitive cells (i.e. chromophores) are required in the polymer matrix to allow photo induction (Chatani, Kloxin et al. 2014). Further, the light (photon) must carry a sufficient amount of energy to trigger the reaction; this can be an obstacle when deigning an SMP (Chatani, Kloxin et al. 2014). When triggered, photochemical reactions can operate through one of three paths: isomerisation, bond formation or bond breaking reactions (Chatani, Kloxin et al. 2014). If induced, any of these three processes can cause a shape change in the polymer; regardless of which it is, the

molecular structure will be modified. There are three useful benefits that photo induction has over other SME induction stimuli. The most important of these benefits is the rapid induction of change – photons typically have a much higher energy than other stimuli e.g. temperature (Chatani, Kloxin et al. 2014). It is approximated that at 365 nm wavelengths, photons have 130 times more available energy than the energy available at 25°C (Chatani, Kloxin et al. 2014). It is immediately apparent that this increase in energy is significant and vital in some cases for appropriate SMP activation. A second important benefit to photo induction is that of temporal activation (Chatani, Kloxin et al. 2014). Essentially, to trigger the SMP, a light is switch on/off. Light activation is easy to control; it is often as easy as the flick of a switch. Typically, lights do not trigger adverse effects in humans. This is a significant benefits over other stimuli, such as heat – in many instances the SME only triggers at non-physiological temperatures, creating a potentially harmful environment for humans (Chatani, Kloxin et al. 2014). Finally, photo induction also affords spatial control of SMP activation (Chatani, Kloxin et al. 2014). That is, the SMP can be triggered in a specific place – other methods do not allow this control, it is universal activation. To sum up, photo induction allows low energy activation, with excellent control over when the effect is triggered, and where (Chatani, Kloxin et al. 2014). This allows more complex activation patterns than other SME stimuli.

2.4.3 pH

Chemical methods (pH) do not appear to be particularly common in the literature. A brief search has yielded only one paper on this topic (Han, Dong et al. 2012). However, it would appear, based on this paper, that pH induction is a powerful tool. Essentially, pH induction is a result of reversible bond formation (Han, Dong et al. 2012). In this example, it would appear that the beta-cyclodextrins and diethylenetriamine molecules crosslink dependent on the pH of the solution (Han, Dong et al. 2012). It is evident that the crosslinking is responsible for the shape memory properties in pH induced SMPs. Reversible crosslinking has been established as a result of pH changes: at pH 7, the materials do not undergo crosslinking, they do however undergo crosslinking at pH 11.5 (Han, Dong et al. 2012). The very nature of crosslinking explains how the material gets its shape memory: the polymer chains are drawn together if crosslinks are present (Han, Dong et al. 2012). Based on this fact, it is clear that reversible crosslinking would be greatly beneficial in SMP applications. pH sensitive SMPs can be used in human biomedical applications (Han, Dong et al. 2012). Ideally, these SMPs should recover at approximately human physiological pH of 7 (Han, Dong et al. 2012).

2.4.4 Electric Fields

It is apparent that the use of electric fields in SMP's is still a developing area. Essentially, to enable electrical stimulation, the polymer must be blended with a conductive element; such as carbon nanotubes (CNTs) (Cho, Kim et al. 2005, Raja, Ryu et al. 2013) or carbon sheets (Lu, Liu et al. 2010). The conductive carbon elements found within electroactive SMPs act by resistive heating (Lu, Liu et al. 2010). That is to say, they resist the flow of electricity, and heat as a result – SMP behaviour is therefore similar to how thermally responsive SMPs act. It has been suggested that electroactive SMPs could be used in light aerial vehicles or electrical actuation (Cho, Kim et al. 2005, Lu, Liu et al. 2010, Raja, Ryu et al. 2013).

2.4.5 Magnetic Fields

Magnetic fields and SMPs are not typically studied, only one paper has been found that references this (Yu, Zhou et al. 2009). To enable magnetic sensitivity, iron (III) oxide (Fe_3O_4) is blended with PCL (Yu, Zhou et al. 2009). Iron oxide is a typical magnetic element; this is well studied and biocompatible. It has been suggested that magnetic SMPs can provide a significant benefit to medical devices as magnetism does not require contact (Yu, Zhou et al. 2009).

2.5 Polymer Processing Techniques

Polymer processing techniques are those employed to turn raw polymer materials into parts, products or fibres. Three processing techniques have been identified in section 2.2. Melt extrusion (2.5.1), injection moulding (2.5.2) and compression moulding (2.5.3) will be explained. It is important to establish how each method operates, the benefits and detriments of each method, and finally, what the output object is. It is important to note that hybrid materials typically undergo several passes of processing (Middleton and Tipton 2000).

2.5.1 Melt Extrusion

Melt extrusion is a relatively common process to produce polymer hybrids. Two broad classes of melt extruder exist: screw and screwless. Three classes of screw extruder exist: single, multi (typically twin), and vane (refer to figure 2: 2, A, B and C). Single and multi-screw extruders are similar; they both use a standard screw; whereas vane extruders employ a screw with offset platforms surrounding the barrel (Treece and Oberhauser 2007, Chen, Zou et al. 2014). The second class, screwless extruders employ a smooth rotating drum (figure 2: 2, D) rubbing on a flat plate (Jayaraman and Halliwell 2009). Essentially, all thermal melt extruders operate in the same way. Polymer resins (powders or granules) are melted within an auger, then forced out through a small die hole (Treece and Oberhauser 2007, Jayaraman and Halliwell 2009, Jia, Qu et al. 2013). The screws and smooth drums exert shear forces on the molten polymers within the auger; this enables extrusion, with higher shear forces producing better results (Treece and Oberhauser 2007, Jayaraman and Halliwell 2009, Jia, Qu et al. 2013). Of the three screw types, single screws produce the lowest quality hybrid polymers: they exert the lowest shear forces during processing (Treece and Oberhauser 2007). The use of a multi-screw extruder reportedly solves this issue (Treece and Oberhauser 2007). Twin screw extruders are the most common type of multi-screw extruder; these exert relatively high shear forces, producing high quality results (Treece and Oberhauser 2007). However, vane extruders reportedly produce the best results of all screw based extruders (Jia, Qu et al. 2013). Due to the offset plates around the barrel, dynamic shear forces are exerted on the materials (Jia, Qu et al. 2013). The use of dynamic forces produces the most homogeneous blends, with the most consistent mechanical properties (Jia, Qu et al. 2013). Very little work has been done with screwless extruders, as such, no comparisons can be made with the screw extruders. In all cases, polymer filaments are produced. These are suitable for use as sutures or tubing (Zhang, Chen et al. 2010, Catanzano, Acierno et al. 2014, Pan, Trempont et al. 2016).

2.5.2 Injection Moulding

In its simplest form, injection moulding is the same as melt extrusion (section 2.5.1). Injection moulding uses a mould and a hydraulic screw, melt extrusion does not (Chinn, Kate et al. 2016, López, Aisa et al. 2016, Zhang, Zhao et al. 2017). Two forms of injection moulding have been identified: conventional (industrial) and microinjection moulding. Both types of injection moulding operate in the same manner (Giboz, Copponnex et al. 2007). The use of a hydraulic screw in injection moulding allows more materials to be pushed into the mould, and the mould to be blocked with the screw head (Chinn, Kate et al. 2016). The mould itself has two panels, one of which is hydraulically operated, ensuring adequate mould seals (Attia, Marson et al. 2009). The hydraulic panel facilitates part removal; the panel is pulled onto ejector pins, removing the part (Attia, Marson et al. 2009). The main limitation of injection moulding is the requirement of a precise mould.

2.5.3 Compression Moulding

Compression moulding is one of the simplest and most commonly used polymer processing techniques in laboratories worldwide (De Focatiis 2012). A polymer is loaded into a heated mould, and compressed to form a part (Schotzko, Reuter et al. 2015). Prior to compression, polymers must be sufficiently heated. Amorphous polymers must be taken passed their glass transition temperatures, whereas semi-crystalline polymers are taken passed their melting points; the mould will remain stable at the required temperature (De Focatiis 2012). Moulds must be cooled prior to part removal. Cooling is carried out by one of two methods, either ambient air temperature, or convection forced (water or air) (De Focatiis 2012). Two moulding methods exist: flash moulding and positive moulding (De Focatiis 2012). Flash moulding requires a support frame for the polymer materials, the frame and materials are compressed by two plates (De Focatiis 2012). Conversely, positive moulding has two plates, one of which fits inside the other, compressing the materials (De Focatiis 2012). Flash moulds are reported to be considerably easier to remove parts from,; positive moulds produce parts that fit near perfectly in the mould, meaning shrinkage of the part is required, or dismantling of the mould (De Focatiis 2012). Compression moulding is stated to be better than injection moulding: the process does not use shear forces (Schotzko, Reuter et al. 2015). However, that significantly restricts the amount of material mixing that can occur (De Focatiis 2012). It is suggested that this method should not be used where material mixing is useful or essential (De Focatiis 2012).

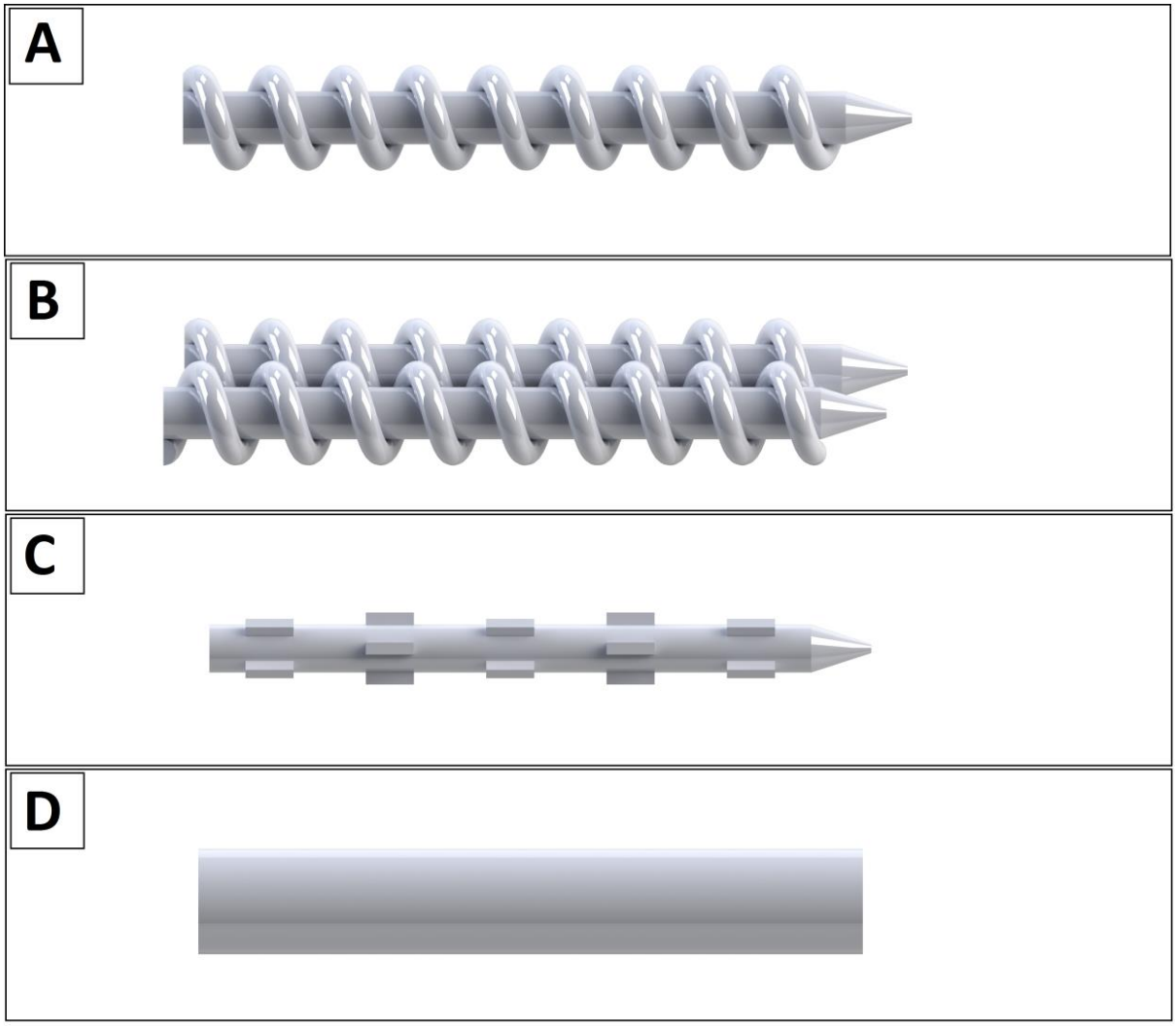

Figure 2: 2 The four types of driving mechanism for melt extrusion. A) Single Screw (SSE). B) Multi (twin) Screw (MSE, TSE). C Vane (VE). D) Screwless/Drum.

2.6 Test Methods

It is essential to determine the appropriate mechanical, *in vitro* and *in vivo* properties of any new combination of materials. The final application of the materials dictates what test methods are appropriate. Tensile, shape recovery and thermal properties are physical properties considered to be of importance to biocompatible polymers. *in vitro* properties are limited to degradation and cytotoxicity properties, while *in vivo* investigate biocompatibility.

2.6.1 Tensile Property Testing

The physical properties of a new material are important to identify. However, prior to testing the physical properties, the materials must undergo conditioning. Material conditioning aims to standardise the temperature and humidity of the materials, to improve repeatability (European Committee for Standization 1997, International Organization for Standardization 2005). Tensile strength is seen to be the most important factor in this project, as such; compressive strength and impact toughness will not be discussed.

Tensile testing investigates the material displacement, and resultant forces across the gauge length of a tested material (Chen, Yeh et al. 2017). In tensile testing, the gauge length is the area that undergoes testing: it rests between the grips (Chen, Yeh et al. 2017). From the output data (force and displacement), several important factors can be determined table 2: 3. Stress and strain are graphed to determine the remainder of the properties listed in table 2: 3; figure 2: 3 displays an example stress strain curve for PLA 100WT% fibres.

Two possible endpoints exist in a tensile test, either sample fracture, or specified displacement. Typically, it is useful to carry out the test until the break point – especially when investigating elastic materials (Chen, Yeh et al. 2017). However, in some instances, it is only necessary to prove that a given material will not fracture at a set displacement – typically a safety test. Some tensile testing data is provided in table 2: 2 (section 2.2), all of which required materials to fracture.

Table 2: 3 Typically Reported Tensile Properties.

Property	**Unit**
Stress	MPa
Strain	%
Tensile Strength	MPa
Yield Strength	MPa
Young’s (Elastic, Tensile)Modulus	MPa
Elongation at Break	%

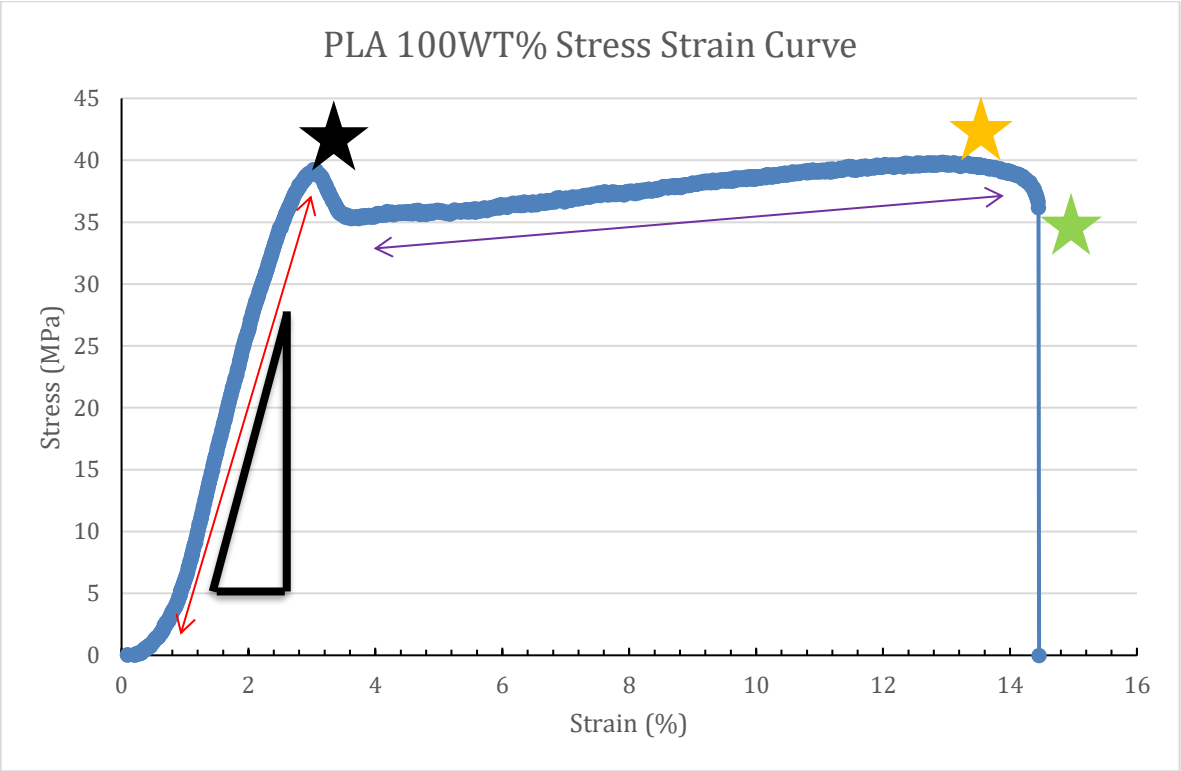

Figure 2: 3 Annotated stress-strain curve. Stars indicate the following: Black: Yield Strength (MPa); Orange: Tensile Strength (MPa); and Green: elongation at break (%). Lines indicate Elastic Deformation: red; and plastic deformation: purple. Young's (elastic, tensile) Modulus (MPa) calculation is indicated by the black triangle

2.6.2 Thermal Properties

Two methods exit for establishing a materials thermal properties: DSC and TGA. The two methods operate in essentially the same manner. An inert gaseous atmosphere (typically argon or nitrogen) is required, with a range of temperatures trialled in both DSC and TGA (Khankrua, Pivsa-Art et al. 2014, Gu, Lv et al. 2017, Yuan, Liu et al. 2017). While the method is similar, the result is different. TGA determines weight loss – degradation occurs; whereas DSC determines thermal transition points – melting (T_m) and glass transition temperatures (T_g) (Gu, Lv et al. 2017, Yuan, Liu et al. 2017). DSC testing reveals different results, dependent on whether a polymer is amorphous or semi-crystalline; melting is a first order response in only semi-crystalline materials (Cadek, Coleman et al. 2002). Amorphous polymers only show a glass transition (Cadek, Coleman et al. 2002).

2.7 *in vitro* Testing

In biocompatible polymers, *in vitro* testing is essential. Polymer degradation behaviour and cytotoxicity must be investigated prior to human testing (2.6.4).

2.7.1 Degradation Testing

Polymers implicated in biomedical applications must undergo enzymatic degradation testing (Jiang, Jiang et al. 2010). A multitude of enzymes exist within the human body; many of these have the potential to interact with polymeric materials (Jiang, Jiang et al. 2010). Wherever possible, degradation testing should be carried out at human physiological temperature, 37.5°C (Vieira, Vieira et al. 2011, Pinho, Rodrigues et al. 2016). Typically, this process involves a buffered solution and one type of enzyme (Jiang, Jiang et al. 2010). Typically, a combination of PBS buffer and trypsin enzyme is applied (Cai, Shi et al. 2003, Almany and Seliktar 2005, Lim, Raku et al. 2005, Moody, Brown et al. 2006, Ghosh, Ali et al. 2010, Bardsley, Wimpenny et al. 2016). All enzymes are found to act on the surface of the material (Puri 1984). Therefore, as surface area increases, the rate of degradation also increases (Puri 1984). Equation 2: 1 displays the equation for the surface area of a cylinder, suggesting that as the radius of the cylinder increases, surface area will increase. In the event of free enzyme being present in the solution, a surface area increase will result in an increased degradation rate (Puri 1984). However, a second phenomenon can be frequently observed with free enzyme: self-autolysis (Nord, Bier et al. 1956). This occurs in enzymes such as trypsin (Nord, Bier et al. 1956). Typically, self-autolysis is most apparent when the enzyme is added to excess (Nord, Bier et al. 1956). Enzymes undergoing self-autolysis suffer a reduction in desired effects; such as degrading a target material (Nord, Bier et al. 1956).

$$A = 2\pi rh + 2\pi r^2 \quad \text{(equation 2: 1)},$$

Where:

A is the surface area;

r is the radius; and

h is the height.

2.7.2 Cytotoxicity

Prior to human testing of any materials, they must be proven safe for cell contact (Mercado, Orellana-Tavra et al. 2016). Cytotoxicity studies are able to provide useful information on materials, at a lower cost than human trials (Riaz Ahmed, Nagy et al. 2017). Typically, cells from the desired active site are used: skin cells (sutures) or bone cells (bone stents/grafts) (Robey and Termine 1985, Corden, Jones et al. 2000, Grenade, De Pauw-Gillet et al. 2017).

2.8 Biocompatibility (in vivo) Testing

In vivo testing is typically one of the last steps in material characterisation. It aims to demonstrate safety in humans (Hamm, Sullivan et al. 2017). Further, animal models are used to determine the lethal dose in 50% of specimens (LD_{50}) (Hamm, Sullivan et al. 2017). LD_{50} is never measured in humans; experiments of this nature would be highly unethical.

2.9 Discussion

Shape recovery is one of the most important properties in this study, as such, an amorphous polymer must be used (Lei, Yu et al. 2017). PLA is an amorphous polymer, stated to be one of the most important biodegradable and biocompatible polymers available (Guttman, DiMarzio et al. 1981, Luzi, Fortunati et al. 2015, Malinowski 2016). A second polymer, PCL, is another important biocompatible and biodegradable polymer (Malinowski 2016). As such, a blend between PCL and PLA materials will be investigated. However, due to thermodynamic incompatibility, the two materials will not blend without the addition of plasticisers or compatabilisers (Malinowski 2016). Glycerol and PEG are commonly used plasticisers for biomedical applications, as such, they will both be trialled in this work (Jung, Deng et al. 2016). Little evidence could be identified for glycerol's use as a plasticiser in PCL:PLA blends. This contributes to the novelty of the hybrid blends. Further, no evidence for PEG-200 with PCL:PLA blends was identified, also contributing to blend novelty. With the potential application in sutures, thermal melt extrusion is the most applicable method: it is used to produce pipes and sutures (Zhang, Chen et al. 2010, Catanzano, Acierno et al. 2014, Pan, Trempont et al. 2016). Compression moulding was not found to be suitable as blending does not occur (De Focatiis 2012). Based on time constraints, thermal shape memory is the most appropriate for testing: it is the easiest and most common method (Behl and Lendlein 2007). The tensile properties of new materials must be characterised. However, the focus is primarily on having a high elongation at break and Young's modulus, and comparison to the component materials; table 2: 4 summaries the cut off points for these. The properties defined in table 2: 4 are based off intermediates between the two constituent polymers (PCL and PLA); refer to table 2: 2. At this stage, the final application of the materials are unknown. Degradation testing will be carried out using trypsin enzymes: this is the most common. However, at this early stage, there is interest in establishing a degradation profile. Whether degradation is required or not is influenced by the application, and required length of time in said application.

Table 2: 4 Minimum Property Values for PCL:PLA Hybrid Fibres.

Property	**Value**
Young's Modulus	1500 MPa
Elongation at Break	250%
Shape Recovery	Essential
Degradation	Profile. No amount is required; want to see how it behaves.

Chapter 3 Fibre Fabrication

3.1 Introduction

Polymer processing is a vital step in developing a new polymeric material. This step determines how homogeneous the final fibres are. Typically, several stages are required to define the most appropriate processing technique. Initially, pilot studies into the method are required. Prior to full scale production, the method must be proven effective. Several factors are considered when determining an appropriate method. The produced fibres must be of high quality; the diameter should be consistent, with no air bubbles present (Sastra, Siregar et al. 2006).

3.2 Materials and Methods

This section provides the materials and methods employed to process the materials. Further, this section gives the details and implications of the single screw melt extruder (SSE) pilot study, section 3.2.2. The method used for screwless extrusion is described in section 3.2.3.

3.2.1 Materials

Fibre processing involved the use of two polymer materials. Polycaprolactone (PCL), Capa 6506 was sourced from Perstorp UK Ltd (UK). PCL was supplied as a fine white powder, and used as supplied. The Capa 6506 line of PCL has an average molecular weight of 50,000 g/mol; with an average particle size of less than 600 μm, with at least 98% of all particles within this range [Capa 6506 Datasheet]. The melting point is quoted as 58 – 60°C on the product data sheet [Capa 6506 Datasheet]. The glass transition temperature of Capa 6506 is not specified in the datasheet; however, PCL has a typical glass transition temperature of approximately -60°C (Koleske and Lundberg 1969). Polylactic acid (PLA) was supplied by Donaghys Industries Ltd, Dunedin (NZ); PLA was originally sourced from NatureWorks LLC Ingeo PLA biopolymers. The supplied PLA was supplied as transparent 3 mm granules, and used as received. However, the product code, and previous storage conditions are unknown; it is possible the material has undergone pre-treatment. Typically, PLA has a glass transition temperature of around 58°C, and a recommended processing temperature of 200 – 205°C (NatureWorks LLC Ingeo 3051D) (Jamshidian, Tehrany et al. 2010).

Two plasticisers were used in the hybridisation process. Glycerol was sourced from Sigma-Aldrich (https://www.sigmaaldrich.com/new-zealand.html) product code: G5516. The supplied glycerol had an average molecular weight of 92.09 g/mol, and was found to be greater than 99% pure [Glycerol G5516 datasheet]. Prior to use, glycerol was diluted in distilled water to one of three concentrations: 5, 10, or 20% glycerol. Polyethylene glycol (PEG-200) with an average molecular weight of 200 g/mol was purchased from Sigma-Aldrich (https://www.sigmaaldrich.com/new-zealand.html) product code: P3015. The supplied PEG-200 was diluted in distilled water, to one of the following: 5, 10, or 20% PEG-200 prior to use.

Initially, an in-house produced single screw thermal melt extruder (SSE) was trialled. The extrusion die on the SSE machine had a diameter of 1 mm, and the screw driving extrusion was a standard, steel single-stage drill-bit; L/D ratio: 12.5:1, with a compression ratio of 1:1. While the exact carbon (C) content of this steel drill bit is unknown, it is expected to be either high (1.5 – 2 C) or low (0.5 – 1 C) steel. This machine has a temperature range of 30 – 250°C. A second thermal extruder was trialled when the SSE was found to be unsuitable. A variable speed rotating drum screwless extruder was obtained from the Chemistry Department, University of Otago, Dunedin. The screwless extruder was purchased by the Chemistry Department, from CSI Custom Scientific Instruments (USA) product code: CSI LE-075. It is reported in the manual provided by CSI Custom Scientific Instruments (USA) that the screwless extruder has a temperature range of 20 – 400°C. Unlike the SSE machine, the screwless extruder uses a rotating smooth drum to drive extrusion; a 3 mm extrusion die was equipped. All materials were weighed out prior to extrusion using a 3-digit Shimadzu Libror EB-280 balance. The EB-280 balanced had an error of 0.01 g (10 mg).

Temperature testing was carried out with a Digitech branded infra-red non-contact digital thermometer purchased from Jaycar Dunedin (NZ) product code: QM7215. This device was quoted as having a detection range of -30 - +260°C, with an error of 2% of the reading. No modifications were made to the device, or any item undergoing temperature measurements. All diameter measurements were made using an electronic digital Vernier calliper (non-Absolute), model number TD2082. The calliper was able to measure values between 0.01 and 150.00 mm, with a resolution of 0.01 mm. The calliper was compliant with ISO 9001:2000 (Quality management system – requirements). While ISO 9001:2000 is a withdrawn standard, there is not substantial difference between that, and the current ISO 9001:2015 standard.

3.2.2 Single Screw Melt Extruder (SSE) Pilot Study

The single screw melt extruder (SSE) was solely used for the purpose of a pilot study; this aimed to ensure PCL and PLA could be both separately processed, and processed to a hybrid. Further work was done ensuring the SSE machine was appropriate for use. To achieve this, three different extrusion runs were carried out.

3.2.2.1 Pilot Method

The SSE machine had a low capacity powder hopper, taking approximately 2 g of material at a time. Material was forced into the auger with the aid of a manually operated piston. Initially, two sets of fibres were produced: 50 fibres containing 100WT% PCL; and 50 fibres containing 100WT% PLA were extruded. For each material set, a variety of temperatures were trialled, table 3: 1 provides the temperatures tested. To ensure that the temperature was accurate, the machine was left to heat for one hour prior to any testing commencing. When switching between the materials, the SSE machine was dismantled and cleaned. This step was required as it ensured that only what was expected to be extruded, was extruded. At each temperature, the fibres were visually inspected to determine suitability. In this instance, suitability was defined as no air-bubbles, correct colour (PCL, white; PLA, transparent), and visual diameter consistency (no large variations). Finally, a PCL:PLA 60:40WT% hybrid was processed through the SSE machine, figure 3: 1 provides an image of this process (table 3: 1 gives the

temperatures used). The hybrid material produced was examined for defects and tensile properties (see section 4: Tensile Properties).

During the extrusion process, it was noted that the temperature displayed did not equal the actual temperatures observed in the machine. As a result, the machine was analysed for how well the displayed temperature represented the actual temperature, and how consistent this temperature was. To achieve this, two set temperatures were trialled: 100±1°C and 200±2°C, table 2 provides a list of temperatures and results for this test. The temperature testing sites are displayed in figure 3: 2. During both 100°C and 200°C testing, the machine was given a 1 hour warm up period. This ensured all surfaces identified in figure 3: 2 were at equilibrium temperature. The temperature test did not involve material extrusion; however, the screw was set to rotate, ensuring the test was representative.

3.2.2.2 Pilot Results and Discussion

Three fibre ratios were extruded: PCL 100WT%, PLA 100WT%, and PCL:PLA 60:40WT% (figures 3: 3 – 5). All three fibre types were able to be successfully extruded. In this instance, a successful extrusion meant consistent fabrication of fibres of at least 200 mm in length, with regular diameters. Fibre were examined for deformities both on the surface and internally (air bubbles). In most cases the fibres examined were smooth to touch; however, many fibres were found to have air-bubbles present internally. It must be noted that the air bubbles reduce the quality of the fibre. The issue of air bubbles is significant during tensile testing: air bubbles are voids in the fibre, these cause points of weakness (Sastra, Siregar et al. 2006). As a result of the processing method, fibres had curved ends: this did not impact the fibre, it was solely a processing artefact.

Over the course of the extrusion process, it was noted that the SSE's displayed temperature was not comparable to the internal temperature of the machine. It was determined that this phenomenon could have a negative impact on the extrusion process: if the temperature is too low, it will not allow for correct extrusion. The results of this test are found in table 3: 2. The difference between the actual temperature and displayed temperature appeared to follow a relatively consistent pattern. It must be noted that the three temperature points taken from the driving screw gave very low temperatures: on average the screw was 69% lower in temperature than the display. In reality, this would prevent polymer extrusion – the polymer will cool to a point where it cannot be extruded. As such, it must be assumed that these measurements possessed a high degree of error, given that the polymer could be extruded. It is reasonable to assume that the screw would cool rapidly after removing it from the device – the auger has three heating coils in it, with radiant heat allowing the screw to be heated; the screw does not possess its own heating element. As mentioned in the materials section (section 3.2.1), the screw was a standard steel drill-bit, with a 5.76 mm diameter. Based on the thermal conductivity of steel, this should cool rapidly when removed from the heat source: 0.5 C WT% steel, 55 $Wm^{-1}K^{-1}$, 1.5 C WT% steel 37 $Wm^{-1}K^{-1}$ at 0°C (Peet, Hasan et al. 2011). Across the temperature range tested (100 and 200°C) the high carbon (1.5 C WT%) steel has a constant thermal conductivity; whereas the low carbon (0.5 C WT%) steel displays a reduction in thermal conductivity: 53 $Wm^{-1}K^{-1}$ at 100°C, and 48 $Wm^{-1}K^{-1}$ at 200°C (Peet, Hasan et al. 2011). Essentially, an increase in temperature gives a decrease in thermal conductivity; however, higher carbon contents reduce this effect significantly (Peet, Hasan et al. 2011). A range of 37 $Wm^{-1}K^{-1}$ (0°C) to 28 $Wm^{-1}K^{-1}$ (1000°C) is observed in high carbon (1.5 C WT%)

steel, while 55 $Wm^{-1}K^{-1}$ (0°C) to 30 $Wm^{-1}K^{-1}$ (1000°C) is observed in low carbon (0.5 C WT%) steel (Peet, Hasan et al. 2011). Thermal conductivity provides an indication of the rate of heat transfer across a material, therefore, a higher thermal conductivity indicates a more rapid heat loss (Peet, Hasan et al. 2011). The main problem associated with the heat loss is the potential for motor damage, If the required temperature for extrusion is set to 140°C (arbitrary), but the actual temperature is between 40 – 75% lower (table 3: 2), this is likely to damage the motor.

A further challenge was the operation of the SSE device. During the extrusion process, materials in the hopper had to be manually compressed. During compression, the majority of the materials would not enter the auger, most erupted up and out the hopper. Further, no variable speed motor was attached. Therefore, screw speed was constant. This resulted in a very limited throughput: the screw speed was relatively slow. The combination of manual compression and slow screw speed resulted in processing issues. Primarily, air bubbles were observed in the fibres. Typically, the air bubbles were caused by the machine's inability to sustain a suitable material input. Voids frequently formed along the screw, causing fibre truncation. It was further established that the SSE machine could not produce a drawn fibre.

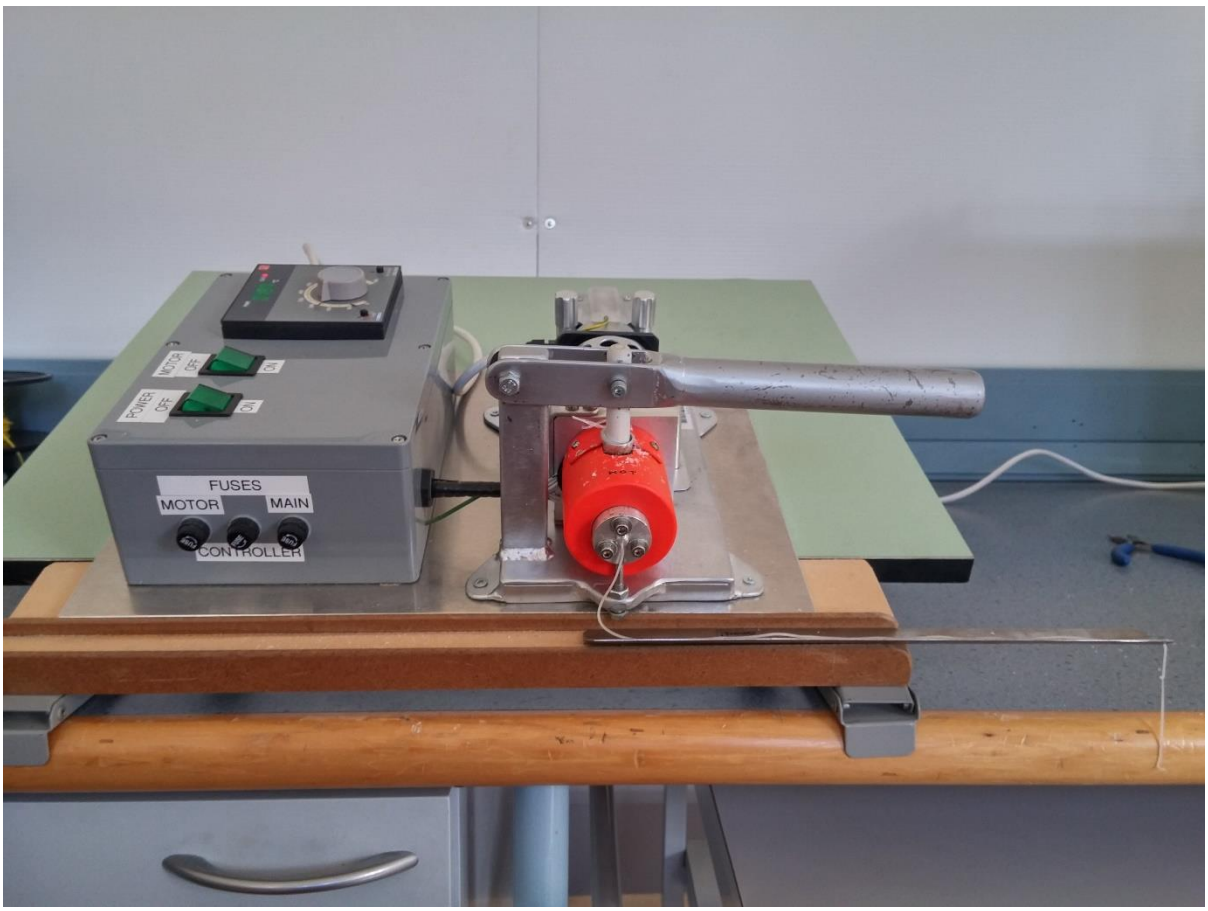

Figure 3: 1 Extrusion using the 1 mm diameter single screw melt extruder.

Table 3: 1 Single Screw Melt Extruder Processed Fibre Pretest

Material	**Ratio (WT%)**	**Temperatures Investigated (°C)**							
PCL	100	60	70	80	90	100			
PLA	100	140	150	160	170	180	190	200	210
PCL:PLA	60:40	70	160	180	200				

Table 3: 2 Single Screw Melt Extruder Actual temperature compared to Displayed temperature (°C)

Location	**Temperature (°C)**	**Percentage Difference (%)**	**Temperature (°C)**	**Percentage Difference (%)**	**Average Difference (%)**
Display (set)	200±2	*N/A*	100±1	*N/A*	*N/A*
Hopper	180	10	88	12	11
Front of Die	112	44	64	36	40
Under Die	125±5	37	65±5	35	36
Screw Base	50	75	30	70	72.5
Screw Middle	70	65	27	73	69
Screw Tip	65	67	36	64	65.5

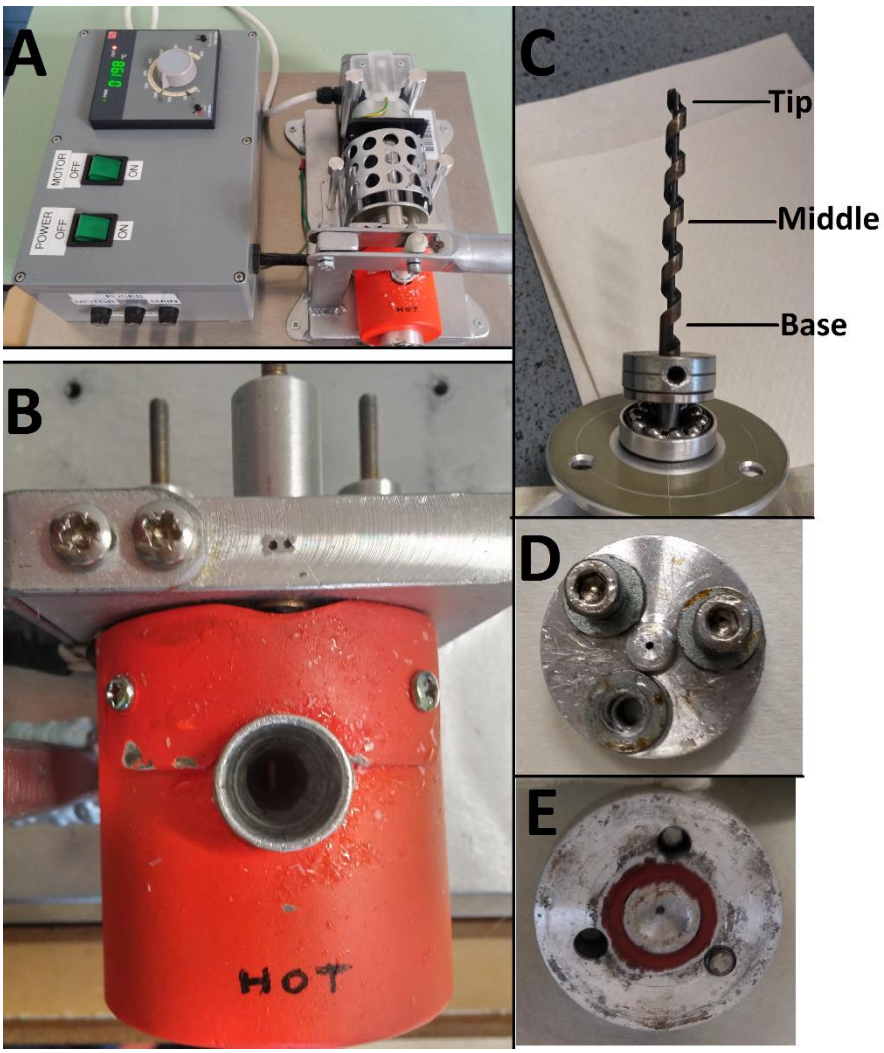

Figure 3: 2 Image series of temperature testing regions. A: The machine, 198°C display temperature. B: The hopper. C: The screw, locations are marked. D and E: are the front and back of the extrusion die respectively.

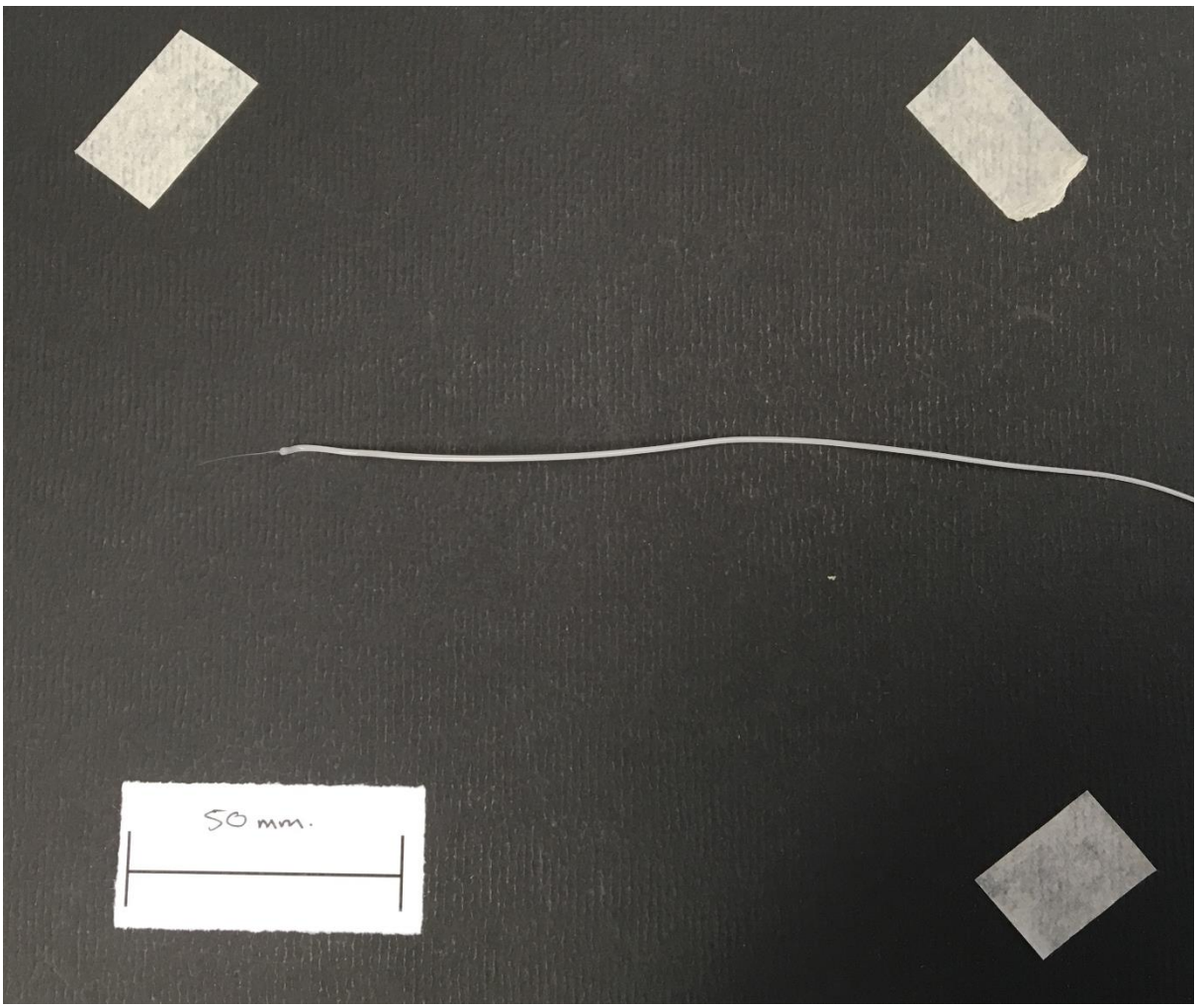

Figure 3: 3 PCL 100WT% fibre. Produced using the 1 mm diameter single screw melt extruder.

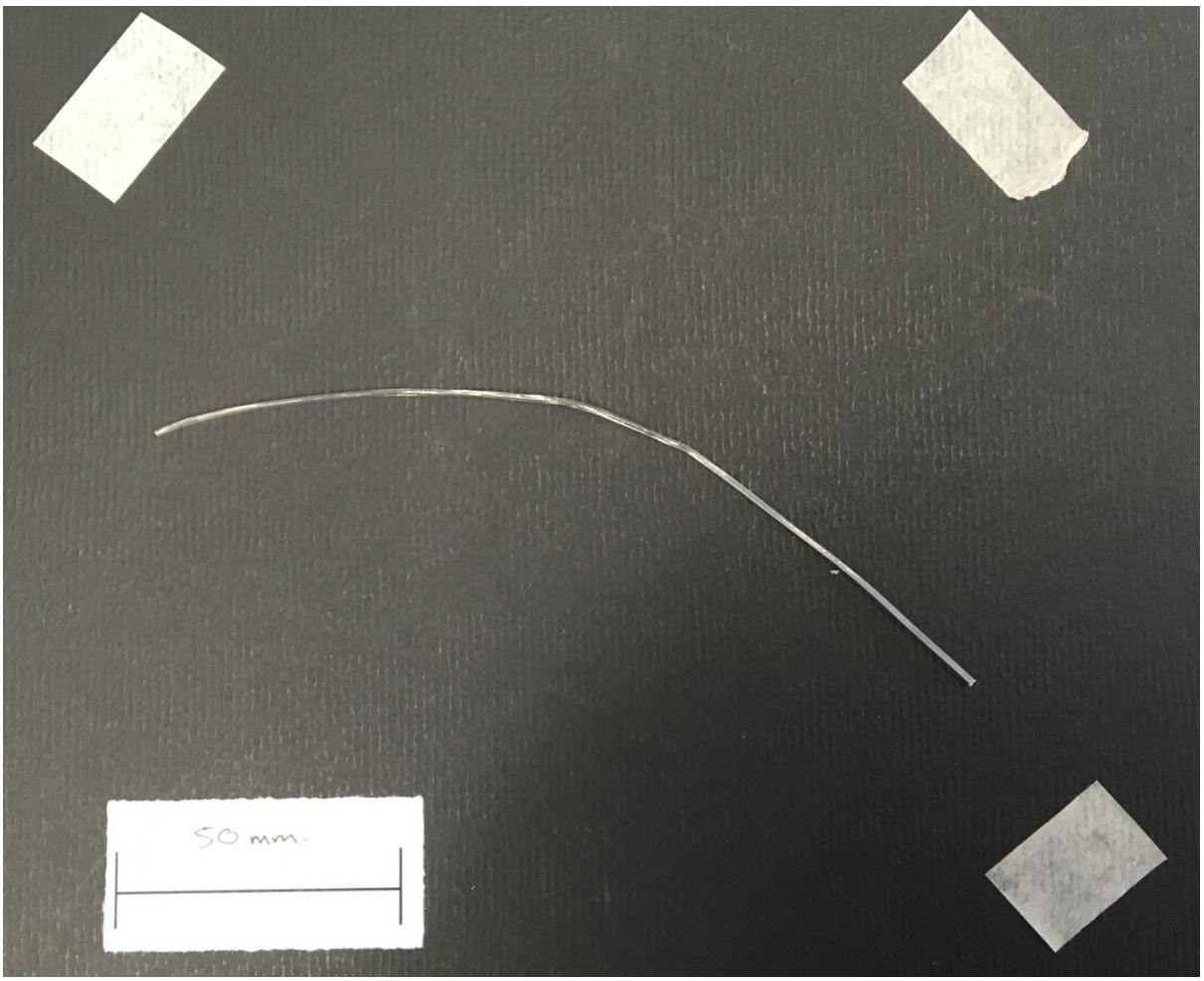

Figure 3: 4 PLA 100WT% fibre. Produced using the 1 mm diameter single screw melt extruder.

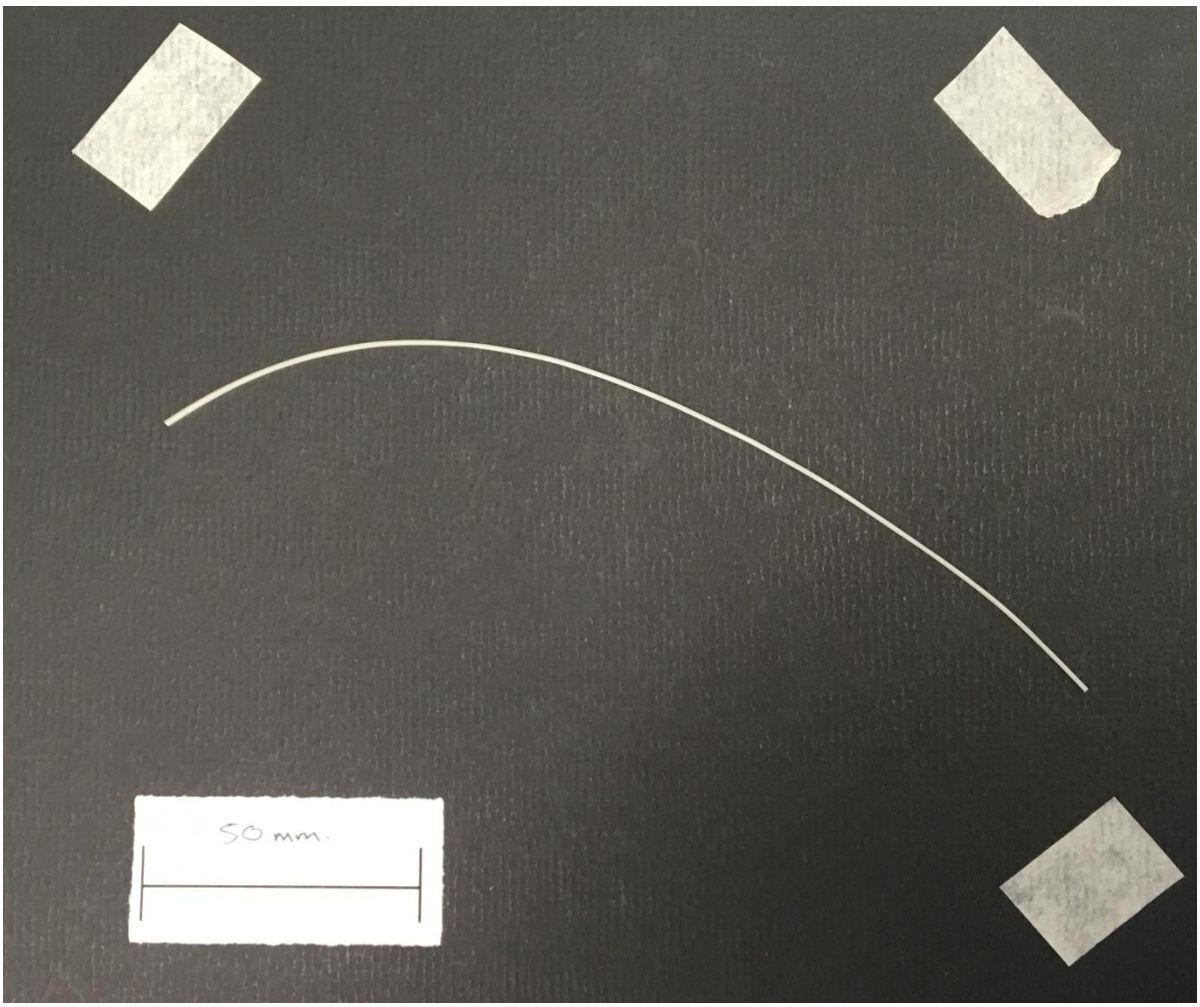

Figure 3: 5 PCL:PLA 60:40WT% fibre. Produced using the 1 mm diameter single screw melt extruder.

3.2.2.3 SSE Pilot Study Summary

Overall, the pilot study demonstrated that PCL:PLA hybrid fibres could be melt extruded. However, air bubbles within the hybrid fibres were observed. The air bubbles were primarily due to the processing method. Further, the processing method meant the conventional approach of drawing fibres could not be applied. As such, a commercially produced, CSI LE 075 screwless extruder was used.

3.2.3 Screwless Extruder

Fibre extrusion with the screwless extruder was a relatively straightforward process. Prior to initiating fibre extrusion, several steps were required. Initially, the machine was allowed to heat: the CSI LE-075 has two thermocouple locations, the head and rotor region. Typically, 30 minutes was allowed to ensure complete and consistent heating. Secondly, the rotor was allowed to turn at low speed – set to 30% of the maximum voltage (motor RPM is unspecified). The motor was not easily damaged at 30% of maximum voltage, making it an appropriate test speed. When extrusion was successful at 30% maximum voltage, the motor speed was increased to 80% to allow higher flow melt extrusion. It was identified early on that 80% of maximum voltage was an easily workable motor speed for extrusion: when drawing the fibres, a balance between extrusion speed and material viscosity was required. At 80% of maximum voltage, the material was extruded at a rate that meant it was still relatively viscous, allowing extrusion and drawing to occur in the desired manner.

Materials were weighed out and set aside prior to extrusion starting. During the extrusion process, the powder hopper was half filled: this was approximately 4 g of materials. It was identified that overfilling the hopper would reduce extrusion efficiency – the hopper would become blocked, reducing/preventing extrusion. In the event that the powder hopper became blocked, the motor speed was reduced to 30% of maximum voltage, and a glass rod used to remove the blockage.

During extrusion, the fibre was hand drawn. Figure 3: 6 displays a single fibre being drawn from the extruder. Trial and error was used to identify the best rate to draw the extruded fibres: eventually, a speed of approximately 2 – 4 mm/second was found to work well. This rate was suitable for the most part, however, at times this rate was either increased or decreased (viscosity dependent). Essentially, the rate at which the fibre was drawn centred on achieving a suitable, consistent diameter. A suitable diameter was arbitrarily defined as at least 100 μm. Nothing under 100 μm worked for other testing.

Figure 3: 6 Fibre drawing process. The drawn fibres are extruded from the screwless melt extruder, and pulled over the metal doorframe.

3.2.3.1 Non-plasticised Fibre Processing

A large variety of non-plasticised fibres were produced (tables 3: 3 – 5). Regardless of the ratio used, the method employed was the same. For each extrusion, a total of 20 g of material, this was found to produce a significant amount of fibre. In the instances of the control fibres, PCL and PLA, 20 g of material was spooned into the hopper, 4 g at a time. In the case of hybrid fibres, a slight change to the method was made.

All hybrid fibres had their respective materials weighed out, these were stirred using a spoon prior to extrusion. All hybrid fibres required further extrusion steps. Following the initial extrusion, hybrid fibres were cut and re-extruded; a process termed passes here. A number of passes were used, 1, 2, 3 and 6. A 2 pass hybrid variant would undergo two extrusion steps, and one cutting step (figure 3: 7). A weight loss of 5 – 15% was observed between passes. To ensure consistency across the fibres, the full 20 g was extruded until the first allocated pass count, then divided in half (10 g) and one half reserved, with the other cut and processed further. In the instance of a PCL:PLA 50:50WT% 3 and 6 pass variants, 10 g of PCL was combined with 10 g of PLA. This was extruded and cut twice (2 passes). Approximately 10 g of fibre was reserved as the 3 pass variant. The remaining 10 g underwent a further 3 passes, to produce the final 6 pass variant.

3.2.3.2 Plasticisation

To plasticise the fibres, glycerol and polyethylene glycol (average molecular weight 200 g/mol) were used. These plasticisers were diluted in distilled water prior to use, into one of three concentrations, see table 3: 6. Three separate material ratios were tested with each plasticiser ratio, at either 1 or 2 passes (table 3: 7). A variation to the method describe in sections 3.2.3 – 3.2.3.1 is used. The materials are weighed out as described above. Following material blending, 6 mL of diluted plasticiser is added. A second blending step is required to ensure adequate soaking of PCL and PLA in the plasticisers: not all of the liquid is soaked up. The materials were given 30 minutes to absorb the plasticiser prior to extrusion.

Table 3: 3 Compositions of Non-plasticised control and hybrid fibres from the Screwless Pilot Study.

Composition	Number	Processing Temperature (°C)	Passes	PCL (WT%)	PLA (WT%)
PCL	1 – 5	75	1	100	0
PCL	6 – 10	80	1	100	0
PCL	11 – 15	85	1	100	0
PCL:PLA	1 – 5	160	3	50	50
PCL:PLA	6 – 10	170	3	50	50
PCL:PLA	11 – 15	180	3	50	50
PCL:PLA	16 – 20	160	6	50	50
PCL:PLA	21 – 25	170	6	50	50
PCL:PLA	26 – 30	180	6	50	50
PLA	1 – 5	160	1	0	100
PLA	6 – 10	170	1	0	100
PLA	11 – 15	180	1	0	100
PLA	16 – 20	190	1	0	100
PLA	21 – 25	200	1	0	100
PLA	26 – 30	210	1	0	100

Table 3: 4 Fibre Compositions for Determination of PCL and PLA Control Fibre Best processing temperature.

Composition	Number	Processing Temperature (°C)	Passes	PCL (WT%)	PLA (WT%)
PCL	1	160	1	100	0
PCL	2	160	1	100	0
PCL	3	160	1	100	0
PCL	1	170	1	100	0
PCL	2	170	1	100	0
PCL	3	170	1	100	0
PCL	1	180	1	100	0
PCL	2	180	1	100	0
PCL	3	180	1	100	0
PCL	1	190	1	100	0
PCL	2	190	1	100	0
PCL	3	190	1	100	0
PLA	1	160	1	0	100
PLA	2	160	1	0	100
PLA	3	160	1	0	100
PLA	1	170	1	0	100
PLA	2	170	1	0	100
PLA	3	170	1	0	100
PLA	1	180	1	0	100
PLA	2	180	1	0	100
PLA	3	180	1	0	100
PLA	1	190	1	0	100
PLA	2	190	1	0	100
PLA	3	190	1	0	100

Table 3: 5 Fibre Compositions for Determination of PCL:PLA Hybrid Fibre Best processing temperature.

Composition Number	Processing Temperature (°C)	Passes	PCL (WT%)	PLA (WT%)
PCL:PLA	160	2	50	50
PCL:PLA	160	3	50	50
PCL:PLA	170	2	50	50
PCL:PLA	170	3	50	50
PCL:PLA	180	2	50	50
PCL:PLA	180	3	50	50
PCL:PLA	160	2	60	40
PCL:PLA	160	3	60	40
PCL:PLA	170	2	60	40
PCL:PLA	170	3	60	40
PCL:PLA	180	2	60	40
PCL:PLA	180	3	60	40
PCL:PLA	160	2	70	30
PCL:PLA	160	3	70	30
PCL:PLA	170	2	70	30
PCL:PLA	170	3	70	30
PCL:PLA	180	2	70	30
PCL:PLA	180	3	70	30
PCL:PLA	160	2	80	20
PCL:PLA	160	3	80	20
PCL:PLA	170	2	80	20
PCL:PLA	170	3	80	20
PCL:PLA	180	2	80	20
PCL:PLA	180	3	80	20

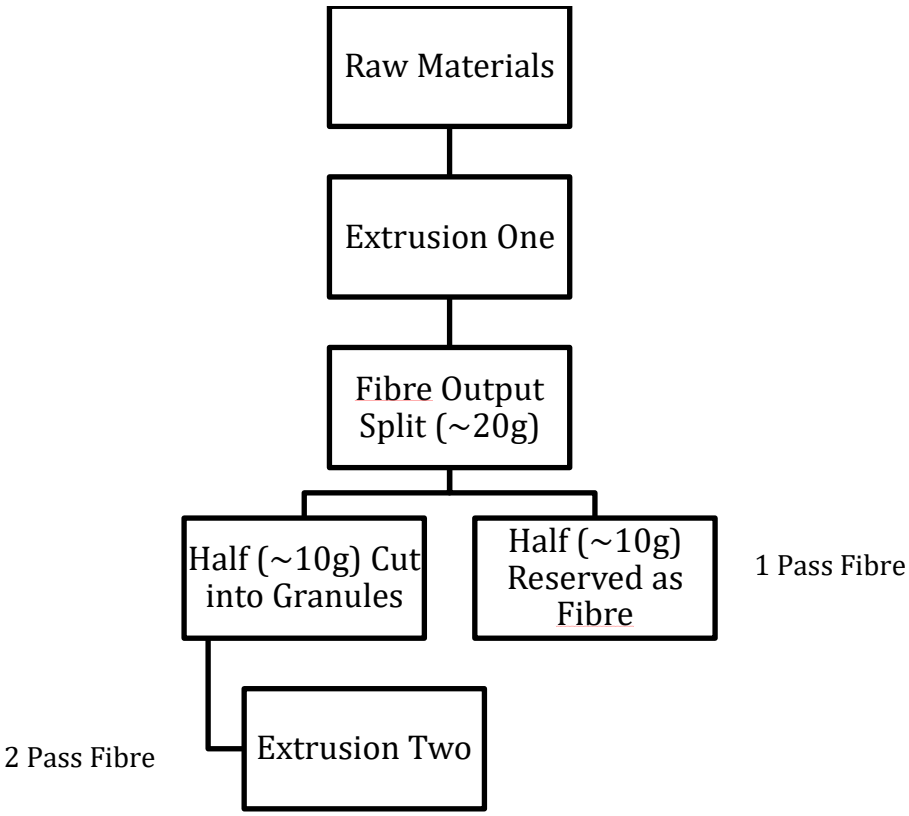

Figure 3: 7 Flow diagram displaying the method to produce 1 and 2 pass fibres.

Table 3: 6 Compositions of Glycerol and PEG-200 Plasticiser Solutions

Concentration (%)	Plasticiser	Glycerol (mL)	PEG-200 (mL)	Distilled Water (mL)
5	Glycerol	5	0	95
10	Glycerol	10	0	90
20	Glycerol	20	0	80
5	PEG-200	0	5	95
10	PEG-200	0	10	90
20	PEG-200	0	20	80

Table 3: 7 Compositions of Plasticised Control and Hybrid Fibres.

Material	Ref.	Processing Temperature (°C)	Passes	PCL (WT%)	PLA (WT%)	Glycerol Concentration (%)	PEG-200 Concentration (%)
PCL	1-5	150±5	1	100	0	5	0
	6-10	150±5	1	100	0	10	0
	11-15	150±5	1	100	0	20	0
	1-5	150±5	1	100	0	0	5
	6-10	150±5	1	100	0	0	10
	11-15	150±5	1	100	0	0	20
PCL:PLA	81-85	150±5	1	30	70	5	0
	86-90	150±5	2	30	70	5	0
	61-65	150±5	1	30	70	10	0
	66-70	150±5	2	30	70	10	0
	71-75	150±5	1	30	70	20	0
	76-80	150±5	2	30	70	20	0
	1-5	150±5	1	50	50	5	0
	6-10	150±5	2	50	50	5	0
	41-45	150±5	1	50	50	10	0
	46-50	150±5	2	50	50	10	0
	21-25	150±5	1	50	50	20	0
	26-30	150±5	2	50	50	20	0
	11-15	150±5	1	70	30	5	0
	16-20	150±5	2	70	30	5	0
	51-55	150±5	1	70	30	10	0
	56-60	150±5	2	70	30	10	0
	31-35	150±5	1	70	30	20	0
	36-40	150±5	2	70	30	20	0

Table 3: 8.Continued: Compositions of Plasticised Control and Hybrid Fibres.

Material	Ref.	Processing Temperature (°C)	Passes	PCL (WT%)	PLA (WT%)	Glycerol Concentration (%)	PEG-200 Concentration (%)
PCL:PLA	61-65	150±5	1	30	70	0	5
	66-70	150±5	2	30	70	0	5
	41-45	150±5	1	30	70	0	10
	46-50	150±5	2	30	70	0	10
	51-55	150±5	1	30	70	0	20
	56-60	150±5	2	30	70	0	20
	71-75	150±5	1	50	50	0	5
	76-80	150±5	2	50	50	0	5
	1-5	150±5	1	50	50	0	10
	6-10	150±5	2	50	50	0	10
	21-25	150±5	1	50	50	0	20
	26-30	150±5	2	50	50	0	20
	81-85	150±5	1	70	30	0	5
	86-90	150±5	2	70	30	0	5
	11-15	150±5	1	70	30	0	10
	16-20	150±5	2	70	30	0	10
	31-35	150±5	1	70	30	0	20
	36-40	150±5	2	70	30	0	20
PLA	1-5	150±5	1	0	100	5	0
	6-10	150±5	1	0	100	10	0
	11-15	150±5	1	0	100	20	0
	1-5	150±5	1	0	100	0	5
	6-10	150±5	1	0	100	0	10
	11-15	150±5	1	0	100	0	20

3.2.4 Fibre Imaging

All fibres produced using the screwless extruder were imaged using the Nikon D90 camera and lighting rig set-up. The Nikon D90 was equip with a AF-S Nikkor 1:3.5 – 6.3G ED VR lens. The lighting rig was acquired from Durst Phototechnik AG (Brixen, Italy) in 1998. Two large reprolamps were attached the rig. The camera was positions 500 mm away from the fibres to be imaged. A spirit level was used to ensure the camera was resting flat.

3.2.5 Fibre Diameter Measurements

All fibres diameters (ø) were measured using a digital Vernier calliper (TD2082). The diameters were measured in four independent locations along the gauge lengths of the fibres used. No measurements were taken within 5 mm of the mount attachment points. The four measurements were taken at approximately 7 mm intervals, and averaged to give the final value for mechanical testing. The range, average and standard deviation of the fibre diameters (ø) for the best fibres are located in table 3: 9 (the remainder can be found in Appendix A, Part 1).

3.3 Observations and Implications

Table 3: 9 provides a summary of the results for the best fibres. Appendix A, Part 1 contains the complete set of tables for fibre quality. Fibre diameter (ø) values were collected for mechanical testing using Vernier Callipers (as per 3.2.5). Figure 3: 8 – 10 provide a selection of images are as points of reference for table 3: 9. The remaining images can be located in appendix A, Part 2.

Table 3: 9 Physical Characteristics of the Best Fibres. The symbol ø is used to represent diameter.

Fibre Code (DD/MM/YY)	PCL:PLA:Gly 30:70:20_1P				
Fibre ø (mm)	Average ø	Range ø	Standard Deviation ø	Visual ø Consistency	Reflectiveness
	0.64	0.56 – 0.72	0.03	Consistent	Reflective
Colour	Opacity	**Observations/Comments:** Smooth surface. Feels tough.			
Silver	Translucent				
Fibre Code (DD/MM/YY)	PCL:PLA:Gly 30:70:20_2P				
Fibre ø (mm)	Average ø	Range ø	Standard Deviation ø	Visual ø Consistency	Reflectiveness
	0.79	0.56 – 0.77	0.05	Consistent	Reflective
Colour	Opacity	**Observations/Comments:** Smooth surface. Feels tough.			
Silver	Translucent				
Fibre Code (DD/MM/YY)	PCL:PEG-200 100:20 6-10				
Fibre ø (mm)	Average ø	Range ø	Standard Deviation ø	Visual ø Consistency	Reflectiveness
	0.65	0.34 – 1.29	0.30	Inconsistent	None
Colour	Opacity	**Observations/Comments:** Feels smooth and wet. Highly irregular diameter.			
White	Opaque				
Fibre Code (DD/MM/YY)	PLA:PEG-200 100:10 1-5				
Fibre ø (mm)	Average ø	Range ø	Standard Deviation ø	Visual ø Consistency	Reflectiveness
	0.43	0.22 – 0.64	0.11	Inconsistent	Moderate
Colour	Opacity	**Observations/Comments:** PCL was present in some parts, this burnt. Smooth to touch.			
Brown	Transparent				

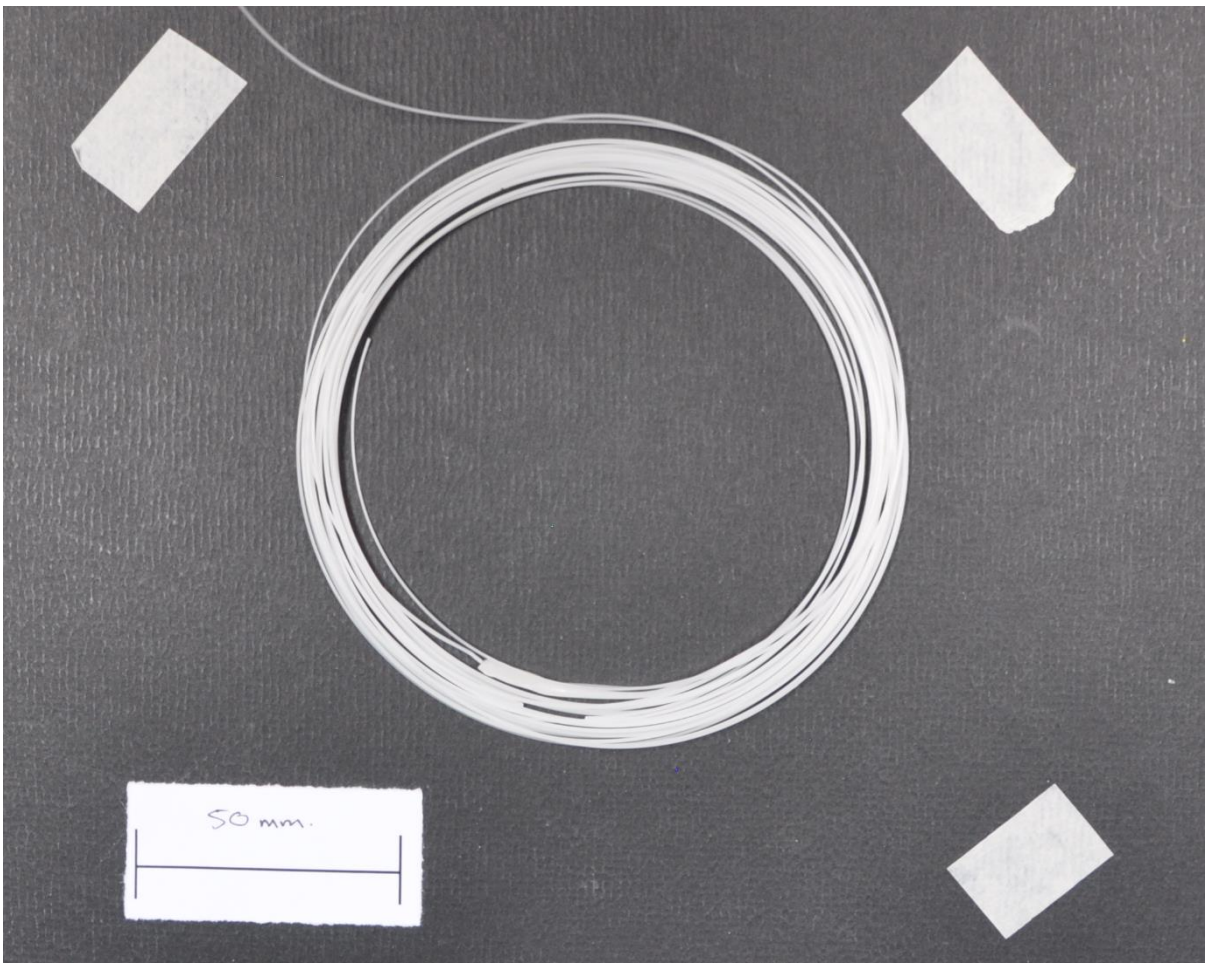

Figure 3: 8 PCL:PLA 30:70WT% fibre after 2 passes, plasticised with 20% PEG-200.

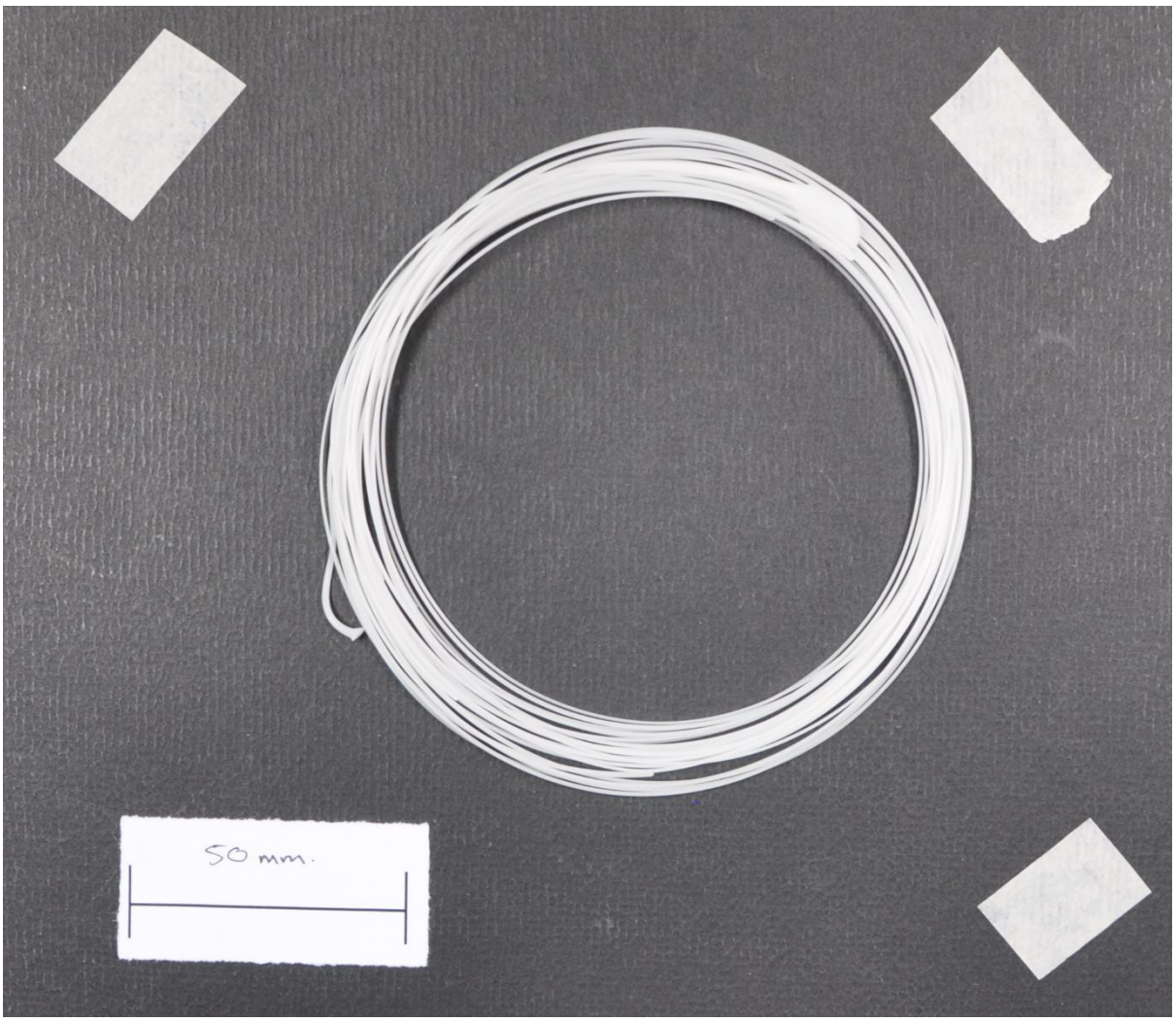

Figure 3: 9 PCL:PLA 50:50WT% fibre after 1 pass, plasticised with 5% PEG-200.

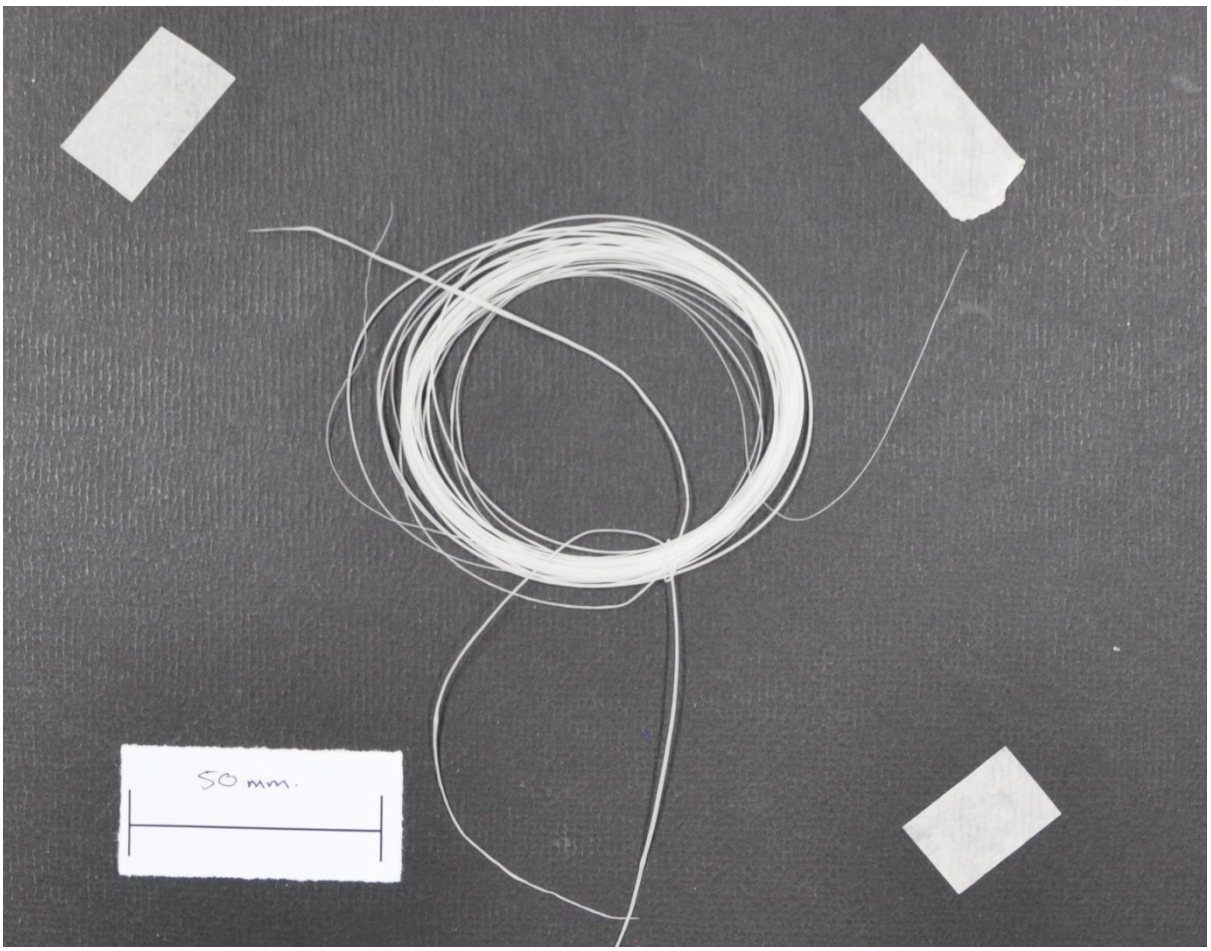

Figure 3: 10 PCL:PLA 70:30WT% fibre after 1 pass, plasticised with 10% PEG-200.

3.3.1 PCL and PLA Consistency

Numerous batches of both PCL and PLA 100WT% control fibres were extruded. This provides insight into the repeatability of fibre processing. Overall, it was observed that PLA was highly repeatable across the entire tested temperature range (140 – 210°C). However, PLA was found to produce a better fibre when extruded at a higher temperature. This phenomenon relates to the recommended extrusion temperature 175°C (Middleton and Tipton 2000) and 210°C [NatureWorks LLC Datasheet]. It must be noted that the recommended temperatures are not necessarily for the PLA used in this work, as such, the processing temperature cannot be guaranteed to be relevant. Further, it was observed that PLA would extrude with relative ease at 140°C, 70°C under the 210°C temperature recommended by NatureWorks LLC. The 70°C discrepancy between the extruder temperature and recommended temperature could be put down to either: using the wrong datasheet (it is unknown what version PLA was used, see Section 3.2.1), or PLA's amorphous nature (Ostafinska, Fortelny et al. 2015). The fact that PLA is an amorphous polymer allowed it to be extruded below the recommended temperature. PLA does not undergo crystalline melting, rather, it softens to a rubbery consistency when taken passed its glass transition temperature (T_g): 60°C (Middleton and Tipton 2000). Further, during low temperature (140°C) extrusion of PLA it was observed that the polymer was tough and rubbery (highly viscous) as it came out of the extrusion die. However, as the temperature approached 210°C, PLA lost its rubbery nature and became free flowing.

Unlike PLA which is processed at higher temperatures, PCL is best processed at relatively low temperatures: 60°C (Wan, Lu et al. 2009). Initially, PCL was processed across a range of low temperatures, 75, 80, 85°C. This is slightly higher than the recommend 60°C temperature (Wan, Lu et al. 2009); however, the extrusion machine would not function below 75°C. Even with the increased temperature, PCL extruded easily, producing consistent fibres. It was observed that at 80 and 85°C, the PCL fibres were relatively thin (figure 3: 11). While PCL extrudes consistently between these temperatures, it has to be blended with PLA. It is important to note that PLA will not extrude at temperatures of 75 – 85°C; while this does exceed the glass transition temperature of 60°C, it is too rubbery to process (Middleton and Tipton 2000). Therefore, PCL was also tested at higher temperatures suitable for PLA processing. To this end, temperatures between 160 – 190°C were trialled. Overall, these fibres were found to be relatively consistent. However, in some instances at temperatures of 180 or 190°C the fibres were observed to have a yellow-brown colour: indicating some degradation.

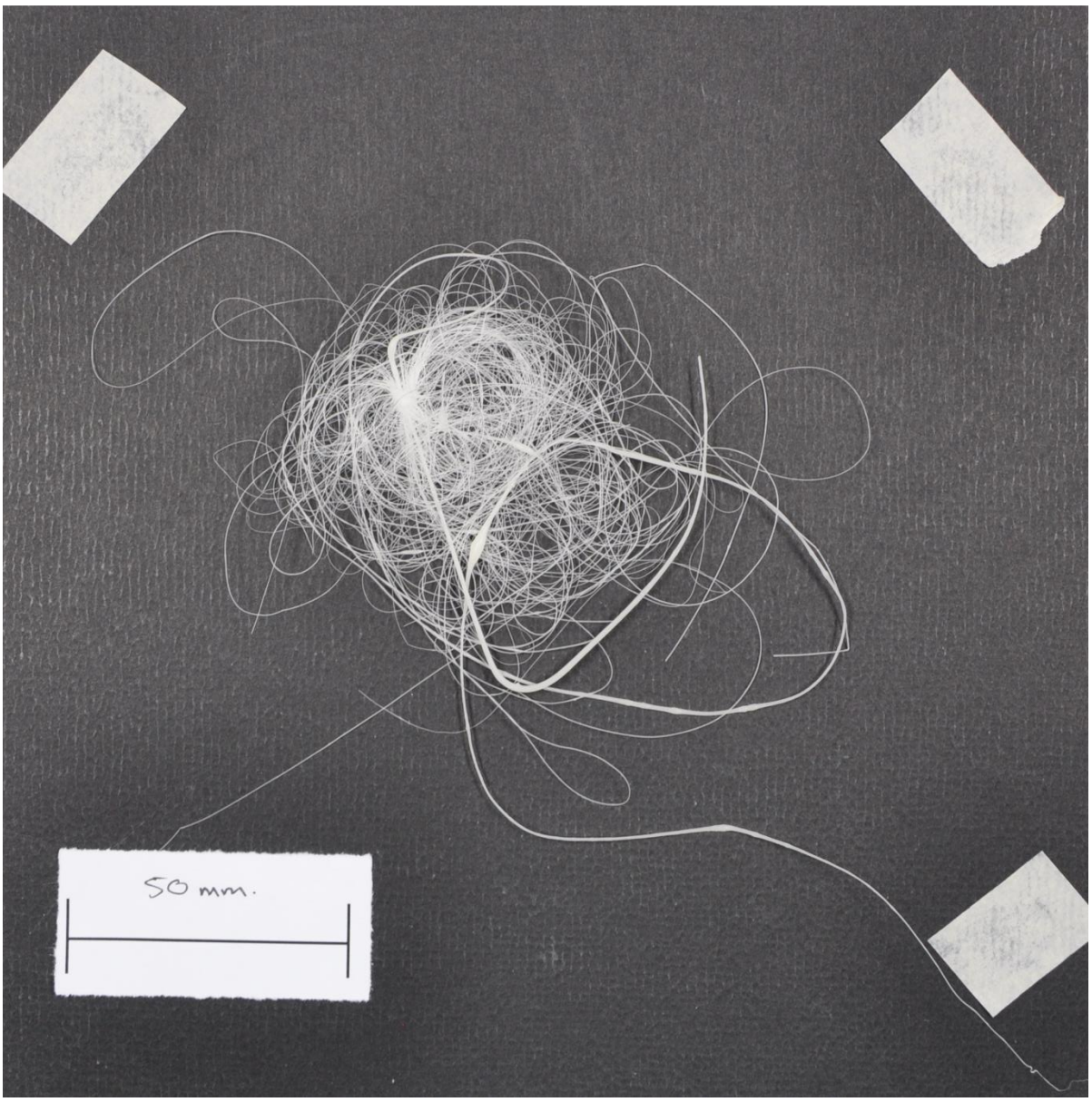

Figure 3: 11 PCL fibre extruded at 80°C. Notice that it is cobweb like in consistency

3.3.2 Processing Challenges

Processing of the various fibre ratios proved to cause a number of processing challenges. These were noted during processing of both PCL control and PCL:PLA hybrid fibres. Fibre degradation was noted during PCL control extrusion, when processed at high temperatures. Further, PCL degradation was observed during hybridisation, at similar temperatures. Finally, the produced PCL:PLA hybrid fibres were of a relatively low quality, which were not suitable for mechanical testing.

3.3.2.1 Degradation during extrusion

During fibre processing, one issue was readily apparent: fibre browning. On its own, the brown/yellow colour of a fibre makes no difference: the fibre colour is not important. However, fibre browning was a visual sign of degradation. Fibres that had degraded were brittle, and unable to elongate. As such, it was determined, that if possible, brown fibres should be avoided. During processing of triplicate repeat PCL 100WT% fibres, no were brown/yellow. However, previous PCL 100WT% fibre processing had displayed fibre yellowing: this indicates the heating was inconsistent. Further, it was observed that the PCL:PLA hybrids fibres exhibited yellowing of the fibres at all tested temperatures (160 – 185°C). As temperature increased, yellowing was increased in hybrid fibres; further, with increased passes, degradation also increased. Degradation of the fibres is clearly a result of the temperature. This phenomenon can explain why additional passes cause more degradation. Essentially, each extrusion of a fibre exposes it to some damaging temperatures: degradation is minimal after the initial extrusion. However, as the fibre is cut and re-extruded, it was exposed to additional damaging temperatures. Each application of the damaging temperature was found to cause exponentially more degradation within the fibres, as such, a 6 pass fibre will be more degraded than a 3 pass fibre (Pospíšil, Horák et al. 1999).

3.3.2.2 Non-Plasticised Hybrid Fibres Processing and Issues

Hybrid fibres proved to be difficult to process using manual melt extrusion and drawing. Typically, the fibres did not have consistent diameters, suffering extreme lows (0.08 mm) or highs (1.50 mm) diameter ranges. Further, during processing, it was observed that the two materials did not melt (or soften) at the same rate. This was expected, as the PCL and PLA possess significantly different processing temperatures. To minimise the temperature difference's effects, multiple passes were required. However, the use of multiple passes caused fibre yellowing during processing. Typically, either 3 or 6 passes were trialled. The overall result of this was inconsistent and highly brittle fibres; essentially, significant degradation had occurred. Interestingly, it was observed during processing that higher PCL hybrids appeared less yellow/brown. PCL:PLA 50:50WT% hybrids were brown in appearance, compared to PCL:PLA 80:20WT% hybrids, which were pale yellow. This phenomenon is the opposite of what would be expected, assuming PCL is the cause of the colour change: if more is present, the effect should be bigger. However, the opposite effect was observed. The PCL powder used was white in colour; as a result, it is possible that this can mitigate the effects of degradation on the colour change. However, this was not investigated further. It was observed that in higher PCL content hybrids, extrusion was more rapid: the molten solution has a lower

viscosity. This increased processing speed meant the materials experienced less of the damaging temperatures; this could explain the observed reduction in degradation.

3.3.3 Effects of Plasticising the Hybrids Fibres

Three separate ratios were attempted (PCL:PLA 70:30, 50:50, 30:70WT%) with the addition of plasticisers (see table 3: 7). This aimed to provide improved processing between the materials. It is essential to note that plasticised fibres were processed at a lower temperature (not significantly) than the previous non-plasticised hybrids. A temperature of 150±5°C was used, as opposed to 160 – 185°C previously. As such, it is possible that the temperature reduction had some effect on fibre processing.

During fibre processing addition of liquid plasticisers disrupted the extrusion process. Two disruptive effects were observed: firstly, the materials suffered minor cooling, slowing extrusion; secondly, the water boiled in the extruder barrel, causing air bubbles in the fibre. Both of these effects were observed in all plasticised fibre during the initial extrusion step. However, these effects were only evident in certain parts of the fibres. In the event that air bubbles formed, they were only spread across about 100 mm of fibre length at a time. Affected areas were not used in any tests. Essentially, these two effects did not alter the results at all; rather, they slowed the process, and caused increased material wastage.

While the extrusion process was slightly more challenging than in non-plasticised fibres, plasticisation significantly improved the quality of the fibres. Further, the second processing step was not subject to the issues of liquid plasticiser. During the second extrusion step, significant improvements to fibre processing were observed, when compared with non-plasticised. The main issue in non-plasticised fibre processing must also be considered: thermal degradation. Across all plasticised fibres, thermal degradation was not apparent. This was considered a significant improvement in the processing method: the fibres were not brittle when plasticised.

Several factors were observed with plasticised fibre. A large number of the plasticised fibres presented a reflective surface: this was absent in all previous hybrids. Typically, plasticised fibres presented a comparatively smooth surface. The presence of a smooth surface is indicative of a more homogeneous blend – lumps are a sign of blend issues. Interestingly, several plasticised fibres had incredibly smooth surfaces: slippery to the touch. In instances where a slippery surface is present, these fibres were of a very high quality. Three sets of fibres presented this effect: a PCL:PLA 70:30WT% fibre plasticised with 10% glycerol after 2 passes, and two PCL 100WT% fibres, plasticised with 10% and 20% PEG-200.

3.5 Summary

Overall, it was noted that thermal degradation was occurring in many of the fibres. This was almost exclusively observed in the non-plasticised hybrid fibres. Both the temperature and number of processing passes was important factors in producing this effect. This suggested that a lower temperature, with less processing passes was required. The addition of plasticisers and the slight processing temperature reduction were found to significantly improve the quality of the fibres.

Based on ease of processing, the best fibres were found to be those containing plasticisers. Overall, the best fibres were determined to be the PCL:PLA 30:70WT% fibres, plasticised with PEG-200. In terms of physical appearance and processing ease, there was no observable difference with plasticiser concentration (5, 10 or 20%).

Chapter 4 Mechanical Testing

4.1 Introduction

The mechanical properties of polymeric hybrids fibres are important to identify. This will allow determination of fibre quality – lower quality fibres show reduced mechanical properties. Initially, two pilot studies were carried out on the materials. The first pilot dealt with the SSE 1 mm fibres (section 3.2.2), the second with lower diameter drawn fibres using the screwless extruder (section 3.2.3). Out of all the properties investigated, the tensile properties are the most vital. The tensile properties are a deciding factor in the quality of the produced fibres. Typically, hybrid fibres that present significantly reduced mechanical properties, when compared to their components, are of very low quality (Pospíšil, Horák et al. 1999). As such, the tensile properties of the produced fibres inform the rest of the project.

4.2 Materials and Methods

Two pilot studies into the tensile testing methods were required. Initially, the 1 mm diameter fibres produced in section 3.2.2 were used. The initial study aimed to demonstrate that the fibre could be tested. However, due to failings with the 1 mm fibre processing, a second pilot test was required. The second pilot study employed the drawn fibres from section 3.2.3. The results from the second pilot study were used to inform the remainder of the testing within this section.

4.2.1 Materials

Across all testing, a polyamide fishing line control fibre was used. The purpose of this was to act as a blank, demonstrating that the machine was acting in a consistent way across all tests. The particular line used was a 6 ¼ lb force green Platypus Classics product.

Prior to any mechanical testing taking place, all samples underwent conditioning. The purpose is this step is to ensure that the materials are all at equilibrium with the environment and improves repeatability. Realistically, due to the nature of testing, a temperature of 23±1°C and humidity of 50±5RH% should have been used (European Committee for Standization 1997). However, the conditioning space is primarily used for textile fibres, which require different conditions. As such, 20±2°C and 65±2RH% were used (International Organization for Standardization 2005).The difference between these conditions is unlikely to have any significant effects. In all cases, the samples were allowed a minimum of 48 hours to condition. It has been reported that after 24 hours, the fibres will have reached equilibrium at these conditions (Ghosh, Ali et al. 2010, Ghosh, Ali et al. 2010) . The conditions of the room were able to be monitored using an Elsec 765C UV+ data logger. This data logger was able to measure both the ambient temperature and the humidity of the room. The temperature was provided with an error of ±0.5°C; and an error of 3.5%RH for humidity, as per the item datasheet.

An Instron 4464 Universal Tester was used for the majority of testing. The Instron machine was located in the conditioned space. This particular Instron machine has a maximum load capacity of 2000 N, and a speed range of 0.05 – 2500 mm/min as reported on the Instron 4464 datasheet. Further, the load accuracy is either, 0.5%, or ±1 N, whichever is higher. Fibres were clamped in place using flat plate grips. The maximum test range on this machine is 1192 mm: excluding the grips. A torque wrench set to 10N/m was used to ensure adequate grip strength for the control specimens. A 100 N load cell was fitted to the Instron 4464 Universal Tester for all testing. A 16 channel ADInstruments Power Lab was connected to the Instron 4464 tester. Across all mechanical testing, the Power Lab setup was the same.

4.2.2 Pilot Study 1: 1 mm Fibres

Fibres processed using the SSE machine undergo tensile testing within this section. Refer to section 3.2.2 for details on how these fibres were produced.

4.2.2.1 Method

Two separate methods were attempted to identify the tensile properties of the 1 mm SSE fibres. Initially, the fibres were placed centrally within the flat plate grips of the Instron 4464 machine. A torque wrench was used to tighten the grips with 10 N/m of torque.

A second pilot method was employed, due to failings in the first. The second pilot method involved attaching materials to the flat plate grips: paper, corrugated cardboard, nitrile gloves, and sandpaper – all independently of each other. In all cases, the flat plate grips were first coated in double-sided cellotape, and the materials were attached. All materials were trimmed to size after grip attachment: ensuring maximum coverage. The materials essentially acted as the new grip faces. All testing was done using single fibres centralised on the grip. A torque wrench set to 10 N/m or torques was employed to tighten the grips.

4.2.2.2 Results and Discussion

Initial tensile testing experiments on the Instron 4464 machine were found to consistently fail. It was identified that in approximately 95% of testing carried out, the fibre would be pulled from the grip: a null result. Typically, a test specimen is pulled from the grip when the exerted grip force is too low. It was decided that the flat plate grips could not exert the required friction on the samples: the grip surfaces were smooth. A new surface was applied to the grips hoping to improve the exerted friction. Of the four new surfaces trialled, only one was found to offer any benefit: the sandpaper. The addition of the sandpaper allowed successful testing to be carried out. However, a serious flaw was identified in this remedial action: the sandpaper surface quickly wore away. Essentially, the sandpaper was only ‘textured’ for five test runs. After five runs, the surface of the sandpaper was entirely removed, exposing the paper underneath. This resulted in the sandpaper requiring changing every five tests. The sandpaper lost a percentage of its coating after each test, as such, lower friction would be applied on each subsequent test. It was decided that this would significantly impact the reliability of the results. The other three materials (paper, cardboard, and nitrile gloves) were found to

increase fibre slippage. Essentially, these were worse than the bare grip surfaces. The corrugated cardboard created a secondary issue: the lumps from the compressed corrugation prevented correct tightening of the grips. The corrugated cardboard essentially prevented fibre gripping altogether.

4.2.3 Pilot Study 2: Drawn Fibres

The drawn fibre pilot investigates if the drawn fibres (produced in section 3.2.3) could be successfully tested. Further, a remedy to the issues found in section 4.2.2 was investigated.

4.2.3.1 Method

Three sets of methods were trialled to test drawn fibres produced in section 3.2.3. Initially, the Instron 4464 Universal Testing machine was employed. All initial testing was done using the bare flat plate grips. Secondary testing was done with the addition of new surfaces to the grips (paper, corrugated cardboard, nitrile gloves and sandpaper). The first test method was carried out using the same methods as described for the 1 mm diameter pilot (4.2.2.1).

Due to the previously mentioned tests not performing correctly, the method was adapted. The drawn fibres were cellotaped and/or glued to a fibre mount. Once attached, the fibres were tested on the Instron 4464 machine using the flat plate grips. The grips were trialled as tightened using a torque wrench (10 N/m), and as finger tight.

4.2.3.2 Results and Discussion

The first phase of tensile testing with drawn fibres used the same method as the 1 mm pilot (section 4.2.2). Initially, individual drawn fibres were tested: the grips could not physically restrain the fibres. Due to the very low diameter of the fibres, it was determine the grips were unsuitable as they were. The addition of new surface materials was attempted, but no improvement was noted. Unlike the 1 mm pilot, sandpaper provided no benefit – the fibre diameter was far too narrow.

However, it was clear the grips themselves were unsuitable but no other grips were available. As such, a system of mounting single fibres on card was devised. A single fibre would be cellotaped to the mount, and allowed to condition. Three methods of attaching the fibre to the mount were attempted: a single layer of cellotape over the fibre; a strip of double sided cellotape between the mount and fibre, with a layer of single sided over the top; and, two mounts attached to each other with double sided cellotape. Images of the three mounts are found in figure 4: 1 – 3. All three methods proved to be equally effective; however, the fibre was able to elongate into the grips: the cellotape could not exert enough force. To remedy this, the fibres were instead glued to the mount (further details can be found in section 4.2.3).

Results from the drawn fibre pilot study are located in table 4: 1. A summary of reported tensile properties can be found in table 2: 1 for both PCL and PLA 100WT%. It can be noted that the values stated within the literature (table 2: 1) vary from those determined within this pilot test. In all cases, the achieved tensile strength values are not the same as the literary values; further, in all but one case, the Young's Modulus achieved are out of range of the literary values (PLA at 200°C is within range). The tensile properties of PCL:PLA 50:50WT% hybrid fibres have been reported previously (Zhao and Zhao 2016). It has been stated that these fibres have a tensile strength of 30±2 MPa, a Young's modulus of 800 MPa and 600±50% elongation at break (Zhao and Zhao 2016). For the most part, the elongation at break values of PCL and PLA 100WT% control fibres are within range. PCL:PLA (50:50WT%) hybrid fibres however, are a factor of 100 out. It is important to note that some variation between the literary values and experimental ones will be present: in no case do the literary values test fibres; rather, sheets are used.

4.2.3.3 Pilot Study Conclusions and Implications

Overall, the pilot studies proved to be useful. It was demonstrated early on that the Instron flat plate grips were not suitable for direct contact with the fibres. Ultimately, the pilot studies were able to demonstrate that a simple fibre mount can enable significant improvements in tensile testing. The use of the mount meant the test behaved in a suitable way: little to no inappropriate elongation and fibres broke within the gauge length.

The primary result of these pilot studies was fibre mount development. The fibre mount was used for the remainder of the tensile property investigation.

Table 4: 1 Mechanical Properties of PCL, PLA and PCL:PLA (50:50WT%) Hybrid Fibres.

Material	Temperature (°C)	Pass	Tensile Strength (MPa)	Yield Strength (MPa)	Young's Modulus (MPa)	**Graph Strain (%)**	**Max Strain (%)**
PCL	75	1	19.66±1.6	19.66±1.6	411.30±66.1	274.14	492.64±301.0
	80	1	50.07±7.9	28.39±4.3	708.80±72.3	575.37	657.28±64.4
	85	1	36.03±1.7	20.26±2.4	195.19±31.4	848.71	686.36±11.6
PLA	160	1	25.60±2.2	NA	1371.41±226.0	4.99	7.76±2.1
	170	1	39.40±5.5	NA	596.40±67.1	7.21	13.40±4.9
	180	1	37.72±11.1	NA	1211.74±204.1	8.53	15.87±5.3
	190	1	36.26±5.7	NA	2347.33±140.5	2.17	3.14±0.9
	200	1	27.89±8.3	NA	1511.41±92.9	4.78	5.49±0.5
	210	1	25.94±1.7	NA	2444.44±372.1	1.31	2.98±2.2
PCL:PLA 50:50WT%	160	3	51.95±17.0	NA	4814.55±1360.1	1.62	2.69±1.1
	170	3	32.78±4.8	NA	1107.69±156.3	4.74	5.85±0.8
	180	3	35.00±16.7	NA	2557.61±1713.8	1.85	4.08±1.7
	160	6	24.87±1.7	NA	1089.98±12.2	3.26	3.41±0.1
	170	6	24.95±9.7	NA	1981.93±943.1	1.77	2.65±0.6
	180	6	32.41±2.8	NA	1166.29±64.4	4.87	4.91±0.0

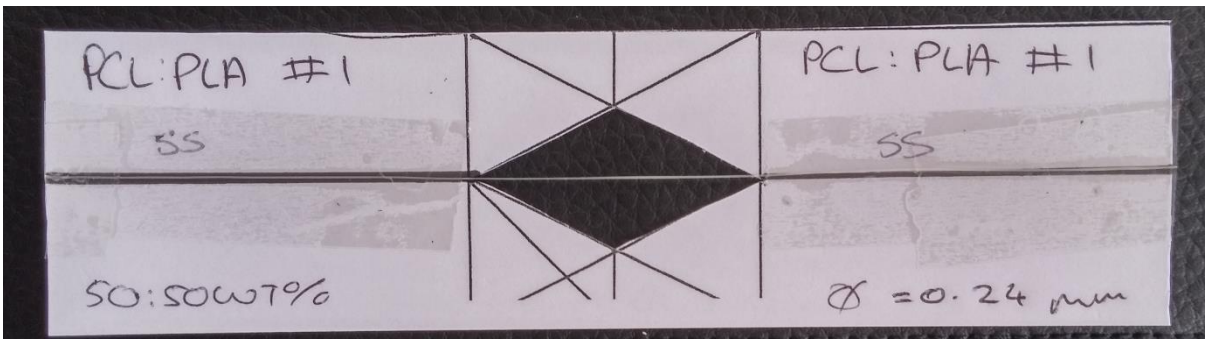

Figure 4: 1 First iteration mount. A paper mount with single sided cellulose tape attachment.

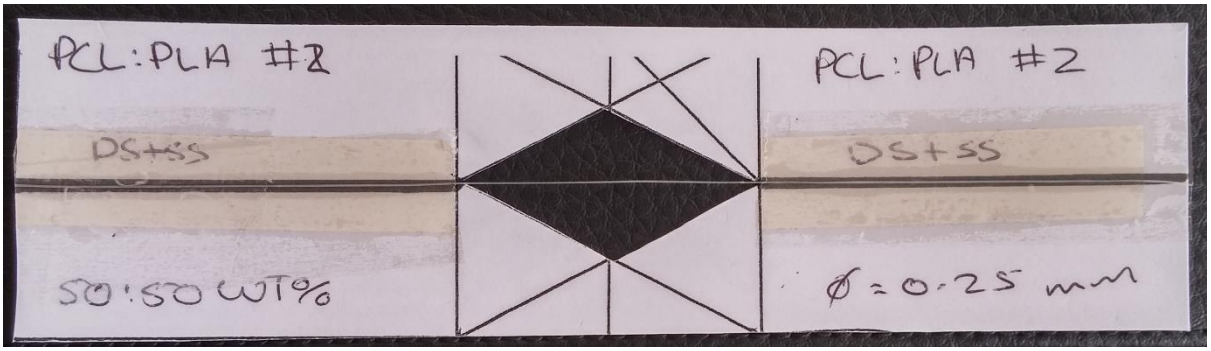

Figure 4: 2 First iteration mount. A paper mount with single sided and double-sided cellulose tape attachment.

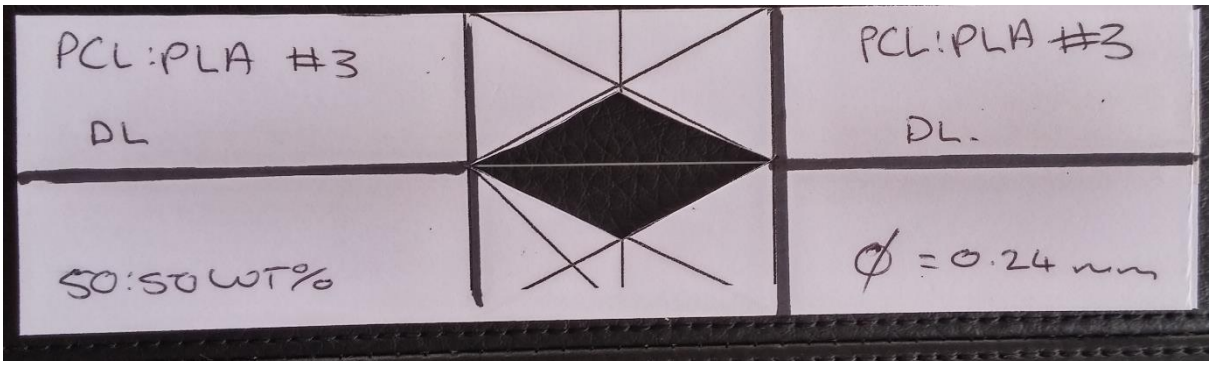

Figure 4: 3 First iteration mount. Two stacked paper mounts, with double-sided cellulose tape attachments on both mounts.

4.2.4 Fibre Mounts

Several iterations of mount design were developed (Ilankeeran, Mohite et al. 2012). Over the course of this work, two materials were used for the mounts: initially, light cardboard (figure 4: 4); ending with paper (figure 4: 5). It was established that the difference between the two materials did not affect the results. All mounts used retained the same markings, and the gauge length remained constant at 40±1 mm. A slight variation was observed in the gauge length of the mount; this was solely due to removal of the rectangle (see figures 4: 4 and 5) and was not found to alter the results.

The method for attaching fibres to the mounts was straightforward. Initially, both the fibre and the mount were attached to a solid surface. Fibres were attached above the fibre line (see figures 4: 4 and 5). This ensured that over the gluing process, neither the mount nor the fibre would move. Once secure, the fibres were glued to the mounts (figures 4: 4 and 5). To ensure even gluing, only one side of the fibre was glued at a time. To ensure adequate drying, the glue was left for 24 hours between each step. Once gluing was complete, fibres were sent to condition prior to testing.

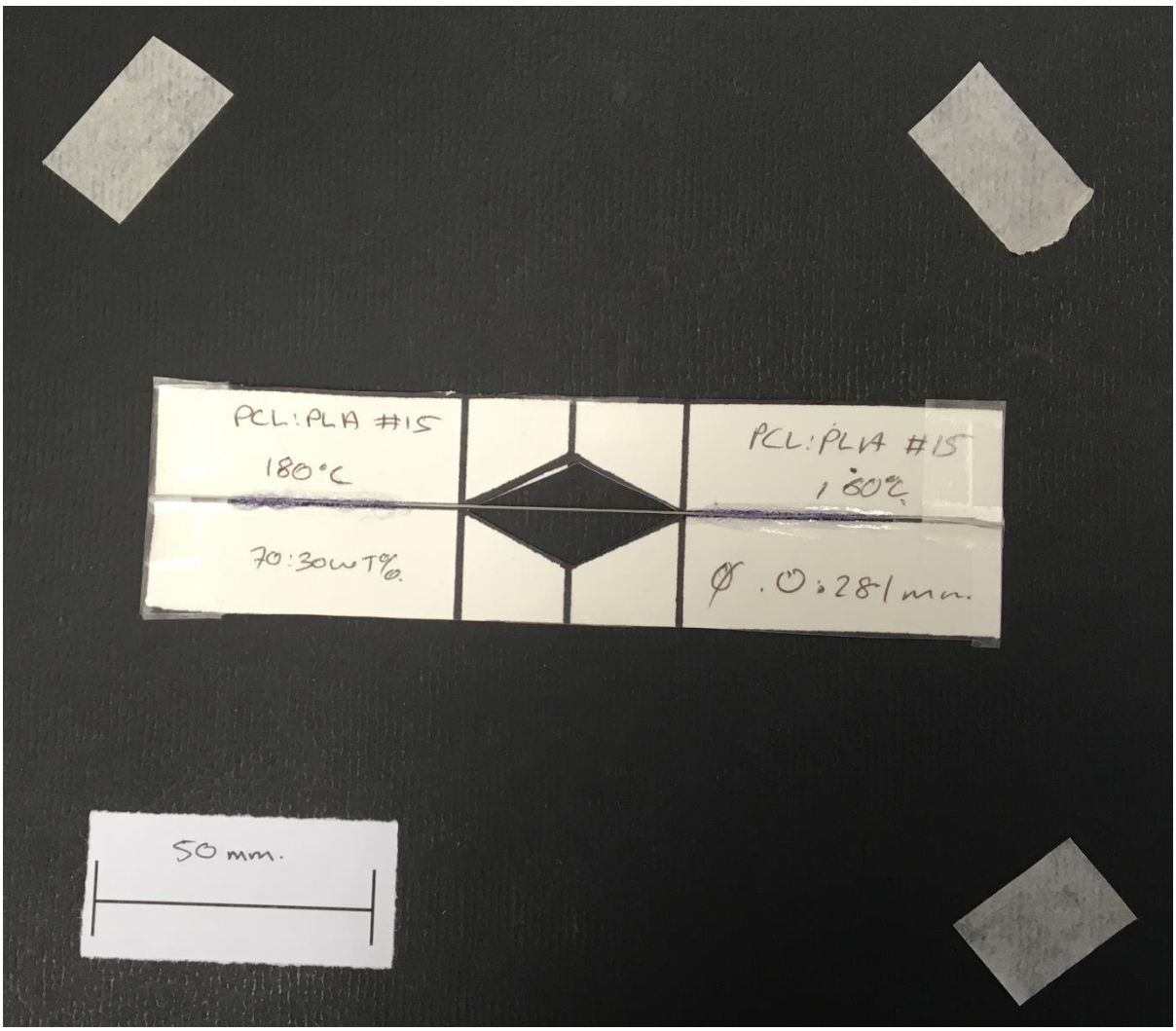

Figure 4: 4 Example of the initial white cardboard mounts. This has the dimensions 145±5x40±5 mm (LxW). The gauge length is 40±2 mm. The fibre is glued along the black centre line.

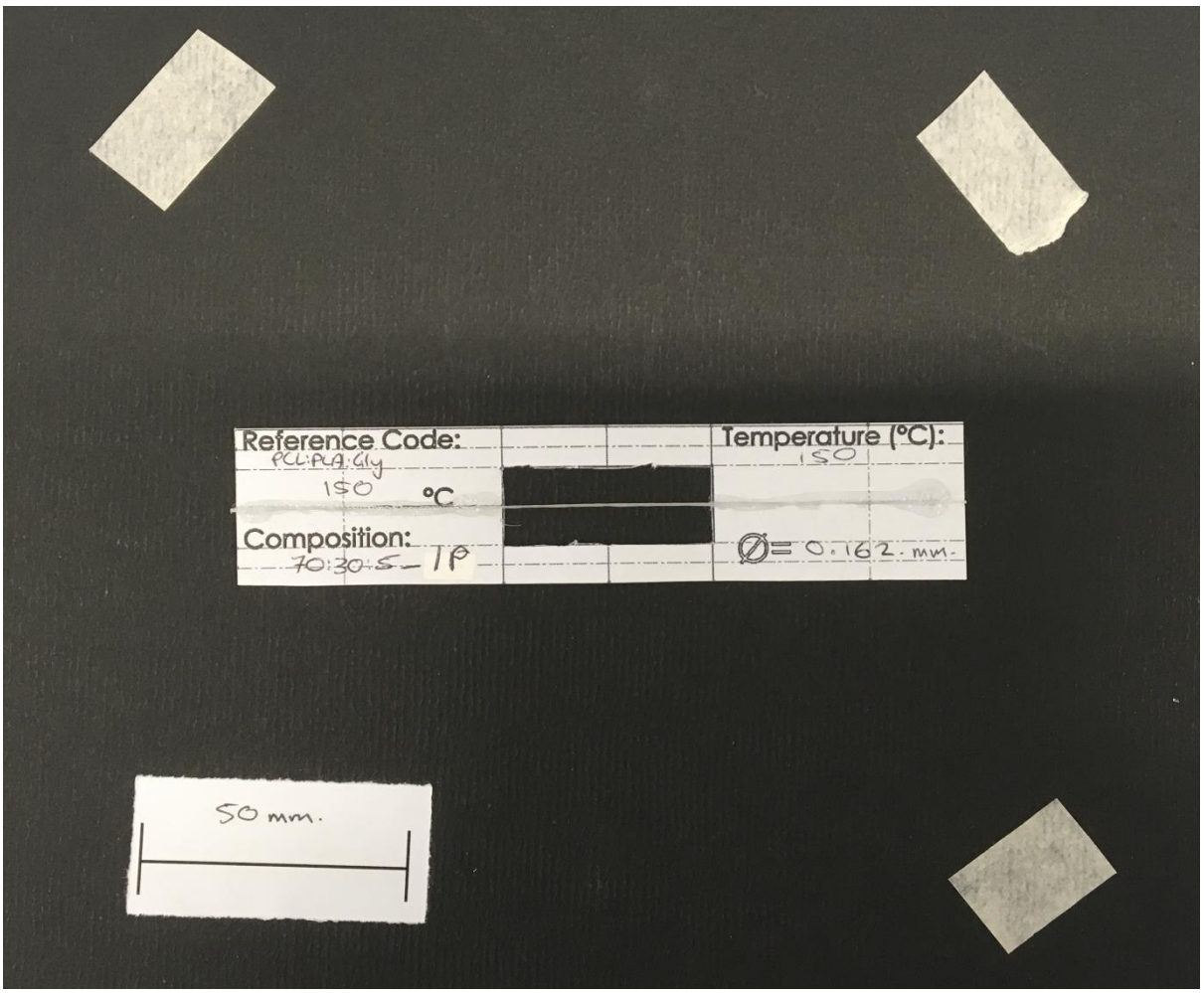

Figure 4: 5 Example of the final white paper mounts. This has the dimensions 140±5x30±5 mm (LxW). The gauge length is 40±2 mm. The fibre is glued along the black centre line

4.2.5 Mechanical Testing

Across all mechanical test steps, the set up was the same. The Instron 4464 Universal Tester was fitted with a 100 N load cell, and a cross-head speed of 20 mm/min was used . All specimens used a 40 mm gauge length. The Instron 4464 flat plate grips were used in all tests (excluding pilot studies); the grips had the centre point marked on the base of the grips. All fibre mounts were loaded into the grips ensuring the fibre itself was coincident with the centre point marks. With fibre testing, the torque wrench was unusable – it cut the fibres. As such, the grips were set to finger tight. Unlike the fibre test specimens, the fishing line blanks required the use of a torque wrench, exerting 10 N/m of torque.

4.2.6 Statistical Analysis

Statistical analysis was carried out on a number of parameters. R studio was used for all statistical analysis reported. However, prior to analysis, several additional R studio packages were required. The four required packages were as follows: nlme, lsmeans, car and estimability. These packages allowed for a variety of useful testing to take place. The first step in the process was to define the independent factors: processing temperature (Temp), PCL and PLA content, number of passes (Pass), plasticiser concentration (Conc), and plasticiser type (Plast); and the dependent factors: tensile strength (TS), Young's modulus (YM) and elongation at break (EB). Refer to Appendix B (part 1) for the scripts required in R studio, and the outputs these gave. Three analyses took place: generalised least squares (GLS), least square means (LSM) and ANOVA type 3. GLS testing was processed using restricted maximum likelihood (REML) methods. The results from GLS testing are not reported. Rather, the GLS test methods were used to calculate both the LSM and ANOVA type 3 results. LSM methods determine the pairwise comparisons between two or more factors; the comparisons employed here are found in Appendix B (part 1). The complete outputs from the scripts are found in Appendix B (part 2), with the data used located in Appendix B (part 3). Intercept values are not provided. These indicate the likelihood of the mean being zero. A zero value is not realistic for any tensile properties in these polymeric fibres.

Statistical analysis could not be carried out on the yield strength values. The large number of missing values means the analysis is meaningless. Methods not employed here could have been trialled, such as a binary analysis. However, this method will not return meaningful results: too many sets have complete presence or absence. In this event, the output is meaningless.

4.3 Results

The initial part of the results looks at determining the best processing temperature for the fibres. That is to say, the temperature where the results are the most consistent with each other, and table 2: 2 displaying the literature values for PCL and PLA. It was vital that this started with the control materials. This provided conformation that the control materials could be processed at the desired temperatures. Hybrid fibres were trialled at a variety of temperatures. The aim was to determine what temperature would produce the most consistent mechanical properties. The initial hybrids produced did not contain plasticisers, as

such, they provided a point of comparison for the plasticised hybrids. Further work was done to analyse whether or not hybrid plasticisation improved the mechanical properties of the fibres, when compared to the non-plasticised variants. A large number of stress-strain curves have been produced. However, the curves are not reported. The stress-strain curves can be found Appendix C.

4.3.1 Ideal Processing Properties

During mechanical testing, it is essential to use the highest quality fibres. To this end, an investigation into how the virgin control fibres behave across a variety of temperatures (160 – 190°C) must be carried out. The ideal processing temperature is directly related to a fibre's mechanical properties. Ideally, a minimal variation in mechanical properties will be observed at the fibre's processing temperature. To determine the ideal fibre processing temperature, only PCL and PLA fibres were studied. A particular emphasis was placed on a loss in elongation characteristics. Ideally, the optimal fibre processing temperature will produce the highest and most consistent elongation at break (table 2: 4). The fibre processing temperature identified as optimum that was used for plasticised hybrid fibres.

Across the PCL 100WT% fibres, several temperature dependent trends were identified. A near complete loss in average yield strength was observed, as temperature increases (table 4: 2). At both 160° and 170°C, yield points were observed; however, 180°C shows no yield points (table 4: 2). A single fibre set displayed a yield point when processed at 190°C: set 1 (table 4: 2). Across the range of temperatures, no trends were observed in average tensile strength or Young's modulus (table 4: 2). Average elongation at break displayed a decrease, in respect to increasing temperature (table 4: 2). Based on the information available in table 4: 2, it appears PCL fibre set 1, at 190°C has a significantly higher elongation at break than the other two sets. With an average of 1101.9% elongation at break, fibre set 1 at 190°C is 120 times the average value for set 2, and near 300 times the value for set 3. This is indicative of an outlier; however, this was a real result, so it is retained. Statistically, no variations in raw tensile strength values were observed (table 4: 3). However, raw values for both Young's modulus and elongation at break produced a temperature dependent change (table 4: 3).

PLA 100WT% fibres displayed a completely different result. The yield strength of PLA fibres is observed in all cases at 160°C; however, this is reduced to 2 sets at 170° and 180°C, with only 1 present at 190°C (table 4: 4). Average tensile strength does not show any variations in response to processing temperature (table 4: 4). The average Young's modulus shows a slight increase as processing temperature increases (table 4: 4). Average elongation at break is reduced in response to increasing processing temperature (table 4: 4). Based on the statistical analysis, no temperature effects were observed in PLA 100WT% fibres (table 4: 5).

Based on the mechanical properties identified for both PCL 100WT and PLA 100WT% fibres, the optimal processing temperature is 160°C. PCL produces the most consistent elongation at break values at 160°C. The ideal processing temperature for PLA fibres could not be identified from the results. PLA showed no change in mechanical properties in respect to temperature.

The most apparent trend identified with the non-plasticised hybrid fibres is the lack of yield points for all fibres (table 4: 6). Average tensile strength and elongation at break measures were consistent across all hybrid fibres and processing temperatures (table 4: 6). The material ratio (PCL:PLA) effects the average Young's modulus (table 4: 6). As PCL content of the ratio increases, Young's modulus decreases (table 4: 6). Neither processing temperature nor number of passes effects any of the average properties (table 4: 6). Statistical analysis of raw data suggests that Young's modulus changes, dependent on the conditions (table 4: 7). However, it must be noted that Young's modulus is significantly affected by material ratio (table 4: 7). Neither temperature nor passes display any significant effects on the raw values (table 4: 7). The exception to this is the raw elongation at break values; the number of passes applied alters the mean (table 4: 7). In no cases do the raw values for tensile strength change, this is essentially independent of the processing properties (table 4: 7). Further testing using an ANOVA type 3 analysis provided no evidence to support any temperature dependant affects (table 4: 8). The sole statistically significant effect observed was that of the PCL:PLA ratio on Young's modulus (table 4: 8).

Table 4: 2 Mechanical properties for PCL 100WT%.

Temperature (°C)	Number	Tensile Strength (MPa)	Yield Strength (MPa)	Young's Modulus (MPa)	Graph Strain (%)	Max Strain (%)
160	*1*	21.2±1	19.7±3	488.3±2	494.47	532.4±45
	2	15.3±1	15.3±1	462.2±6	425.38	533.1±80
	3	18.1±2	18.1±2	407.7±19	525.47	538.6±14
170	*1*	18.6±1	17.7±2	472.1±13	404.92	479.8±85
	2	14.6±5	12.3±2	526.4±21	7.50	60.0±70
	3	20.0±5	18.2±3	463.4±58	575.37	814.7±295
180	*1*	18.0±1	*None*	528.4±51	5.92	7.7±2
	2	16.4±2	*None*	470.8±52	3.88	6.8±2
	3	22.5±0.3	*None*	497.3±10	6.72	9.0±2
190	*1*	31.9±5	23.2±4	579.7±61	863.56	1101.9±332
	2	20.9±2	*None*	453.2±9	7.92	9.2±2
	3	13.0±2	*None*	450.4±58	3.02	3.8±0.5

Table 4: 3 Statistical Analysis on PCL. Significant values are underlined and italicised. Factor of Significance 0.05. Rounded to 4 D.P.

	Methods						
	LSMEANS						**ANOVA**
	Contrasts						
Property	160-170	160-180	160-190	170-180	170-190	180-190	Temperature
Tensile Strength	0.8789	0.9640	0.2208	0.9936	0.6193	0.4651	0.2498
Young's Modulus	0.9675	0.0735	0.1157	0.2007	0.2798	0.9991	*0.0202*
Elongation at Break	0.9975	*0.0315*	0.9808	0.0571	0.9975	0.1017	*0.0131*

Table 4: 4 Mechanical properties for PLA 100WT%.

Temperature (°C)	Number	Tensile Strength (MPa)	Yield Strength (MPa)	Young's Modulus (MPa)	Graph Strain (%)	Max Strain (%)
160	*1*	29.6±5	29.6±5	1954.6±21	9.35	35.5±40
	2	49.7±10	49.7±18	2296.6±274	4.02	30.6±34
	3	20.5±4	20.5±4	1431.0±295	6.72	95.5±123
170	*1*	31.3±11	31.3±11	2399.0±375	3.14	4.1±0.9
	2	35.8±3	*None*	2280.4±276	2.84	4.7±2
	3	35.6±11	35.6±11	2263.4±448	11.41	23.4±11
180	*1*	34.94±14	*None*	2281.5±106	3.21	5.6±2
	2	33.08±0.7	33.08±0.7	2294±122	2.91	3.7±0.5
	3	26.98±3	26.98±3	1923.1±130	5.37	8.5±3
190	*1*	23.82±3	*None*	2339.4±398	1.33	2.6±1
	2	24.52±8	23.38±2	2685.5±66	1.58	3.7±2
	3	30.58±10	*None*	2604.3±248	2.14	3.1±0.7

Table 4: 5 Statistical Analysis on PLA. Significant values are underlined and italicised. Factor of Significance 0.05. Rounded to 4 D.P.

	Methods						
	LSMEANS Contrasts						**ANOVA**
Property	160-170	160-180	160-190	170-180	170-190	180-190	Temperature
Tensile Strength	0.5954	0.9901	0.2094	0.7592	0.8829	0.3187	0.1602
Young's Modulus	0.9849	0.7212	0.3297	0.8877	0.5047	0.9092	0.3081
Elongation at Break	0.0890	0.0740	*0.0459*	0.9997	0.9942	0.9985	*0.0216*

Table 4: 6 Mechanical properties of Non-plasticised PCL:PLA Hybrids

Ratio (WT%)	Temperature (°C)	Pass	Tensile Strength (MPa)	Yield Strength (MPa)	Young's Modulus (MPa)	Graph Strain (%)	Max Strain (%)
50:50	160	2	7.58±1.8	NA	761.85±331.3	1.10	2.40±1.2
	160	3	11.10±0.45	NA	910.57±18.6	1.36	2.26±0.7
	170	2	6.16±1.3	NA	1239.15±275.9	0.62	1.81±0.9
	170	3	15.99±2.54	NA	954.40±146.8	3.18	3.38±0.2
	180	2	16.88±6.0	NA	1189.44±10.8	2.57	2.25±0.6
	180	3	14.06±0.4	NA	901.30±16.1	3.47	3.61±0.1
60:40	160	2	9.82±2.6	NA	718.89±241.9	2.12	2.61±0.4
	160	3	14.08±1.2	NA	1020.11±130.1	3.28	3.73±0.4
	170	2	10.09±3.2	NA	714.66±29.2	1.90	3.07±0.8
	170	3	6.65±0.4	NA	948.86±20.5	0.82	3.40±1.9
	180	2	16.34±0.3	NA	873.58±158.7	3.87	4.19±0.2
	180	3	15.09±2.3	NA	974.42±167.0	2.94	4.04±1.0
70:30	160	2	16.67±1.2	NA	946.41±11.66	2.64	3.18±0.5
	160	3	17.06±6.7	NA	798.75±101.5	4.87	5.32±0.3
	170	2	7.02±3.1	NA	492.33±229.9	1.94	2.64±0.5
	170	3	10.87±0.5	NA	683.39±43.1	2.27	4.05±1.5
	180	2	9.60±1.3	NA	658.30±23.0	1.86	2.34±0.6
	180	3	11.46±2.1	NA	751.71±9.9	2.37	2.72±0.3
80:20	160	2	12.65±1.0	NA	676.63±108.8	3.00	3.57±0.4
	160	3	15.24±1.1	NA	599.62±145.7	3.77	4.81±0.8
	170	2	15.90±2.0	NA	702.96±34.2	5.62	5.73±0.1
	170	3	13.02±1.7	NA	611.05±150.7	4.27	4.87±0.7
	180	2	14.49±2.1	NA	539.29±85.3	3.59	4.22±0.8
	180	3	15.01±0.9	NA	636.35±36.4	3.57	5.36±1.6

Table 4: 7 LSMEANs Analysis on Non-plasticised Hybrid Fibres. Significant values are underlined and italicised. Factor of Significance 0.05. Rounded to 4 D.P.

	Ratio	**50:50WT%**		**60:40WT%**		**70:30WT%**		**80:20WT%**	
Property	*Contrasts*	**2**	**3**	**2**	**3**	**2**	**3**	**2**	**3**
Tensile Strength	*160-170*	0.8971	0.9612	0.8061	0.9256	*0.0012*	0.5409	0.6010	0.9417
	160-180	0.2819	0.8854	0.5173	0.8927	*0.0268*	0.2098	0.9701	0.8170
	170-180	0.1272	0.7419	0.8832	0.6869	0.5082	0.7923	0.4580	0.9587
Young's Modulus	*160-170*	0.9744	0.7028	0.6773	*0.0329*	*0.0001*	0.6731	0.9736	0.9953
	160-180	0.9216	*0.218*	0.6463	*0.0368*	0.0987	0.7751	0.5104	0.9914
	170-180	0.8196	0.1338	0.9986	0.9988	0.0543	0.2845	0.6471	0.9744
Elongation at Break	*160-170*	0.8075	0.4200	0.8517	0.9595	0.8631	0.3484	*0.0264*	0.5466
	160-180	0.6652	0.2981	0.2807	0.8847	0.6153	*0.0168*	0.7236	0.1957
	170-180	0.3053	0.9698	0.5796	0.7373	0.9048	0.3181	0.1454	0.7643

Table 4: 8 ANOVA type 3 Analysis on Non-plasticised Hybrid Fibres. Significant values are underlined and italicised. Factor of Significance 0.05. Rounded to 4 D.P.

Property	**Temperature**	**Ratio**	**Passes**	**Temperature:Ratio:Passes**
Tensile Strength	0.1145	0.2557	0.4700	0.2023
Young's Modulus	0.8303	*0.0033*	0.6578	*0.0138*
Elongation at Break	0.3270	0.5431	0.8820	0.2783

4.3.2 Effect of Plasticisation

Based on the results determined results in section 4.3.2, plasticised hybrids were produced.

4.3.2.1 Plasticised Control Fibres

Across the plasticised PCL 100WT% fibres, very little variation is observed in the average mechanical properties (table 4: 9). All plasticised PCL 100WT% fibres underwent yielding (table 4: 9). Average tensile strength and Young's modulus values were near constant across the data (table 4: 9). However, the average elongation at break displayed plasticiser dependent changes (table 4: 9). When glycerol plasticiser was used, a 20% solution concentration produced a lower elongation than 5 or 10% (table 4: 9). Conversely, when PEG-200 plasticiser was used, the lowest elongation resulted from a 5% solution concentration (table 4: 9). Statistical analysis of the raw data produced results not in keeping with the averages. Statistically, the plasticiser type and concentration were both, individually and cumulatively, found to effect the results (table 4: 10). However, Young's modulus showed no statistically significant effects as a result of any factors (table 4: 10). The lack of any statistical effects on Young's modulus was supported in table 4: 11; no differences were observed between the two plasticises, or their concentrations. The raw values from tensile strength displayed, at 5% concentration, a difference between glycerol and PEG-200 plasticiser types (tables 4: 11 and 12). Elongation at break produced a useful result. A comparison between glycerol and PEG-200 as plasticisers demonstrated no difference at 10%; however, both 5 and 20% plasticiser concentrations produced a difference as a result of plasticiser type (table 4: 11). This was supported when comparing the plasticiser concentrations independently. PEG-200 plasticised fibres showed difference between 5 and 10% and 5 and 20% (table 4: 12). However, no difference was observed between the raw elongation at break attributable to 10 and 20% PEG-200 plasticisers (table 4: 12). This means that a 5% PEG-200 loading is all that is required in PCL 100WT% fibres. Conversely, glycerol plasticisation demonstrated that 5 and 10% loadings were the same; the difference was between 5 and 20%, and 10 and 20% (table 4: 12). This would suggest a minimum of 10% glycerol loading is required in PCL 100WT% fibres.

The average values for plasticised PLA 100WT% fibres showed large variations in the tested mechanical properties (table 4: 13). Only five of the six PLA 100WT% plasticised fibres produced a yield point: a 5% loading of glycerol plasticiser did not yield (table 4: 13). For the most part, the average Young's modulus values are similar across all fibres (table 4: 13). The non-yielding 5% glycerol loaded PLA 100WT% fibre shows a substantially increased Young's modulus, approximately 1500 MPa higher than the next highest (table 4: 13). The average tensile strength values produced different values dependent on both plasticiser type and concentration (table 4: 13). When glycerol plasticised, PLA 100WT% fibres produced three seemingly distinct tensile strengths, with the highest at 5% glycerol (table 4: 13). Conversely, PEG-200 plasticised fibres produced a high average tensile strength at both 5 or 10% loadings; with a 20% loading halving the tensile strength (table 4: 13). In both glycerol and PEG-200 plasticised PLA 100WT% fibres, three distinct averages for elongation at break were observed. When glycerol plasticised, a 20% solution concentration produced the highest elongation at break, however, only 10% was required for PEG-200 plasticised fibres to reach their peak (table 4: 13). Statistical analysis of the raw data for both tensile strength and elongation at break supported these observations (table 4: 14). It must be noted however that

Young's modulus reported significant variations as a result to both and individual and cumulative effect of plasticiser type and concentration (table 4: 14). Based on tables 4: 15 and 16, it appears that the sole reason for the reported variations in Young's modulus is the 5% glycerol plasticised PLA 100WT% fibre: this is the only significant interaction identified.

4.3.2.2 Plasticised Hybrid Fibres

Two factors are considered with plasticised hybrid fibres. Firstly, the effect of PCL:PLA ratio on the mechanical properties, at a constant plasticiser value. Secondly, the effect of plasticiser concentration on the properties, assuming a constant PCL:PLA ratio.

4.3.2.2.1 Effect of PCL:PLA Blend Ratio

The basis of the fibres is the ratio of the component materials, PCL and PLA. As such, it is important to determine what effects this ratio has on the mechanical properties, so the best fibres can be produced. Across the glycerol and PEG-200 plasticised fibres, a similar trend is observed in regards to PCL:PLA ratios (tables 4: 17 and 18). In both instances, average elongation at break displays a reduction in respect to PCL content; that is, PCL:PLA 30:70WT% has a higher elongation at break than the 70:30WT% hybrids (tables 4: 17 and 18).). In all cases, PCL:PLA 30:7WT% plasticised fibres display the highest average values for the three mechanical properties (tables 4: 17 and 18). The ability of the fibres to undergo yield is compromised by the increase in PCL content; at PCL:PLA 30:70WT%, all fibres undergo yield (tables 4: 17 and 18). However, at a PCL:PLA 50:50WT% ratio, only five of the 12 fibres yield (tables 4: 17 and 18). None of the fibres undergo yielding in the PCL:PLA 70:30WT% sets (tables 4: 17 and 18).

Statistical analysis on the raw data values provided the expected results: the ratio of PCL:PLA is significant (table 4: 19). Overall, the interactions can be separated out further (table 4: 20). It is readily apparent that a large number of differences attributable to PCL:PLA ratio are presentation (table 4: 20). Of the potential interactions, 46% show significant effects as a result of a ratio change (table 4: 20). Interestingly, the majority (56%) of the interactions in table 15 are attributable to glycerol plasticised materials. This suggests that the mechanical properties in PEG-200 plasticised hybrid fibres were more consistent. A total of seven sets produced no differences in raw values attributable to PCL:PLA ratio (table 4: 20). When plasticised with glycerol, elongation at break shows no ratio dependent differences at a 10% concentration (table 4: 20). Further, at 5% glycerol concentration and 1 pass, elongation at break shows no ratio dependent differences (table 4: 20). PEG-200 plasticisation produces a different result to this. At 2 passes, a 5% PEG-200 solution shows no elongation at break variations (table 4: 20). Further, 20% PEG-200 plasticised fibres had no ratio dependent variations at 2 passes (table 4: 20). Interestingly, 10% PEG-200 plasticised fibres at 1 pass have constant tensile strength and elongation at break values (table 4: 20).

4.3.2.2.2 Effect of Plasticiser Concentration

An increasing concentration of glycerol or PEG-200 as plasticisers for PCL:PLA 30:70WT% fibres appears to improve elongation at break (tables 4: 17 and 18, figures 4: 6 and 7). Conversely, an increasing plasticiser concentration reduces the tensile and yield strengths of the PCL:PLA 30:70WT% fibres (tables 4: 17 and 18). In all but two cases, there is no statistical support for these apparent trends (table 4: 21). Glycerol plasticised fibres show a significant difference in mean tensile strength between concentrations of 10 and 20% (table 4: 21). PCL:PLA 30:70WT% fibres plasticised with PEG-200 displayed a significant difference in mean elongation at break between 5 and 20% plasticiser concentrations (table 4: 21). Between glycerol and PEG-200 PCL:PLA 30:70WT% plasticised fibres, almost no differences in mean mechanical properties are observed (table 4: 21). At a 10% plasticiser concentration, a significant difference in tensile strength is observed between glycerol and PEG-200 plasticised fibres. A comparison between the glycerol concentrations in figure 4: 6 show a consistent elongation at break. However, a different observation is made when comparing the PEG-200 concentrations (figure 4: 7). A PEG-200 20% solution allowed the PCL:PLA 30:70WT% fibres to extend considerably more than the 5% or 10% equivalents (figure 4: 7).

PCL:PLA 50:50WT% plasticised fibres appear to have plasticiser type dependent trends. When plasticised with glycerol, an increasing concentration (5 – 20%) has little effect on the mechanical properties (table 4: 18). The elongation at break appears to be consistent at both 5 and 20% glycerol concentrations; however, at 10%, two elongation extremes were reached (table 4: 17). A 10% glycerol solution gives the PCL:PLA 50:50WT% fibres either a 218% elongation (at 1 passes), or a 4.14% elongation (at 2 passes) (table 4: 17). Tensile strength is reduced across the glycerol concentration range; the PCL:PLA 50:50WT% 10% 2 passes variant displays the lowest, at 16.0 MPa (table 4: 17). Young's modulus of 50:50WT% (PCL:PLA) fibres is variable. At a 10% solution, with 2 passes, a 897.2 MPa Young's modulus is achieved; further, when plasticised with a 20% solution, a 1 passes, a 987.5 MPa value is displayed (table 4: 17). In both cases, this is a reduction on the rest of the set (1686.3 MPa or higher). PEG-200 plasticised PCL:PLA 50:50WT% fibres display a more variable elongation at break and Young's modulus, when compared with the same glycerol plasticised fibres (table 4: 18). Half of the PEG-200 fibres lack a yield point; these same fibres display low (below 10%) elongation at break (table 4: 18). Tensile strength and Young's modulus showed little variation as a result of the PEG-200 concentration (table 4: 18). For the most part, none of these trends are statistically supported (tables 4: 19 and 20). When a glycerol plasticiser was incorporated, tensile strength display significant variations in tensile strength between 5 – 10%, and 5 and – 20% glycerol concentrations (table 4: 19). PEG-200 plasticised fibres did not display any significant variations in tensile strength (table 4: 19). Both glycerol and PEG-200 plasticised fibres displayed a significant Young's modulus difference between plasticiser concentrations of 5 – 10% (table 4: 19). When the two plasticisers were compared, a difference at 5% concentration was observed in PCL:PLA 50:50WT% fibres for all three mechanical properties: tensile strength, Young's modulus, and elongation at break (table 4: 20). No other statistically significant variations in mean mechanical property were identified between the two plasticisers (table 4: 20).

Across the PCL:PLA 70:30WT% datasets the results are similar (tables 4: 17 and 18). When compared with the PCL:PLA 30:70WT% and 50:50WT% hybrids, the 70:30WT% hybrids have reduced mechanical properties (table 4: 21). However, for the most part, elongation at break displays no difference between PCL:PLA 50:50WT% and 70:30WT% hybrids (table 4: 21). The

exception to this is 5% PEG-200 plasticised fibres (table 4: 21). No variations in mechanical properties resulted from either plasticiser concentration (table 4: 19), or plasticiser type (table 4: 20).

4.3.2.2.3 Differences Between 1 and 2 Pass Variants

The pass system showed several differences between the average mechanical properties (tables 4: 17 and 18). However, this is difficult to judge in a non-statistical manner. For the most part, average tensile strength and Young's modulus do not show any pass dependent effects (tables 4: 17 and 18). Average elongation at break however does show a pass dependent effect (tables 4: 17 and 18). A consistent change is not present; in some instances the 1 pass variant is higher, in others it is lower (tables 4: 17 and 18). Statistically, there is little evidence for differences in mean as a result of the pass system (table 4: 19 and 23). When considering solely the number of passes, the raw Young's modulus displays a significant difference (table 4: 19). However, this is a result of the result of Young's modulus's dependence on the ratio. Table 4: 23 provides a more reliable statistical analysis of the pass system. When plasticised with glycerol, only a 5% concentration in PCL:PLA 30:70WT% fibres was there a difference (table 4: 23). PEG-200 plasticised fibres displayed a total of three statistically significant effects (table 4: 23). When a PCL:PLA 30:70WT% fibre was plasticised with 10% PEG-200, Young's modulus had a significant pass dependent effect (table 4: 23). Further, the 20% PEG-200 plasticised PCL:PLA 30:70WT% fibres displayed a change in elongation at break in response to the number of passes (table 4: 23). A PCL:PLA 50:50WT% fibre, plasticised with 5% PEG-200 produced a significant effect on elongation at break, in respect to number of passes (table 4: 23).

4.3.2.2.4 Presence or Absence of Yielding

Statistical analysis could not be performed on yield strength values. It can be seen in both tables 4: 17 and 18 that a number of fibres did not yield. Statistical analysis using the same methods as previously described could not be carried out, due to the large number of missing yield strengths. Alternate statistical methods could have been carried out; however, these require that no data set has either a 100% presence or absence of values. This was not observed in this data. Trends based on the average values can be speculated on (tables 4: 17 and 18). Across both glycerol and PEG-200 plasticised hybrids, the same trend is observed: as PCL content increases, the ability to yield seems to be compromised (tables 4: 17 and 18). At a ratio of PCL:PLA 30:70WT%, all fibres underwent yielding, irrespective of the other factors (plasticiser type, concentration, passes). Conversely, at PCL:PLA 70:30WT%, none of the fibres underwent yielding (table 4: 17 and 18). Interestingly, a PCL:PLA 50:50WT% hybrid fibre plasticised with glycerol produced a yield in four out of six (66.7%) instances (table 4: 12). Whereas, PEG-200 plasticised PCL:PLA 50:50WT% hybrids in table 4: 17 showed only three of the six (50%) undergoing yielding. Regardless of plasticiser type, the lack of yield in PCL:PLA 50:50 WT% fibres did not appear to have any contributing factors.

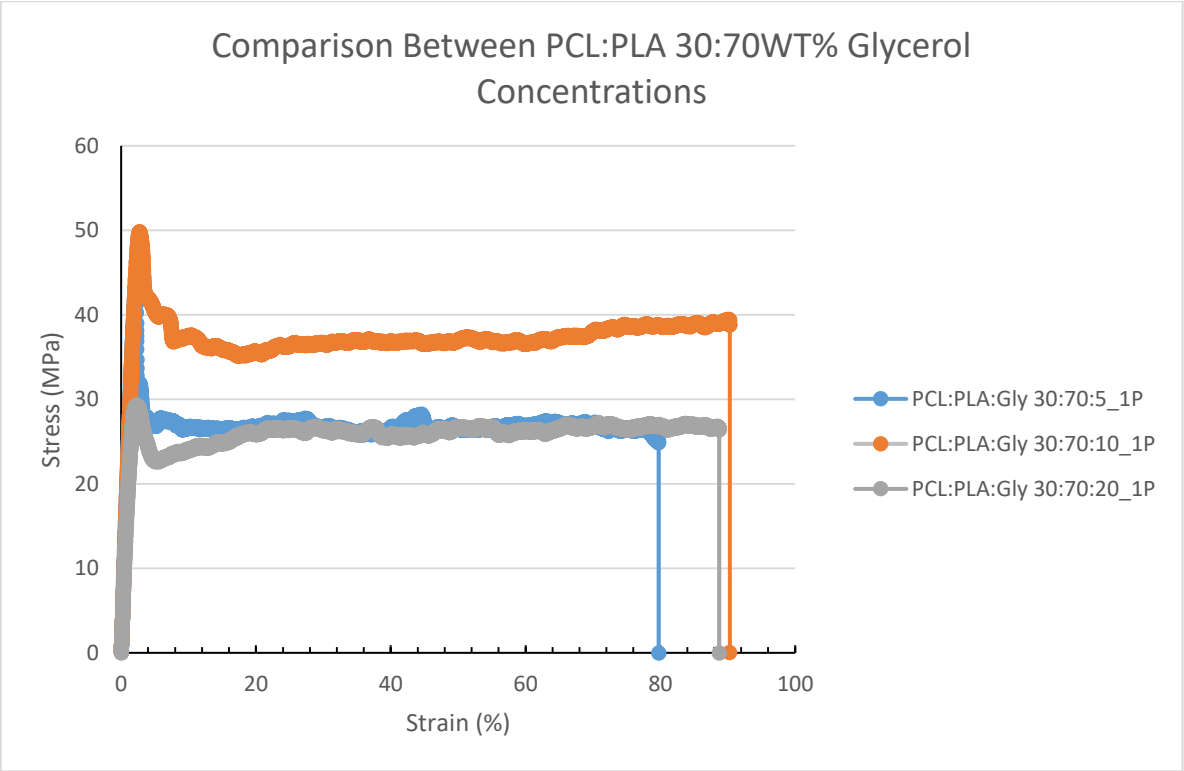

Figure 4: 6 Comparative graph displaying the effect of varying the Glycerol concentration on PCL:PLA 30:70WT% fibres. Blue circle: 5% glycerol. Orange circle: 10% glycerol. Grey circle: 20% glycerol.

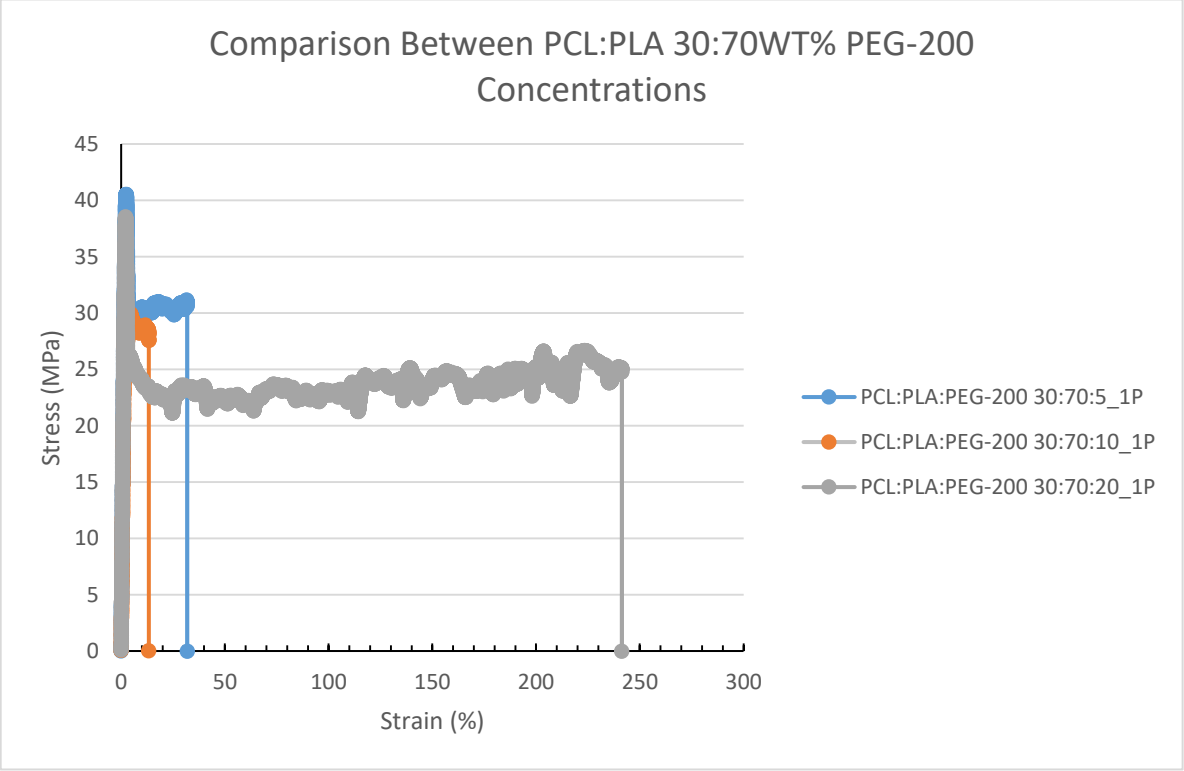

Figure 4: 7 Comparative graph displaying the effect of varying the PEG-200 concentration on PCL:PLA 30:70WT% fibres. Blue circle: 5% PEG-200. Orange circle: 10% PEG-200. Grey circle: 20% PEG-200.

Table 4: 9 PCL 100WT% fibres Plasticised with Glycerol and PEG-200.

Glycerol (%)	PEG-200 (%)	Number	Tensile Strength (MPa)	Yield Strength (MPa)	Young's Modulus (MPa)	Graph Strain (%)	Max Strain (%)
10		1-5	21.4±1.7	17.73±1.0	395.1±12.2	701.82	818.55±89.8
20		6-10	18.4±0.8	12.1±1.6	369.3±27.3	446.22	459.10±15.9
5		11-15	21.7±5.1	13.7±2.8	380.5±103.0	654.47	772.94±86.2
	10	1-5	21.5±3.5	16.26±1.3	370.8±110.4	750.18	851.36±106.1
	20	6-10	22.6±3.7	15.3±0.6	322.1±33.5	850.34	897.59±40.8
	5	11-15	16.4±0.7	14.2±0.5	361.6±8.4	272.47	466.55±137.2

Table 4: 10 ANOVA type 3 Analysis on PCL 100WT% plasticised controls. Significant values are underlined and italicised. Factor of Significance 0.05. Rounded to 4 D.P.

Property	Plasticiser Type	Plasticiser Concentration	Plasticiser Type: Plasticiser Concentration
Tensile Strength	*0.0020*	*0.0063*	*0.0034*
Young's Modulus	0.7117	0.9960	0.9164
Elongation at Break	*0.0007*	*0.0000*	*0.0000*

Table 4: 11 LSMEANs Comparisons for plasticised PCL 100WT% controls fibres. Comparisons are made between plasticiser types. Significant values are underlined and italicised. Factor of Significance 0.05. Rounded to 4 D.P.

Property	*Contrasts*	5	10	20
Tensile Strength	*Gly-PEG-200*	*0.0093*	0.8425	0.1157
Young's Modulus	*Gly-PEG-200*	0.7181	0.5147	0.2123
Elongation at Break	*Gly-PEG-200*	*0.0203*	0.7444	*0.0001*

Table 4: 12 LSMEANs Comparisons for plasticised PCL 100WT% controls fibres. Comparisons are made between plasticiser concentrations. Significant values are underlined and italicised. Factor of Significance 0.05. Rounded to 4 D.P.

Property	*Contrasts*	**Glycerol**	**PEG-200**
Tensile Strength	*5-10*	0.8514	0.1401
	5-20	0.0660	0.1121
	10-20	0.1262	0.9998
Young's Modulus	*5-10*	0.9967	0.8802
	5-20	0.9979	0.9867
	10-20	0.9986	0.8642
Elongation at Break	*5-10*	0.8642	*0.0217*
	5-20	*0.0008*	*0.0030*
	10-20	*0.0003*	0.8358

Table 4: 13 PLA 100WT% fibres Plasticised with Glycerol and PEG-200.

Glycerol (%)	**PEG-200 (%)**	**Number**	**Tensile Strength (MPa)**	**Yield Strength (MPa)**	**Young's Modulus (MPa)**	**Graph Strain (%)**	**Max Strain (%)**
5		1-5	63.1±6.2	N/A	3574.0±350.0	2.3	2.37±0.1
20		6-10	35.2±18.8	35.2±18.8	2169.7±322.1	49.4	84.01±44.2
10		11-15	27.3±3.6	27.3±3.6	2657.9±136.8	4.85	10.18±3.8
	10	1-5	52.8±13.4	52.8±13.4	2657.9±71.4	94.0	121.92±22.2
	20	6-10	27.5±4.5	27.5±4.5	2463.8±201.4	10.3	15.83±3.9
	5	11-15	50.9±2.6	50.9±2.6	2579.4±93.9	5.17	6.81±1.3

Table 4: 14 ANOVA type 3 Analysis on PLA 100WT% plasticised controls. Significant values are underlined and italicised. Factor of Significance 0.05. Rounded to 4 D.P.

Property	**Plasticiser Type**	**Plasticiser Concentration**	**Plasticiser Type: Plasticiser Concentration**
Tensile Strength	*0.01137*	*0.0000*	*0.0000*
Young's Modulus	*0.0191*	*0.0000*	*0.0164*
Elongation at Break	*0.0000*	*0.0000*	*0.0000*

Table 4: 15 LSMEANs Comparisons for plasticised PLA 100WT% controls fibres. Comparisons are made between plasticiser type. Significant values are underlined and italicised. Factor of Significance 0.05. Rounded to 4 D.P.

Property	*Contrasts*	**5**	**10**	**20**
Tensile Strength	*Gly-PEG-200*	*0.0264*	*0.0019*	0.3946
Young's Modulus	*Gly-PEG-200*	*0.0372*	0.5140	0.1333
Elongation at Break	*Gly-PEG-200*	*0.0005*	*0.0001*	0.0506

Table 4: 16 LSMEANs Comparisons for plasticised PLA 100WT% controls fibres. Comparisons are made between plasticiser concentrations. Significant values are underlined and italicised. Factor of Significance 0.05. Rounded to 4 D.P.

Property	*Contrasts*	**Glycerol**	**PEG-200**
Tensile Strength	*5-10*	*0.0005*	0.5156
	5-20	0.0935	*0.0001*
	10-20	0.7812	*0.0006*
Young's Modulus	*5-10*	0.1176	0.8858
	5-20	*0.0014*	0.9105
	10-20	0.0702	0.9679
Elongation at Break	*5-10*	*0.0345*	*0.0001*
	5-20	0.0553	*0.0229*
	10-20	0.0864	*0.0001*

Table 4: 17 PCL:PLA Hybrid Fibres Plasticised with Glycerol.

Glycerol (%)	Ratio (WT%)	Pass	Tensile Strength (MPa)	Yield Strength (MPa)	Young's Modulus (MPa)	Graph Strain (%)	Max Strain (%)
5	30:70	1	43.4±4.1	43.4±4.1	2284.9±250.0	79.76	97.91±13.3
5	30:70	2	41.0±6.1	41.0±6.1	2163.5±291.3	143.97	216.4±55.7
10	30:70	1	49.9±3.0	49.9±3.0	2132.8±54.8	90.32	120.43±32.7
10	30:70	2	43.0±0.7	43.0±0.7	2172.3±28.5	51.30	62.73±12.1
20	30:70	1	29.4±14.5	29.4±14.5	2066.2±419.5	88.75	203.52±83.8
20	30:70	2	32.9±7.8	32.9±7.8	2049.5±247.7	80.88	188.58±5.4
5	50:50	1	48.9±11.6	None	2423.6±760.0	3.0	12.50±12.3
5	50:50	2	38.2±16.5	38.2±16.5	1547.6±605.6	8.7	56.7±47.1
10	50:50	1	27.2±9.5	27.2±9.5	1686.3±11.6	113.02	180.63±47.9
10	50:50	2	16.0±0.7	None	897.2±37.0	2.50	2.76±0.2
20	50:50	1	31.1±10.3	31.1±10.3	987.5±357.9	32.7	47.49±12.5
20	50:50	2	32.2±9.2	32.2±9.2	1864.4±85.1	16.2	20.39±4.5
5	70:30	1	16.0±1.9	None	482.4±74.3	5.0	5.65±0.7
5	70:30	2	13.5±1.3	None	469.3±107.1	4.2	7.08±2.1
10	70:30	1	17.4±1.5	None	643.9±21.7	4.57	5.57±0.7
10	70:30	2	18.9±1.2	None	549.3±35.5	5.37	6.31±0.7
20	70:30	1	8.9±1.1	None	436.4±48.8	5.8	3.98±1.2
20	70:30	2	19.3±0.9	None	461.7±1.4	9.1	9.76±0.7

Table 4: 18 PCL:PLA Hybrid Fibres Plasticised with PEG-200.

PEG-200 (%)	Ratio (WT%)	Pass	Tensile Strength (MPa)	Yield Strength (MPa)	Young's Modulus (MPa)	Graph Strain (%)	Max Strain (%)
5	30:70	1	40.5±7.3	40.5±7.3	2102.2±284.3	31.83	92.63±57.9
5	30:70	2	34.3±5.2	34.3±5.2	2307.7±145.1	45.75	58.78±15.8
10	30:70	1	30.0±3.9	29.3±3.4	1839.1±658.3	13.34	38.22±17.8
10	30:70	2	30.0±9.1	30.0±9.1	2011.7±640.3	306.53	323.06±21.5
20	30:70	1	38.5±4.1	38.5±4.1	2169.3±166.3	241.31	301.89±83.3
20	30:70	2	24.6±4.3	24.6±4.3	1952.4±573.8	119.90	234.44±95.0
5	50:50	1	34.1±1.6	34.1±1.6	1860.0±190.7	108.05	239.20±103.1
5	50:50	2	17.1±2.4	None	1105.6±127.8	3.27	4.54±1.3
10	50:50	1	23.1±2.0	None	945.2±133.3	3.4	4.04±0.5
10	50:50	2	27.9±2.7	27.9±2.7	1210.2±228.7	73.4	99.51±29.3
20	50:50	1	25.9±3.6	25.9±3.6	1703.9±107.8	124.6	214.3±68.0
20	50:50	2	25.2±2.2	None	1124.5±91.2	3.3	3.95±0.7
5	70:30	1	21.0±4.0	None	949.20±178.0	3.77	5.83±1.7
5	70:30	2	19.7±0.9	None	535.2±13.6	6.13	6.56±0.3
10	70:30	1	8.2±1.0	None	648.2±21.2	1.4	3.34±2.1
10	70:30	2	13.1±1.2	None	593.7±52.1	2.7	4.44±1.2
20	70:30	1	14.1±1.4	None	573.8±6.2	3.7	5.43±1.4
20	70:30	2	15.1±0.6	None	582.4±13.4	3.9	4.17±0.2

Table 4: 19 Significant Interactions resulting from Individual factors, and Combined. Significant values are underlined and italicised. Factor of Significance 0.05. Rounded to 4 D.P.

Mechanical Property	Plast	Conc	PCL	Pass	Plast:Conc:PCL:Pass
Tensile Strength	0.2793	*0.0367*	*0.0000*	0.2383	0.6216
Young's Modulus	*0.0293*	*0.0291*	*0.0000*	*0.0302*	0.3598
Elongation Break	0.4501	0.7537	*0.0475*	0.7395	0.2462

Table 4: 20 Effect of PCL content, with respect to Plasticiser type, concentration and number of passes. Significant values are underlined and italicised. Factor of Significance 0.05. Rounded to 4 D.P.

		Concentration	5		10		20	
Plasticiser	Mechanical Property	Contrasts	1	2	1	2	1	2
Glycerol	Tensile Strength	30-50	0.8382	0.7029	*0.0105*	*0.0001*	0.5804	0.9549
		30-70	*0.0001*	*0.0032*	*0.0001*	*0.0001*	*0.0018*	*0.0043*
		50-70	*0.0001*	*0.0002*	0.1603	0.9352	*0.0314*	*0.0017*
	Young's Modulus	30-50	0.1308	0.9984	*0.0220*	*0.0013*	0.1851	0.2067
		30-70	*0.0001*	*0.0001*	*0.0001*	*0.0001*	*0.0001*	*0.0001*
		50-70	*0.0001*	*0.0001*	0.0542	0.2778	*0.0031*	*0.0001*
	Elongation at Break	30-50	0.1017	0.0729	0.9048	0.9063	0.1404	*0.0062*
		30-70	0.0791	*0.0343*	0.1928	0.6175	*0.0399*	*0.0026*
		50-70	0.9926	0.9461	0.0816	0.8636	0.8383	0.9564
PEG-200	Tensile Strength	30-50	0.4365	*0.0425*	0.8822	0.2122	0.0912	0.9969
		30-70	*0.0055*	*0.0226*	0.0792	*0.0006*	*0.0018*	0.0870
		50-70	0.1247	0.9663	0.2065	0.0735	0.3246	0.1022
	Young's Modulus	30-50	0.3073	0.0527	0.5882	*0.0001*	0.2278	0.3332
		30-70	*0.0014*	*0.0001*	*0.0461*	*0.0001*	*0.0001*	*0.0002*
		50-70	0.0816	*0.0283*	0.3255	0.8926	*0.0043*	*0.0186*
	Elongation at Break	30-50	0.2206	0.9721	0.2742	*0.0385*	*0.0072*	0.1535
		30-70	0.3129	0.7536	0.0694	*0.0042*	*0.0001*	*0.0087*
		50-70	*0.0067*	0.8755	0.7630	0.7024	0.0974	0.4675

Table 4: 21 Effect of Plasticiser Concentration, with respect to PCL content, plasticiser type, and number of passes. Significant values are underlined and italicised. Factor of Significance 0.05. Rounded to 4 D.P.

			30		50		70	
Plasticiser	Mechanical Property	Contrasts	1	2	1	2	1	2
Glycerol	Tensile Strength	5-10	0.9827	0.3843	*0.0033*	*0.0002*	0.9992	0.9304
		5-20	0.0904	0.9604	*0.0012*	0.7144	0.5253	0.9822
		10-20	0.0607	0.2527	0.9456	*0.0032*	0.5484	0.8506
	Young's Modulus	5-10	0.2044	0.7957	0.0399	*0.0112*	0.8380	0.9442
		5-20	*0.0288*	0.7365	*0.0451*	0.6335	0.9067	0.8312
		10-20	0.6451	0.9943	0.9986	0.1064	0.5862	0.6403
	Elongation at Break	5-10	0.8865	0.2546	0.1109	0.9753	0.9996	0.9999
		5-20	0.9589	0.6133	0.9017	1.0000	0.9998	0.9994
		10-20	0.7384	*0.0349*	0.2511	0.9753	0.9999	0.9998
PEG-200	Tensile Strength	5-10	0.2281	0.9306	0.6415	0.9159	0.8002	0.2619
		5-20	0.6521	0.2004	0.5329	0.7906	0.8527	0.4738
		10-20	0.3076	0.3617	0.9835	0.9649	0.9946	0.9133
	Young's Modulus	5-10	0.1355	0.9890	0.3233	0.0575	0.7602	0.9850
		5-20	0.9977	0.1845	0.9925	0.6847	0.4376	0.5841
		10-20	0.1190	0.2374	0.3843	0.2960	0.8587	0.6876
	Elongation at Break	5-10	0.7187	*0.0365*	*0.0435*	0.9668	1.0000	0.9978
		5-20	*0.0010*	0.0637	0.5532	0.7977	1.0000	0.9987
		10-20	*0.0107*	0.9706	0.3414	0.9181	0.9999	0.9999

Table 4: 22 Effect of Plasticiser type, with respect to PCL content, plasticiser concentration and number of passes. Significant values are underlined and italicised. Factor of Significance 0.05. Rounded to 4 D.P.

			30		50		70	
	Mechanical Property	Contrasts	1	2	1	2	1	2
5	Tensile Strength	Gly-PEG	0.2829	0.9317	*0.0052*	*0.0022*	0.7423	0.4469
	Young's Modulus	Gly-PEG	*0.0326*	0.3659	0.0930	0.1637	0.1303	0.4241
	Elongation at Break	Gly-PEG	0.4526	0.0751	*0.0037*	0.8441	0.9775	0.9818
10	Tensile Strength	Gly-PEG	*0.0047*	0.1132	0.6856	0.1657	0.7882	0.2439
	Young's Modulus	Gly-PEG	*0.0191*	0.9023	0.5105	0.4431	0.7983	0.7530
	Elongation at Break	Gly-PEG	0.6263	*0.0237*	0.1414	0.8172	0.9923	0.9567
20	Tensile Strength	Gly-PEG	0.3875	0.1733	0.7947	0.0862	0.3826	0.8215
	Young's Modulus	Gly-PEG	0.6181	0.1109	0.5395	0.1893	0.4744	0.6964
	Elongation at Break	Gly-PEG	*0.0080*	0.6453	0.1316	0.4043	0.9950	0.9532

Table 4: 23 Effect of Pass Number, with respect to PCL content, Plasticiser Type and Concentration. Significant values are underlined and italicised. Factor of Significance 0.05. Rounded to 4 D.P.

			30:70			50:50			70:30		
Plasticiser	Mechanical Property	Contrasts	5	10	20	5	10	20	5	10	20
	Tensile Strength	1-2	0.2422	0.9771	0.4971	0.3485	0.0856	0.0527	0.9537	0.6486	0.3380
Glycerol	Young's Modulus	1-2	*0.0335*	0.8430	0.2357	0.7909	0.4562	0.2130	0.7555	0.948	0.8777
	Elongation Break	1-2	0.7405	0.4298	0.3195	0.8575	0.10470	0.8007	0.9832	0.9841	0.9774
	Tensile Strength	1-2	0.9911	0.2026	0.1227	0.2202	0.9495	0.6243	0.6236	0.6558	0.8887
PEG-200	Young's Modulus	1-2	0.3595	*0.0082*	0.3611	0.9767	0.3931	0.4954	0.6801	0.8989	0.8632
	Elongation Break	1-2	0.4748	0.3075	*0.0318*	*0.0106*	0.9397	0.3506	0.9760	0.9802	0.9808

4.4 Discussion

Comparisons between the various processing temperatures were discussed. This allows identification of the temperature that produces the highest quality fibres. Further, comparisons are made between the plasticised and non-plasticised fibres. This aims to determine if plasticising the fibres was beneficial.

4.4.2 PCL and PLA Repeatability

When PCL control fibres are processed, a high repeatability is noticed: this indicates the process is good. PCL control fibres exhibited a temperature dependent effect. It was determined that, as processing temperature increases, PCL's mechanical properties reduce. This was proposed to relate to PCL undergoing thermal degradation. It has been reported that PCL 100WT% materials degrade at 358° (Zhao and Zhao 2016). While the actually degradation temperature was never tested with PCL, it must be noted that clear degradation symptoms were present. The PCL fibres, especially when processed at 180 or 190°C displayed reduced properties, and yellowing of the fibre (Pospíšil, Horák et al. 1999). PCL's thermal degradation occurs at these temperatures because of several factors: the internal temperature of the machine, and the molecular weight of PCL. It is not possible to determine the real temperature the material is exposed to, as several factors must be considered. Firstly, the temperature as a result of electrical heating: this is approximately the reported temperature (180 or 190°C). However, the screwless extrusion machine applies shear forces to allow extrusion. When applied to the polymer, the shear forces heat the material, increasing the 'real' temperature to be above the displayed temperature (Pospíšil, Horák et al. 1999). This increase has the potential to take the actual applied temperature passed the reported thermal degradation temperature for PCL (358°C) (Zhao and Zhao 2016). Further, a polymers thermal degradation rate is a result of its molecular weight (Mittal, Sahana et al. 2007). The CAPA 6506 (PCL used) datasheet stats the molecular weight as 50,000 g/mol, no error is provided. Variations to the molecular weight will alter the degradation rate (Mittal, Sahana et al. 2007). Based on the machine's temperature, slight variations in the molecular weight of PCL could significantly alter the speed of degradation. In the event that the extruded PCL's molecular weight is lower in comparison to the quoted value, degradation symptoms would be expected to appear at an increased rate (Mittal, Sahana et al. 2007). Based on the observations for PCL 100WT% fibres, a 160°C extrusion temperature produces the best results. The results observed at 160°C are within the expected error or literary values (Monticelli, Calabrese et al. 2014).

In terms of repeatability, PLA control fibres were found to be highly consistent. Over the range of temperatures used, PLA does not show any significant differences. The fact that PLA's mechanical properties show no temperature dependent effects is highly beneficial in this work. Ideally, PLA would be processed at the lowest possible temperature, providing higher quality hybrid fibres (PCL works best at lower temperatures). One likely explanation for PLA's consistency is that it is amorphous (Guttman, DiMarzio et al. 1981). Essentially, an amorphous polymer will show very little in terms of temperature dependent effects (Guttman, DiMarzio et al. 1981). An amorphous polymer does not undergo melting in the same manner as a crystalline polymer – no crystal-structure changes occur (Guttman, DiMarzio et al. 1981).

4.4.3 PCL:PLA Hybrid Fibre

It was readily apparent that the non-plasticised hybrid fibres blended poorly (see section 3.3). Typically, it was noted that the fibres were brittle, with some discolouration; these effects were more pronounced when the fibres underwent 3 passes. These are signs of a degraded fibre (Pospíšil, Horák et al. 1999). The fibres showed a significant reduction in mechanical properties, a further indication of thermal degradation (Pospíšil, Horák et al. 1999). No hybrid fibre displayed properties in keeping with the minimum criteria (table 2: 4). Primarily, this is a result of issues with interfacial bonding between the two materials (PCL and PLA); issues in bonding produce mechanically weak, unusable fibres (Malinowski 2016). There is a large amount of support in this issue: materials with vastly different glass transition temperatures do not blend well (El-Hadi 2014). What this means is that a plasticiser must be added to the blend to produce acceptable fibres (El-Hadi 2014). For this reason, glycerol and PEG-200 were investigated as plasticisers.

For the most part, plasticisation of the hybrid blends improved the blend properties. The fibres were not found to exhibit traces of degradation (see section 3.3). This is a significant improvement over the non-plasticised hybrids. The significant improvement in mechanical properties would suggest that the plasticisation process has been successful: no distinct glass transitions are present (El-Hadi 2014). Based on the results displayed in tables 4: 17 and 18, an interesting trend has been observed. The plasticisation process (both PEG-200 and glycerol) proved to be significantly more successful when PLA content was high (tables 4: 17 and 18). One possible explanation for this is the plasticiser primarily effecting PLA. The glass transition temperature of PLA, 60°C (Urquijo, Guerrica-Echevarría et al. 2015) can be beneficially reduced in this system. However, PCL has a -60°C glass transition temperature (Wan, Lu et al. 2009); further reductions to this are not beneficial. A higher PLA content could be proportional to a higher reduction in the glass transition temperature of PLA, resulting in a higher quality blend. However, further work would be required to prove this effect.

Based on the mechanical property criteria specified in table 2: 4 several suitable fibres can be identified. Briefly, the mechanical properties criteria are: fibres will have high elongation at break (over 300%), and have a reasonable Young's modulus (2500 MPa or higher, inclusive of standard deviation). Table 4: 24 displays the four hybrid fibres that fit these criteria. The criteria from table 2: 4 were not suitable for the plasticised control fibres. PCL 100WT% fibres were not found to reach a 2500 MPa Young's modulus; likewise, PLA 100WT% fibres did not reach a 300% elongation at break. However, for the sake of comparison, the control fibres were essential. As such, new criteria were defined, based on literature. It was desired that the plasticised control fibres would not display a significant reduction in mechanical properties, based on the non-plasticised literary values in table 2: 2. Four plasticised control fibres were found to meet these criteria; one PLA and three PCL fibres (table 4: 24). The elongation at break and Young's modulus were improved by plasticising; whereas the PCL fibres displayed a small Young's modulus increase, and the same elongation at break (within error) as the literary values reported by Monticelli, Calabrese et al. (2014).

Based on the eight fibres that meet their respective criteria, a clear trend is noted (table 4: 24). Hybrid fibres plasticised with PEG-250 had more improved properties when compared to glycerol plasticised fibres, with six of the eight fibres containing PEG-250 (table 4: 24). Further analysis of glycerol plasticised fibres was not beneficial to this work as too few fibres met the

criteria. Four hybrid fibres were chosen to be progressed for degradation (section 5) and shape recovery (section 6) testing, these are summarised in table 4: 25. PCL:PLA 30:70WT% fibres, with 25% PEG-250 had both 1 and 2 pass variants meet the criteria, therefore these were progressed. Plasticised PCL fibres had a 25% solution meet the criteria, therefore this was used, due to its similarities with the hybrid (all 25% PEG-250). However, a single PLA fibre was found to meet the criteria: PLA 100WT% plasticised with 10% PEG-250. While this used a lower PEG-250 content (10% instead of 25%), it was the only PLA fibre that was suitable.

4.5 Summary

Overall, several conclusions were made in relation to mechanical properties of the produced hybrid fibres. During the repeatability testing, PCL exhibited a temperature dependent degradation to mechanical properties, where a higher temperature increased the reduction. In this same scenario, PLA was found to lack any processing temperature dependent change in its mechanical properties. PCL:PLA hybrid fibres had low mechanical properties when not plasticised. The non-plasticised hybrid were unusable for future work. Plasticisation of the PCL:PLA hybrid blends proved successful. A set of four fibres were identified (table 4: 25) as the best hybrid fibres based on the relevant criteria mentioned in table 2: 4. These fibres were progressed for shape recovery (section 5) and degradation (section 6) studies.

Table 4: 24 Best Plasticised Hybrid and Control Fibres based on The Mechanical Property Criteria Given in Table 2: 4

Material	Ratio (WT%)	Tensile Strength (MPa)	Yield Strength (MPa)	Young's Modulus (MPa)	Graph Strain (%)	Max Strain (%)
PCL:PLA:Gly	30:70:20_1P	32.9±7.8	32.9±7.8	2049.5±247.7	80.88	316.42
PCL:PLA:PEG-200	30:70:20_0P	38.5±4.1	38.5±4.1	2169.3±166.3	241.31	419.72
PCL:PLA:PEG-200	30:70:20_1P	24.6±4.3	24.6±4.3	1952.4±573.8	119.90	352.42
PCL:PLA:PEG-200	50:50:5_0P	34.1±1.6	34.1±1.6	1860.0±190.7	108.05	359.92
PLA:PEG-200	100:10	52.8±13.4	52.8±13.4	2657.9±71.4	94.0	148.37
PCL:Gly	100:10	21.4±1.7	17.73±1.0	395.1±12.2	701.82	920.37
PCL:PEG-200	100:10	21.5±3.5	16.26±1.3	370.8±110.4	750.18	997.97
PCL:PEG-200	100:20	22.6±3.7	15.3±0.6	322.1±33.5	850.34	949.89

Table 4: 25 Fibres Progressed for Shape Recovery (section 5) and Degradation (section 6) Testing.

Material	Ratio (WT%)	Tensile Strength (MPa)	Yield Strength (MPa)	Young's Modulus (MPa)	Graph Strain (%)	Max Strain (%)
PCL:PEG-200	100:20	22.6±3.7	15.3±0.6	322.1±33.5	850.34	949.89
PCL:PLA:PEG-200	30:70:20_0P	38.5±4.1	38.5±4.1	2169.3±166.3	241.31	419.72
PCL:PLA:PEG-200	30:70:20_1P	24.6±4.3	24.6±4.3	1952.4±573.8	119.90	352.42
PLA:PEG-200	100:10	52.8±13.4	52.8±13.4	2657.9±71.4	94.0	148.37

Chapter 5 Shape Recovery

5.1 Introduction

Establishing the shape recovery ability and properties of the materials is important. The ability of a material to exhibit shape recovery is important for some biomedical applications, such as sutures (Lendlein and Langer 2002). While five stimuli methods have been identified (section 2.4), only thermal shape recovery is investigated here. The methods employed to test thermal shape recovery are solely meant to gain preliminary insight into how the fibres behave. The methods will be further refined in a separate study to characterise the shape recovery behaviours of the optimal fibres.

5.2 Materials and Methods

The materials and methods employed in shape recovery testing are described here.

5.2.1 Materials

Across all shape recovery testing, the same equipment was used. Two solutions were required for shape recovery testing: heated water, and cold water. To achieve this, a Lab Companion TS-14S hotplate and magnetic stirrer was used. This device could heat up to 350°C with a 0.1°C resolution. A glass petri dish was filled with water and heated on top of this to create the water bath. Cold water was in a second, non-heated petri dish. All temperature measurements were taken using a Digitech QM7215 non-contact thermometer. This device has a range of -30 – +260°C, with a 2% error.

The materials used in this section were those fabricated in the materials processing chapter 3. The original materials were cut to 70 mm lengths prior to testing. The best fibres referred to in this chapter are those identified in table 4: 20. Fifty-two polymer fibres were used in this section; table 5: 1 indicates the polymer ratios used.

Table 5: 1 Materials used in Shape Recovery Testing

Polymer Constituents	Ratio (WT%)	Passes	Glycerol Content (%)	PEG-200 Content (%)
PCL	100	1	0	0
	100	1	5	0
		1	10	0
		1	20	0
	100	1	0	5
		1	0	10
		1	0	20
PCL:PLA	50:50	3		0
	70:30	3		0
	30:70	1	5	0
		2	5	0
		1	10	0
		2	10	0
		1	20	0
		2	20	0
	50:50	1	5	0
		2	5	0
		1	10	0
		2	10	0
		1	20	0
		2	20	0
	70:30	1	5	0
		2	5	0
		1	10	0
		2	10	0
		1	20	0
		2	20	0

Table 5: 2.Continued Materials used in Shape Recovery Testing

Polymer Constituents	Ratio (WT%)	Passes	Glycerol Content (%)	PEG-200 Content (%)
PCL:PLA	30:70	1	0	5
		2	0	5
		1	0	10
		2	0	10
		1	0	20
		2	0	20
	50:50	1	0	5
		2	0	5
		1	0	10
		2	0	10
		1	0	20
		2	0	20
	70:30	1	0	5
		2	0	5
		1	0	10
		2	0	10
		1	0	20
		2	0	20
PLA	100	1	0	0
	100	1	5	0
		1	10	0
		1	20	0
	100	1	0	5
		1	0	10
		1	0	20

5.2.2 Methods

A petri-dish of 70 mL water was heated on the hot plate to a variety of temperatures. The petri dish was placed centrally on the hot plate, with no overhang; this ensured equal heat distribution. Initially, testing involved a single 70 mm fibre from each set placed into 37.5°C water (requiring a machine temperature of 43°C), following the method detailed above. Typically, 37.5°C is identified as human physiological temperature (Vieira, Vieira et al. 2011, Pinho, Rodrigues et al. 2016). This test is important to investigate shape recovery for biocompatible materials. A second run of experiments involving the best fibres (identified in table 4: 20) were carried out across a broad range of temperatures: 30 – 90°C. However, it was noted that the hot plate temperature was, in most cases, considerably higher than the water temperature. Table 5: 2 displays a comparison of the water temperature and the required hot plate temperature. For each temperature tested, a new 70 mm fibre was used. In all cases, the fibre was completely submerged in 70 mL of heated water, and left for 30 seconds. The fibre was then removed and deformed (curled into a circle), then cooled in a 1000 mL beaker of cold water for 30 seconds. Finally, the fibre was again submerged in the 70 mL of hot water, and recovery to its original shape timed until recovery had stopped.

Table 5: 3 Comparison of Required to Machine Temperatures for Shape Recovery

Required Temperature (°C)	**Hot Plate Temperature (°C)**
30	33
40	47
50	60
60	75
70	90
80	130
90	190

5.3 Results

Two shape memory studies were performed. The initial study tested all plasticised fibres for their shape recovery ability at human physiological temperature (37.5°C). The second study performed used only the best fibres as defined in table 4: 25 across a 30 – 90°C temperature range.

5.3.1 In Vitro Study Under Human Physiological Temperature (37.5°C)

In total, there were 52 different fibre sets tested at human physiological temperature, 37.5°C (table 5: 3). Of those 52 fibres, 18 (35%) were found to not exhibit shape recovery. PCL (100WT%) fibres, plasticised or not, did not display shape recovery. One plasticised PLA fibre, PLA 100WT% plasticised with 5% glycerol also did not exhibit shape recovery. It must be noted that said fibre had a milky-yellow appearance, as opposed to the typical PLA appearance of clear and transparent. This suggests the fibre was contaminated during processing. Out of all hybrid fibres plasticised with PEG-200, only one did not exhibit shape recovery: PCL:PLA 70:30WT%, plasticised with 20% PEG-200, 1 pass variant. Seven of the glycerol plasticised PCL:PLA fibres did not exhibit shape recovery. The remaining 34 fibres (65%) were found to exhibit shape recovery.

Across those that exhibited shape recovery, 31 fibres had identical responses: a 5 second recovery time. Two fibres recovered slower, at 20 seconds: PCL:PLA 50:50WT% 5% glycerol plasticised, 1 pass variant; and PLA 100WT%. One fibre produced an instant response: PLA 100WT% plasticised with 20% PEG-200. Two non-plasticised hybrid fibres underwent shape recovery testing at 37.5°C: PCL:PLA 50:50WT% and 70:30WT%. Neither of these fibres exhibited shape recovery when tested at 37.5°C. The significant improvement in shape recovery properties when the fibres were plasticised suggests that the process was successful.

Table 5: 4 Results from Physiological Temperature Testing: Shape Recovery.

Material	Ratio	Pass	Set Ref Number	Response to 37.5°C	Recovery Time (s)
PCL	100	1	N/A	None	N/A
PCL:Gly	100:10	1	1-5	None	N/A
	100:20	1	6-10	None	N/A
	100:5	1	11-15	None	N/A
PCL:PEG-200	100:10	1	1-5	None	N/A
	100:20	1	6-10	None	N/A
	100:5	1	11-15	None	N/A
PCL:PLA:Gly	50:50:5	1	1-5	Yes	20
		2	6-10	None	N/A
	70:30:5	1	11-15	Yes	5
		2	16-20	Yes	5
	50:50:20	1	21-25	None	N/A
		2	26-30	Yes	5
	70:30:20	1	31-35	None	N/A
		2	36-40	None	N/A
	50:50:10	1	41-45	Yes	5
		2	46-50	None	N/A
	70:30:10	1	51-55	Yes	5
		2	56-60	Yes	5
	30:70:10	1	61-65	Yes	5
		2	66-70	None	N/A
	30:70:20	1	71-75	Yes	5
		2	76-80	Yes	5
	30:70:5	1	81-85	None	N/A
		2	86-90	Yes	5

Table 5: 5.Continued Results from Physiological Temperature Testing: Shape Recovery.

Material	Ratio	Pass	Set Ref Number	Response to 37.5°C	Recovery Time (s)
PCL:PLA:PEG-200	50:50:10	1	1-5	Yes	5
		2	6-10	Yes	5
	50:50:20	1	11-15	Yes	5
		2	16-20	Yes	5
	70:30:10	1	21-25	Yes	5
		2	26-30	Yes	5
	70:30:20	1	31-35	None	N/A
		2	36-40	Yes	5
	30:70:10	1	41-45	Yes	5
		2	46-50	Yes	5
	30:70:20	1	51-55	Yes	5
		2	56-60	Yes	5
	30:70:5	1	61-65	Yes	5
		2	66-70	Yes	5
	50:50:5	1	71-75	Yes	5
		2	76-80	Yes	5
	70:30:5	1	81-85	Yes	5
		2	86-90	Yes	5
PLA	100	1	N/A	Yes	20
PLA:Gly	100:5	1	1-5	None	N/A
	100:20	1	6-10	Yes	5
	100:10	1	11-15	Yes	5
PLA:PEG-200	100:10	1	1-5	Yes	5
	100:20	1	6-10	Yes	Instant/unmeasurable
	100:5	1	11-15	Yes	5
PCL:PLA	50:50	3	N/A	None	N/A
	70:30	3	N/A	None	N/A

5.3.2 Best Fibre Test

Of the best fibres identified in the mechanical testing section (table 4: 20), PCL was deemed to be not appropriate for shape recovery testing as it will melt when the temperature exceeds 60°C (Monticelli, Calabrese et al. 2014). Further, PCL was not observed to recover at 37.5°C (table 5: 3). Table 5: 4 summarises the results from the best fibre shape recovery study. Further, figures 5: 1 – 4 provide a series of images to demonstrate what the fibre looks like at each stage of the shape recovery test. High quality images are available for every stage of best fibre testing in Appendix D.

The best fibres, based on mechanical properties underwent shape recovery testing across a range of temperatures (30°C – 90°C). All of the fibres tested were able to display shape recovery across all temperatures (table 5: 4). However, recovery occurred at varying rates in response to the temperature. PLA 100WT% fibres plasticised with 10% PEG-200 displayed complete recovery at all temperatures. At lower temperatures (30°C – 40°C) PLA 100WT% fibres plasticised with 10% PEG-200 took 5 seconds to recover completely. However, at temperatures of 50°C and higher, PLA 100WT% fibres plasticised with 10% PEG-200 fibres underwent what is being termed here as heat constriction. This is the phenomenon that occurs when the materials contract as a result of the heat. The constriction resulted in a new, semi-deformed conformation. As such, the fibres were only able to recover to the semi-deformed shape (figure 5: 1 – 4).

The two hybrid fibres, PCL:PLA 30:70 plasticised with 20% PEG-200 1 and 2 pass variants, produced almost identical results to each other (table 5: 4). At 30°C, neither hybrid material displayed complete recovery. The recovery times at 40°C varied, dependent on whether the hybrid underwent 1 or 2 pass. The 1 pass variant took 20 seconds to fully recover, while the 2 pass variant recovered in 5 seconds. At 50°C, the complete recovery of both hybrid fibres took 5 seconds. Heat constriction was apparent in both 1 and 2 pass variants from 60°C – 90°C; in all cases, the effects were instant. The fibres however, could only recover to the point of heat constriction (figures 5: 1 – 4).

Figure 5: 1 PCL:PLA 30:70WT% plasticised with 20% PEG-200 2 pass variant. Permanent shape.

Figure 5: 2 PCL:PLA 30:70WT% plasticised with 20% PEG-200 2 pass variant. Thermal Contraction.

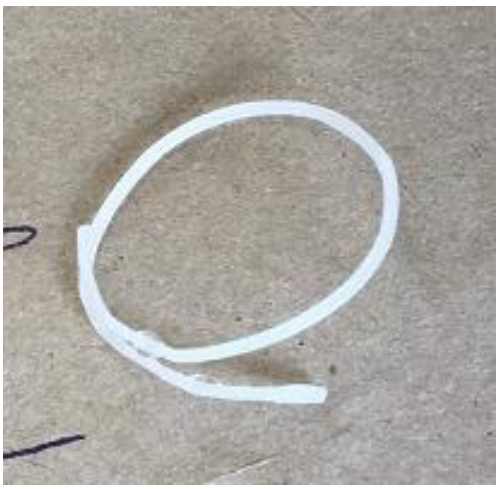

Figure 5: 3 PCL:PLA 30:70WT% plasticised with 20% PEG-200 2 pass variant. Deformed shape

Figure 5: 4 PCL:PLA 30:70WT% plasticised with 20% PEG-200 2 pass variant. Recovered shape

Table 5: 6 Results of Shape Recovery Testing for the Best Fibres

Temperature (°C)	**PLA:PEG-200**	**PCL:PLA:PEG-200**	
	100:10	*30:70:20_1P*	*30:70:20_2P*
30	Complete recovery. ~t=5 sec.	Incomplete recovery after 30 seconds.	Incomplete recovery after 30 seconds.
40	Complete recovery. ~t=5 sec.	Complete recovery to pre-30°C conformation. ~t=20 secs.	Complete recovery to pre-30°C conformation. ~t=5 sec.
50	Thermal contraction.	Complete recovery. ~t=5 sec.	Complete recovery. ~t=5 sec.
60			
70	Thermal contraction occurs on all fibres. Recovering to the point of heat constriction.		
80	Recovery was instant in all cases. As soon as the fibres made contact with the heated water, they recovered.		
90			

5.4 Discussion

The results from both shape recovery studies are discussed in sections 5.4.1 and 5.4.2.

5.4.1 Human Physiological Temperature

In no case were PCL 100WT% fibres observed to display shape recovery. The ability of a material to undergo thermal transitions is important for their ability to display shape recovery (Behl and Lendlein 2007). In the case of PCL 100WT% fibres, two thermal transition points are observed: glass transition, -60°C, and melting 60°C (Jamshidian, Tehrany et al. 2010). As a result of these transition points, PCL undergoes recovery at temperatures above -60°C. However, the temperatures applied to the fibres here were considerably higher than PCL's glass transition. As a result, PCL 100WT% fibres could not undergo shape fixation, a temperature below the thermal transition temperatures is required (Behl and Lendlein 2007). Within the tested temperature range, PCL's melting point was observed (60°C); however, a polymer will not undergo shape recovery after it has melted. It is possible, that if temperatures were applied around PCL's glass transition, it would in fact undergo shape recovery. No future work needs to be done around the glass transition of PCL: it is not appropriate for human use.

Unlike PCL 100WT% fibres, all but one PLA 100WT% fibre exhibited shape recovery. A single PLA 100WT% fibre, plasticised with 5% glycerol did not exhibit shape recovery (table 5: 3). However, this fibre was milky yellow in colour, rather than transparent and colourless; this would suggest the fibre was contaminated. The one major difference between the two materials are their thermal transition points: PLA's glass transition is 60°C, with no melting point (Jamshidian, Tehrany et al. 2010). As such, the temperatures applied here are more suited for PLA's glass transition. Further, PLA is an amorphous polymer, while PCL is semi-crystalline (Middleton and Tipton 2000). PLA fibres can easily undergo molecular chain realignment as there is not defined molecular structure in amorphous materials (Guttman, DiMarzio et al. 1981). An effect on shape recovery was observed with both types of plasticiser (glycerol and PEG-200). When not plasticised, PLA 100WT% fibres had a slower recovery than the plasticised variants. The PLA 100WT% fibres were found to take 20 seconds to completely recovery, when plasticised this was reduced to 5 seconds. One fibre, PLA 100WT% plasticised with 20% PEG-200 was observed to recover instantly, much faster than both the control and other plasticiser concentrations. The two plasticisers (Glycerol and PEG-200) used here function to reduce the glass transition temperature of the material they are applied to (Byun, Kim et al. 2010). The reduction in proposed glass transition temperature could explain why the plasticised PLA fibres recover faster: the applied temperature is closer to the transition point, so a more pronounced effect was observed A reduction in glass transition temperature to 21°C in PLA, with the addition of 20% PEG-400 has been reported (Mekonnen, Mussone et al. 2013). However, the glass transition temperatures of the plasticised fibres was never tested. As such, future work would aim to quantify the reduction to glass transition temperatures.

There were inconsistencies in plasticised hybrid fibre recovery. Glycerol plasticisation of hybrid fibres appeared to be substantially less effective than PEG-200 plasticisation. In the case of glycerol plasticised hybrid fibres, only 61% exhibited shape recovery (11/18), whereas

94% of hybrid fibres plasticised with PEG-200 exhibited shape recovery (17/18). Within the glycerol plasticised hybrid set, there appears to be a trend in whether or not fibres recover. Regardless of the glycerol concentration (5, 10, or 20%) PCL:PLA 50:50WT% hybrids display one fibre or the pair unable to recover. PCL:PLA 30:70WT% fibres plasticised by 5% glycerol at 1 passes did not display shape recovery. Similarly, the 2 pass variant of PCL:PLA 30:70WT% fibre plasticised with 10% glycerol did not recover. When a PCL:PLA 70:30WT% ratio was plasticised with 20% glycerol fibres did not exhibit shape recovery. The large number of fibres that could not undergo shape recovery suggest that glycerol is not the optimal plasticiser for these materials. Unlike glycerol plasticised hybrid fibres, only a single PEG-200 plasticised hybrid fibre lacked shape recovery: PCL:PLA 70:30WT% 2 pass variant. The significant difference in shape recovery is a result of how the two separate plasticisers operated on the materials. There is some evidence reported in the literature that PLA and glycerol are immiscible (Müller, Bere et al. 2016). It must be noted that Müller, Bere et al. (2016) used difference processes and materials to the work carried out for this project. This could have prevented adequate plasticisation of the materials.

While only 61% of the plasticised hybrid fibres exhibited shape recovery, this is a significant improvement on the non-plasticised hybrids. Neither the PCL:PLA 50:50WT% or 70:30WT% non-plasticised fibres exhibited shape recovery. This would suggest that, for the most part, plasticising the hybrid fibres improved their ability to undergo shape recovery.

5.4.2 Best Fibre Test

The best fibres summarised in table 4: 20 underwent a series of tests. PCL (100WT%) best fibres were excluded from this analysis. Any fibre that contains PCL 100WT%, was demonstrated to not exhibit a shape recovery (table 5: 3). Further, the 60°C melting temperature of PCL meant half of the temperatures tested (60°C – 90°C) were not suitable (Middleton and Tipton 2000). It was determined that due to the lack of shape recovery at 37.5°C, and PCL's melting point (60°C), testing PCL 100WT% fibres across this range would not yield any useful results.

During shape recovery testing at 30°C, two different effects were observed. PLA fibres completely recovered, while hybrid fibres only partially recovered. This effect is primarily observed as a result of the differing polymer contents in the fibres. Hybrid fibres are liable to exhibit blend homogeneity issues (Middleton and Tipton 2000). PCL does not exhibit shape recovery, therefore in the event that the hybrid fibres are not optimally blended, reductions to shape recovery are expected. All three fibre types tested in at temperatures of 40°C displayed complete shape recovery. Both PLA 100WT% (10% PEG-200 plasticised) and the 2 pass hybrid fibre variant exhibited complete shape recovery after 5 seconds at 40°C (table 5: 4). The 1 pass variant of PCL:PLA 30:70WT%, plasticised with a 20% PEG-200 solution did exhibit shape recovery, but took 20 seconds to recover at 40°C. This would suggest that the 1 pass hybrid fibre variant lacked blend homogeneity, thereby reducing its recovery time. At a temperature of 50°C, the two PCL:PLA 30:70WT%, 20% PEG-200 plasticised fibres both displayed complete shape recovery after 5 seconds. This would suggest that the 50° is hot enough to overcome blend homogeneity issues. However, PLA 100WT% 10% PEG-200 plasticised fibres exhibited thermal contraction. It has been suggested that amorphous polymers undergo thermal contraction when their glass transition temperatures are exceeded (Kobayashi, Okajima et al. 1967). This would suggest that PLA 100WT% fibres plasticised with

10% PEG-200 are displaying a reduction in glass transition temperature. PLA 100WT% materials are suggested to have a 60°C glass transition temperature (Middleton and Tipton 2000). The difference in the two values would suggest that PLA's glass transition temperature has been reduced by 10°C, to 50°C.

The response of all three fibres to temperatures of, and exceeding, 60°C is identical. All fibres undergo thermal contraction when submerged in the water (figure 5: 2 displays this effect). In this work, the fibres curled in response to heat. However, the response to heat disrupted the recovery process. Any fibre that curled in response to heat could not recover to the initial conformation. No testing was carried out to demonstrate the ability of the fibres to reverse thermal contraction. Future work could be centred on this; heating the fibres to above 60°C, then attempting shape recovery at 40°C. This was not attempted here. Thermal contraction causes the fibres to recover to their contracted state, rather than their permanent shapes. The two PCL:PLA 30:70WT% hybrid fibres, plasticised with 20% PEG-200 appear to exhibit thermal contraction at PLA's glass transition temperature: 60°C (Middleton and Tipton 2000). The discrepancy between the two hybrid fibres, and PLA fibre suggests that the plasticiser has not affected the glass transition temperature in the hybrid fibres. Thermal contraction occurs below PLA's reported 60°C glass transition temperature in PLA 100WT% 10% PEG-200 plasticised fibres; but at it in the 1 and 2 pass PCL:PLA 30:70WT% 20% PEG-200 plasticised fibres.

5.5 Summary

In terms of shape recovery, it is better to use PEG-200 as the plasticising agent than glycerol. No PCL 100WT% fibres were found to undergo shape recovery; while all but one (contamination) PLA fibre exhibited shape recovery. The best fibres were able to undergo shape recovery at all temperatures investigated. In temperatures of, or exceeding, 60°C, the fibres exhibited thermal contraction.

Chapter 6 *in vitro* Trypsin Digestion

6.1 Introduction

The aim of this project was to produce a biocompatible material; enzyme digestions are an important first step in this process. The use of trypsin as the digestive enzyme functions as a preliminary study. This allows initial quantification of potential degradation profiles for the various fibres. However, based on the application(s) for the materials, a variety of degradation profiles are required. Currently, no application has been defined for this material. As such, further work will be undertaken.

6.2 Materials and Methods

The materials and methods employed in *in vitro* trypsin digestion are discussed here.

6.2.1 Materials

Trypsin was purchased from Sigma-Aldrich (SKU: T1426). Once received, the trypsin was immediately stored in a freezer to prevent denaturation. Approximately 2 hours prior to use, trypsin was removed from storage and placed in a fridge to defrost. After use, the remaining trypsin was returned to the freezer for storage. Phosphate Buffered Saline (PBS) tablets were purchased from Sigma-Aldrich (SKU: P4417). PBS tablets were dissolved in distilled water prior to use, with one tablet per 200 mL water yielding a 0.01 M solution as per the instructions provided with the product. In this case, a 0.05 M solution was required. As such, 5 tablets per 200 mL water were required. Hydrochloric acid (HCl) concentrate was purchased from Sigma-Aldrich (SKU: H1758). HCl concentrate was diluted in distilled water to a concentration of 0.05 M. Sodium Hydroxide (NaOH) pellets were purchased from Sigma-Aldrich (SKU: S5881). NaOH pellets were dissolved in distilled water to produce a 0.5 M stock solution; the stock solution was further diluted to 0.05 M.

The best fibres identified in table 4: 20 were employed here. These fibres were cut from the same batches as those used in mechanical testing (section 4) and fibre processing (section 3). For the purposes of this section, the two hybrid fibres (PCL:PLA 30:70WT% 20% PEG-200 plasticised) will be referred to only has 1 pass or 2 pass hybrids. No other hybrid fibres are tested for enzymatic degradation. Coloured strings were used to label the samples. Three different colours of thread were used: dark green (Mölnlycke Sytrad), pale yellow (Mettler, Metrosene series), and grey (Scanfil PLC). All three threads are stated to be 100% polyester.

A Daihan Scientific WCB-11 water circulating bath was used. This device has an 11 L capacity, and circulates the water to ensure even heating. The temperature range for the WCB-11 is stated to be 20°C – 100°C with an error of ±0.1°C. The effective space within the machine is quoted as 120x155x150 mm (LxWxH).

A desiccator was employed to remove moisture from the samples. The desiccator was a glass canister containing a wire rack and desiccant. The desiccant used was Silica gel, 2.5 – 6 mm self-indicating (sourced from ThermoFisher Scientific, SKU: S/0761/60). To ensure an adequate seal on the desiccator, Vaseline was spread around the lid's rim. Vaseline's active ingredient is listed as white petrolatum 100%. The desiccator was placed into the Contherm Thermotec 2000 oven.

A&D Company Ltd, HR-250AZ Super Hybrid Sensor 5-digit balance was used. All samples, and trypsin weights were taken using this balance. In all cases, weights were taken with a muffin cup holding the materials.

To measure the pH values, a Digitech QM-1670 Hand Held pH Meter, purchased from Jaycar Electronics, Dunedin (https://www.jaycar.co.nz/hand-held-ph-meter/p/QM1670). Prior to use, this device was calibrated with the provided control solution, using the method specified. Briefly, the pH meter was inserted into the control solution, and the tuning screw adjusted until the correct (pH 7.0) was displayed. The pH meter can detect pH 1 – 14, with a resolution of 0.1. The quoted device accuracy is 0.2.

6.2.2 Methods

6.2.2.1 Degradation Solution

Three different solutions were prepared for degradation testing: PBS control, 0.1 mg/mL and 0.05 mg/mL solution types (Almany and Seliktar 2005). In all instances, a 40 mL solution of 0.05M PBS was added to a falcon tube (Almany and Seliktar 2005). The PBS used was from a premade stock solution; prior to the addition of trypsin, the solution was pH balanced. For trypsin's activity, a pH of 7.4 was required (Almany and Seliktar 2005). However, the stock PBS solution exhibited a pH of 7.2; two solutions were added to adjust this. Initially, 0.05 M NaOH (alkaline) solution was added: this increased the pH. To ensure a correct pH reading, the solution was thoroughly mixed prior to measurement. In the event that the pH went over 7.4, an acid, 0.05 M HCl, was added to reduce the pH. This process was repeated until a consistent pH value of 7.4 was achieved.

The aliquoted PBS solutions were labelled to indicate the contents: those labelled PBS were left aside as control solutions with no trypsin. Two trypsin concentrations were used in the test solutions: 0.1 mg/mL, and 0.05 mg/mL, trypsin to PBS. In all cases, 40 mL of PBS was used, as such, either 4 mg (0.1 mg/mL) or 2 mg (0.05 mg/mL) of trypsin were required. Trypsin was weighed out using the high accuracy A&D Company Ltd, HR-250AZ balance. After the addition of trypsin, the solutions were inverted three times. This ensures the solutions are mixed well, with no trypsin on the walls of the tubes.

6.2.2.2 Sample Set-Up

During degradation testing, only the fibres identified as the best, table 4: 20 were used. All fibres used were 70 mm long; these were cut to size from the same stock as those produced in section 3, and tested in section 4. All fibres had coloured polyester string of varying length attached. The string acted as a labelling system. Table 6: 1 provides a summary of what string colour/length translated to what sample. One string was tied to one sample prior to the initial desiccation; figures 1 – 3 display this.

Table 6: 1 Polyester String Labelling Key

Numbering		**Time**	
Sample Number	**Length (mm)**	**Colour**	**Period (Days)**
1	200	Grey	7
2	300	Green	14
3	400	Yellow	21

6.2.2.3 Desiccation

All samples were sorted into their respective material types and placed into labelled brown paper bags. Bags were placed into a desiccation chamber – paper was used as it allows for airflow. To desiccate the samples, the materials were left in the desiccator for 24 hours, in an oven heated to 37.5°C (Vieira, Vieira et al. 2011). Samples were removed and weighed following desiccation. All samples underwent an additional 24 hours of degradation at 37.5°C following their respective degradation times (Vieira, Vieira et al. 2011).

6.2.2.4 Degradation

All samples underwent the same method for *in vitro* degradation. Following the initial 24 hour desiccation step, samples were randomly allocated to groups – maintaining nine samples per group, strings were attached to fibres as labels, as per table 6: 1. The labelled samples were placed into falcon tubes; the strings were attached to the outside of the tube (figure 6: 4). The tubes were placed inside the water bath heated to 37.5°C (Ghosh, Ali et al. 2010), and left for the required period of time (7, 14 or 21 days). At the three seven day intervals (7, 14 and 21), the required samples were removed from the tubes (table 6: 1) and desiccated following the method reported in section 6.2.2.3. PA fishing lines were used as a control to establish if the solutions were working. Due to the strings being used as labels for the fibres, these needed to be tested separately. It was important to identify if the strings degraded, as this could be an influencing factor in the weight loss of the fibres.

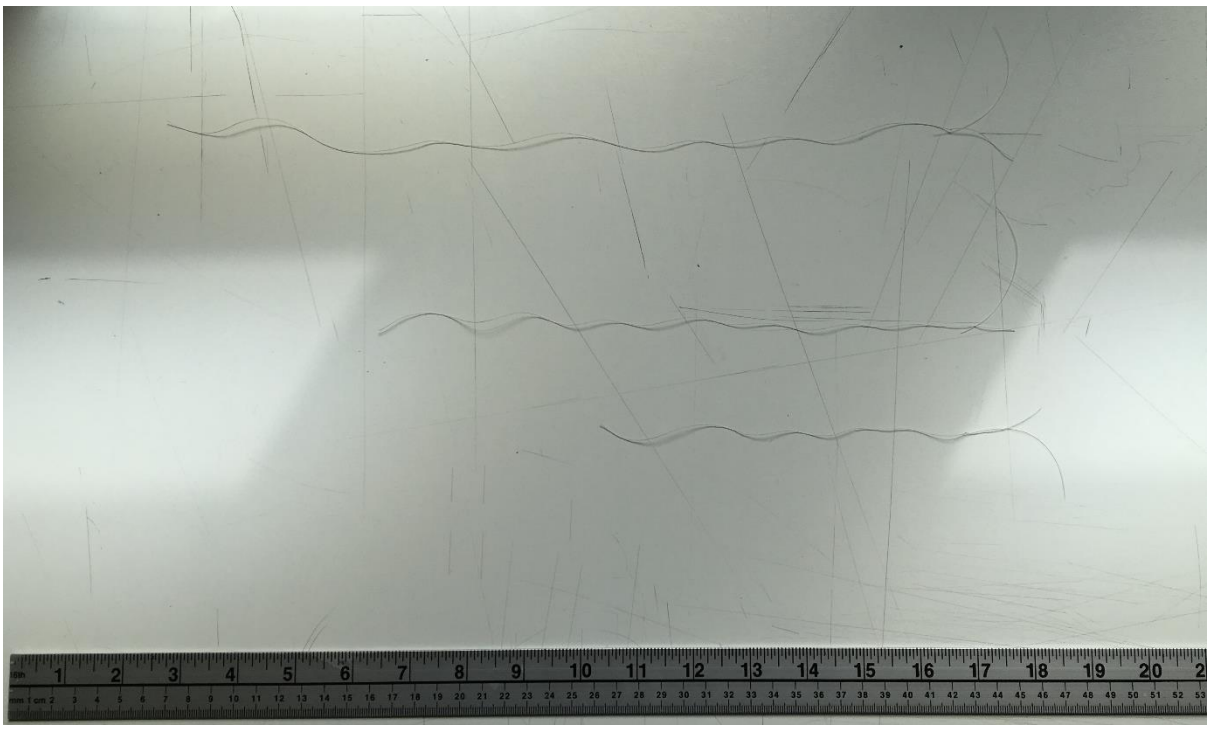

Figure 6: 1 Fibres labelled with grey string for 7 days of degradation.

Figure 6: 2 Fibres labelled with green string for 14 days of degradation.

Figure 6: 3 Fibres labelled with yellow string for 21 days of degradation.

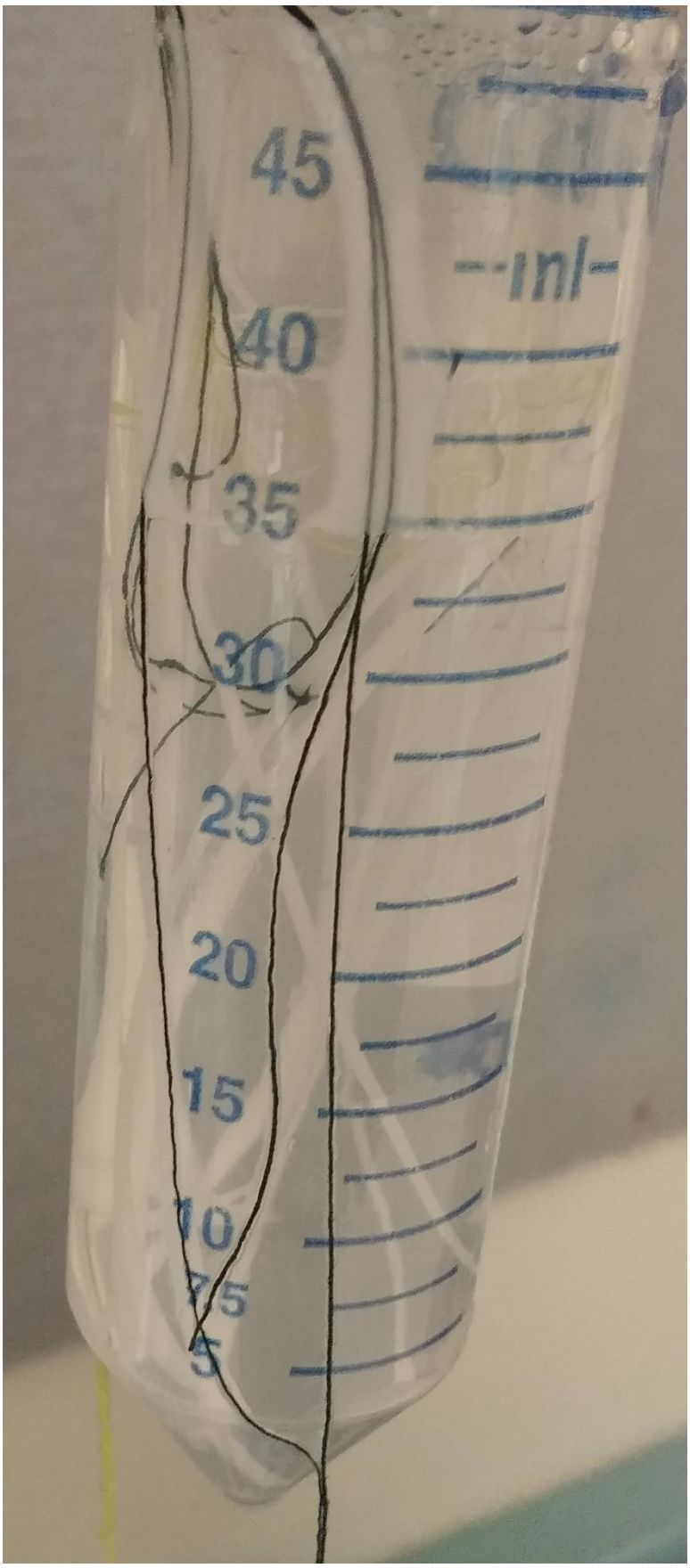

Figure 6: 4 String labels attached to the outside wall of the falcon tube. Each colour is grouped together.

6.2.2.5 Statistical Analysis

The method employed for statistical analysis of the degradation results followed that which was described for mechanical testing (section 4.2.6). The R scripts applied for these datasets are found in Appendix E, Part 1. Generalised least square, restricted maximum likelihood fitted (GLS REML) was carried out at each stage. GLS data is not reported here. Comparisons were made between materials and solution type at each time point. Further, the same method was applied to compare solution type, with degradation duration when comparing the trends across a single material. All statistical outputs are located in Appendix E, Part 2, these used the data located in Appendix E, Part 3. In all cases, unweighted testing was carried out. The output from GLS REML was used in both the type 3 ANOVA and least squares mean (LSM) testing. In all cases, LSM testing used pairwise comparisons. When looking at the individual material interactions at each time point, pairwise comparisons were made between with the material and solution type. These looked at what was attributable to changing materials under a constant solution type; and, changing solution type, under a constant material. However, when comparing the trends for each material, pairwise comparisons were made between solution type and degradation duration. Unlike the mechanical testing section (4.2.6), the intercept values are reported here. Statistical analysis using R studio provides an intercept probability. That is, the likelihood that the average values have a mean of zero.

6.3 Results

There are several important factors to compare within the degradation testing. Firstly, it is vital that the solutions causing the most and least weight loss can be identified: PBS control, 4 mg trypsin, or 2 mg trypsin. Comparisons should be made between the three solutions (PBS control, 4 mg and 2 mg of trypsin) to determine if trypsin has an effect; and what this effect is. Further results should determine how the hybrids behave, compared to the PCL and PLA controls. It is also important to determine any differences between the 1 and 2 pass hybrids. An overall summary of weight loss (%) over the duration of the testing is found in table 6: 2. A large percentage error has been identified on the values in table 6: 2. The median error is 58%, with a range of 3 – 507%. As such, conclusions based off this data are of a low quality. For all tables 6: 3 – 10, the statistical output values are rounded to 4 D.P.

Table 6: 2 Trypsin Digestion Weight Loss (%). Values displayed are the mean±SD.

Polymer Characteristics					**Solution Type**		
Material	Ratio (WT%)	PEG-200 Concentration (%)	Passes	Degradation Period	PBS Control	4 mg Trypsin	2 mg Trypsin
PCL	100	20	1	7	3.4±2.5	2.3±1.2	1.1±2.1
				14	13.6±9.4	6.9±2.7	3.1±1.9
				21	36.7±13.9	20.6±7.2	26.7±12.2
PCL:PLA	30:70	20	1	7	7.5±2.4	7.7±8.5	25.6±5.8
				14	8.0±8.6	15.7±0.5	23.7±7.2
				21	5.0±3.2	30.5±3.0	16.2±2.4
PCL:PLA	30:70	20	2	7	4.3±2.0	2.7±1.5	-2.5±2.0
				14	5.4±2.8	1.5±2.0	-12.4±4.5
				21	-3.0±1.8	-1.3±1.8	-14.8±5.6
PLA	100	10	1	7	1.8±0.9	3.1±3.9	0.9±0.4
				14	9.8±5.7	2.0±3.5	15.7±16.8
				21	-0.6±3.0	12.6±5.4	15.9±7.5
PA	NA	0	NA	7	11.9±4.0	7.4±3.7	14.9±7.0
				14	15.5±5.5	18.9±7.4	9.4±13.8
				21	15.9±13.3	9.6±5.5	13.2±2.2
Strings	NA	0	NA	7	-3.5±14.0	3.1±15.7	10.9±11.2
				14	-1.2±5.6	4.1±6.8	6.9±8.2
				21	-3.6±6.4	5.6±6.4	3.9±2.9

6.3.1 Day 7: in vitro Digestion

Considerable variations in weight loss were identified after 7 days of degradation (figure 6: 5). However, large standard deviations (error bars) were observed in these samples, as such, very few real differences in mean were observed. Statistically, in neither the PBS control nor the 4 mg trypsin solution were any significant variations detected between the material types (table 6: 3). However, three significant interactions were identified when degradation was carried out in 2 mg solutions of trypsin (table 6: 3). Statistically significant variations in mean were observed between the 1 and 2 pass hybrid variants; and the 1 pass hybrid with both PCL and PLA (table 6: 3). Table 6: 4 indicates that the 1 pass hybrid variant is the only material to undergo any changes in response to solution type. The 2 mg trypsin solution was observed to produce statistically significant differences in mean weight loss of 1 pass hybrid fibres, when compared with the PBS control, and the 4 mg trypsin solution (table 6: 4). Table 6: 5 indicated that only solution type was found to effect the mean weight loss across the dataset. It must be noted that table 6: 5 does not display a significant intercept value; as such, the mean weight loss could be zero (no weight loss).

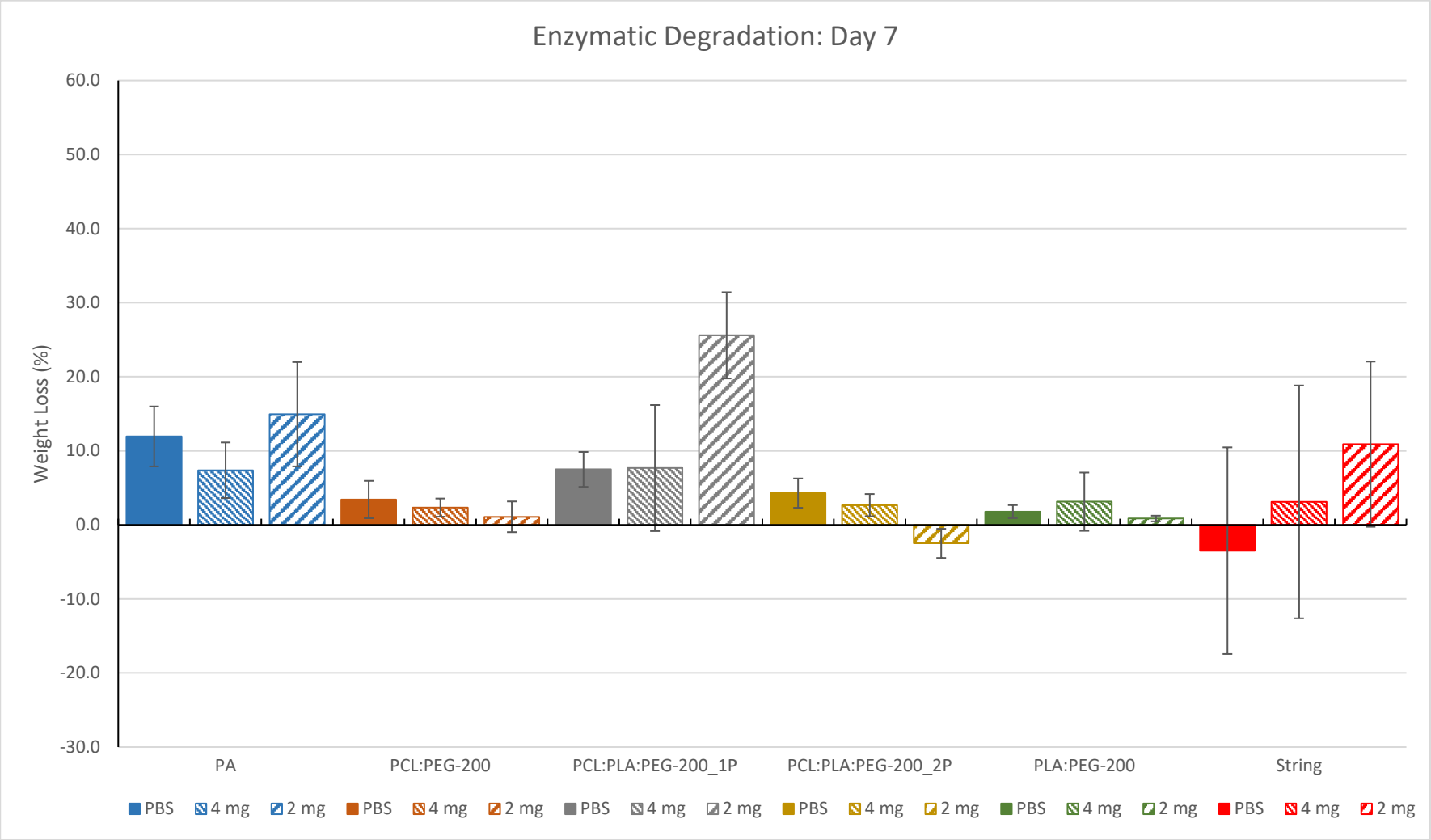

Figure 6: 5 Bar graph indicating the weight loss mean±SD (%) of samples after 7 days. Colours indicate the materials: Blue, Polyamide; Brown, 20% PEG-200 plasticised PCL; Grey, 1 pass 20% PEG-200 plasticised hybrid PCL:PLA 30:70WT%;Yellow, 2 pass 20% PEG-200 plasticised hybrid PCL:PLA 30:70WT%; Green, 10% PEG-200 plasticised PLA; Red, labelling strings. The solution types are indicated by pattern: solid, PBS; narrow stripe, 4 mg trypsin; thick stripe, 2 mg trypsin.

Table 6: 3 Day 7: LSMEANs Material Interactions Summary. Significant values are underlined and italicised. Factor of Significance 0.05. Rounded to 4 D.P.

	Solution		
Contrasts	**PBS Control (0 mg)**	**2 mg**	**4 mg**
1P-2P	0.9964	*0.0020*	0.9737
1P-PA	0.9850	0.6050	1.0000
1P-PCL	0.9895	*0.0092*	0.9654
1P-PLA	0.9542	*0.0084*	0.9829
1P-Strings	0.5701	0.2608	0.9829
2P-PA	0.8581	0.1183	0.9793
2P-PCL	1.0000	0.9940	1.0000
2P-PLA	0.9990	0.9956	1.0000
2P-Strings	0.8491	0.3546	1.0000
PA-PCL	0.7976	0.3205	0.9722
PA-PLA	0.6552	0.3030	0.9870
PA-Strings	0.2147	0.9899	0.9870
PCL-PLA	0.9999	1.0000	1.0000
PCL-Strings	0.9004	0.6830	1.0000
PLA-Strings	0.9663	0.6615	1.0000

Table 6: 4 Day 7: LSMEANs Solution Type Interactions Summary. Significant values are underlined and italicised. Factor of Significance 0.05. Rounded to 4 D.P.

	Materials					
Contrasts	**1P**	**2P**	**PA**	**PCL**	**PLA**	**Strings**
0-2	*0.0267*	0.5711	0.8921	0.9346	0.9892	0.0913
0-4	0.9997	0.9686	0.7786	0.9850	0.9781	0.5835
2-4	*0.0283*	0.7196	0.5008	0.9812	0.9381	0.4800

Table 6: 5 Day 7: Type 3 ANOVA of Material Interactions. Significant values are underlined and italicised. Factor of Significance 0.05. Rounded to 4 D.P.

Interaction	**P-Value**
(Intercept)	0.1109
Material	0.2932
Solution Type	*0.0077*
Material*Solution Type	0.1746

6.3.2 Day 14: in vitro Digestion

It would appear, based on the graphed averages alone, that there are many different weight changes (figure 6: 6). However, the standard deviations (error bars) overlap on almost all cases. Statistically, there are few significant effects on the mean. Table 6: 6 indicates that the only statistically significant weight losses occurred when a 2 mg trypsin solution was used for the digestion. Within the 2 mg trypsin solution digestions, the 1 and 2 pass hybrid variants exhibit a significant difference in mean, as does the 2 pass hybrid with PLA (table 6: 6). Table 6: 7 failed to identify any statistically significant changes in mean weight loss in response to changing solution types. Overall, a significant difference in means result from an interaction between the material and solution type (table 6: 8). No significant intercept value was reported in table 6: 8; suggesting the mean weight loss across the dataset could be equal to zero (no weight loss).

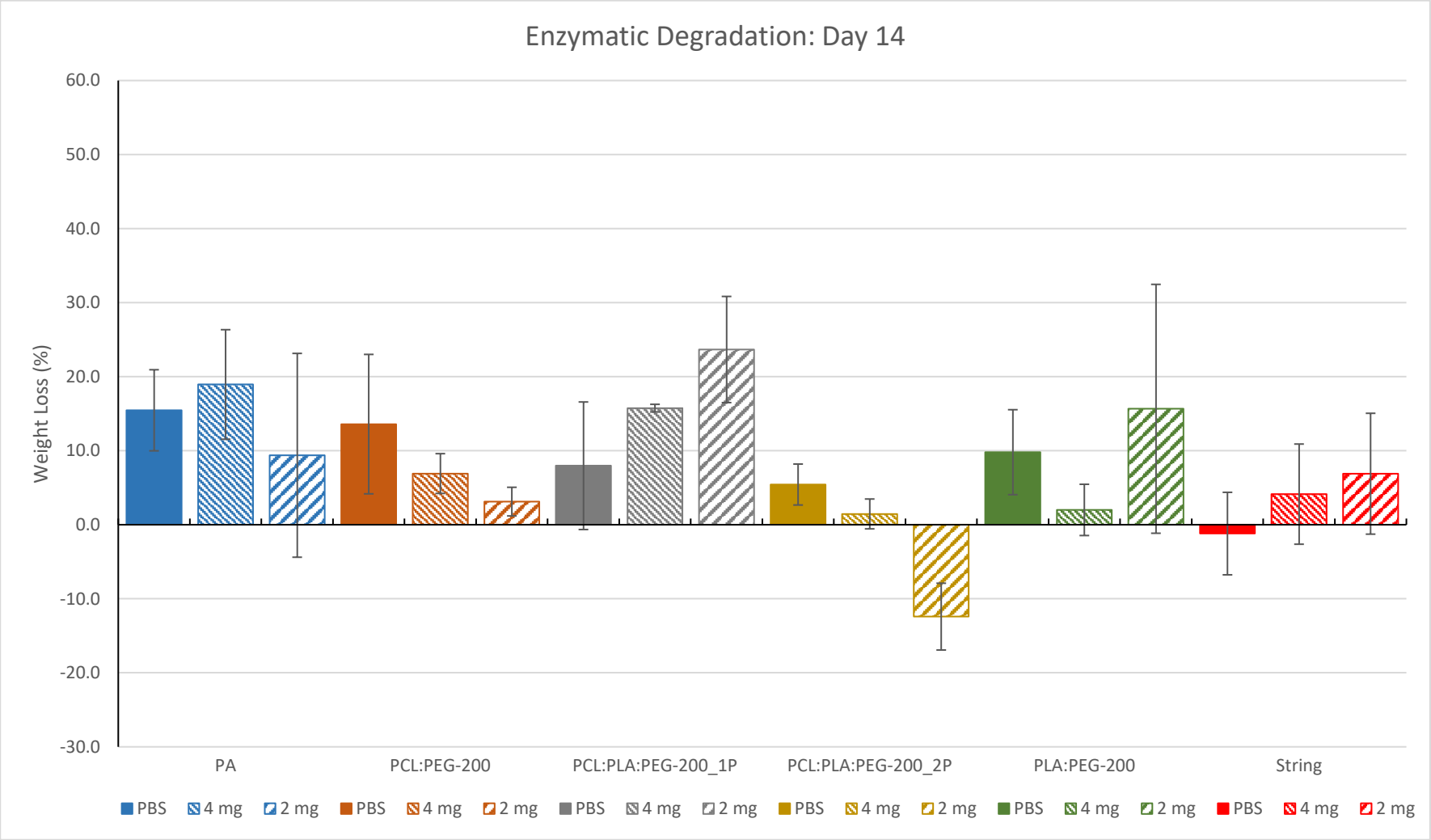

Figure 6: 6 Bar graph indicating the weight loss mean±SD (%) of samples after 14 days. Colours indicate the materials: Blue, Polyamide; Brown, 20% PEG-200 plasticised PCL; Grey, 1 pass 20% PEG-200 plasticised hybrid PCL:PLA 30:70WT%;Yellow, 2 pass 20% PEG-200 plasticised hybrid PCL:PLA 30:70WT%; Green, 10% PEG-200 plasticised PLA; Red, labelling strings. The solution types are indicated by pattern: solid, PBS; narrow stripe, 4 mg trypsin; thick stripe, 2 mg trypsin.

Table 6: 6 Day 14 LSMEANs Material Interactions Summary. Significant values are underlined and italicised. Factor of Significance 0.05. Rounded to 4 D.P.

	Solution		
Contrasts	**PBS Control (0 mg)**	**2 mg**	**4 mg**
1P-2P	0.9993	*0.0003*	0.4119
1P-PA	0.9133	0.4119	0.9980
1P-PCL	0.9732	0.0905	0.8417
1P-PLA	0.9999	0.8910	0.4541
1P-Strings	0.8224	0.2425	0.6327
2P-PA	0.7562	0.0613	0.2049
2P-PCL	0.8787	0.3173	0.9771
2P-PLA	0.9911	*0.0073*	1.0000
2P-Strings	0.9489	0.1270	0.9992
PA-PCL	0.9999	0.9588	0.5961
PA-PLA	0.9726	0.9570	0.2331
PA-Strings	0.2501	0.9994	0.3715
PCL-PLA	0.9955	0.5537	0.9855
PCL-Strings	0.3740	0.9959	0.9990
PLA-Strings	0.6852	0.8438	0.9997

Table 6: 7 Day 14 LSMEANs Solution Type Interactions Summary. Significant values are underlined and italicised. Factor of Significance 0.05. Rounded to 4 D.P.

	Materials					
Contrasts	**1P**	**2P**	**PA**	**PCL**	**PLA**	**Strings**
0-2	0.1042	0.0565	0.6949	0.3504	0.7139	0.5347
0-4	0.5566	0.8587	0.8883	0.6452	0.5538	0.7591
2-4	0.5456	0.1643	0.4144	0.8695	0.1740	0.9289

Table 6: 8 Day14 Type 3 ANOVA of Material Interactions. Significant values are underlined and italicised. Factor of Significance 0.05. Rounded to 4 D.P.

Interaction	**P-Value**
(Intercept)	0.1312
Material	0.2651
Solution Type	0.1105
Material*Solution Type	*0.0414*

6.3.3 Day 21: in vitro Digestion

A large variation in the average values was observed after 21 days of degradation (figure 6: 7). A total of 5 (of 18) samples show an increase in weight (figure 6: 7). Fourteen interactions were identified in response to changing material types (table 6: 9). However, only eight of the 14 interactions were deemed to be useful. Any interaction with either PA or string controls were insignificant. Neither the PA or string controls were being investigated here; rather, they were to demonstrate the enzyme was functional (PA), and to demonstrate that the string would not lose weight, confounding the results. The PBS control digestion identified three statistically significant differences in mean between PCL fibres and the 1 and 2 pass hybrid variants; and a difference between PCL and PLA (table 6: 9). A further three useful interaction were identified when 2 mg trypsin solutions were employed (table 6: 9). The 2 pass hybrid variants were found to exhibit a different weight loss profile to the 1 pass variant; further, both PCL and PLA were displayed different weight loss profiles to the 2 pass hybrid variant (table 6: 9). In the case of the 4 mg trypsin solution, only two significant interactions were identified (table 6: 9). Both the 1 pass hybrid variant and PCOL fibres were found to exhibit significantly difference mean weight losses when compared with the 2 pass hybrid variant (table 6: 9). Table 6: 10 indicates that only the 1 pass hybrid variant experienced solution type dependent weight loss. PBS control solutions and the 4 mg trypsin solution were found to exhibit statistically significant differences in weight loss in the 1 pass hybrid variant (table 6: 10). Across the dataset, both material and solution type, and the interaction between the two were demonstrated to produce statistically significant mean weight loss differences (table 6: 11). However, no significant intercept value was present, suggesting the overall weight loss could be equal to zero (no weight loss) (table 6: 11).

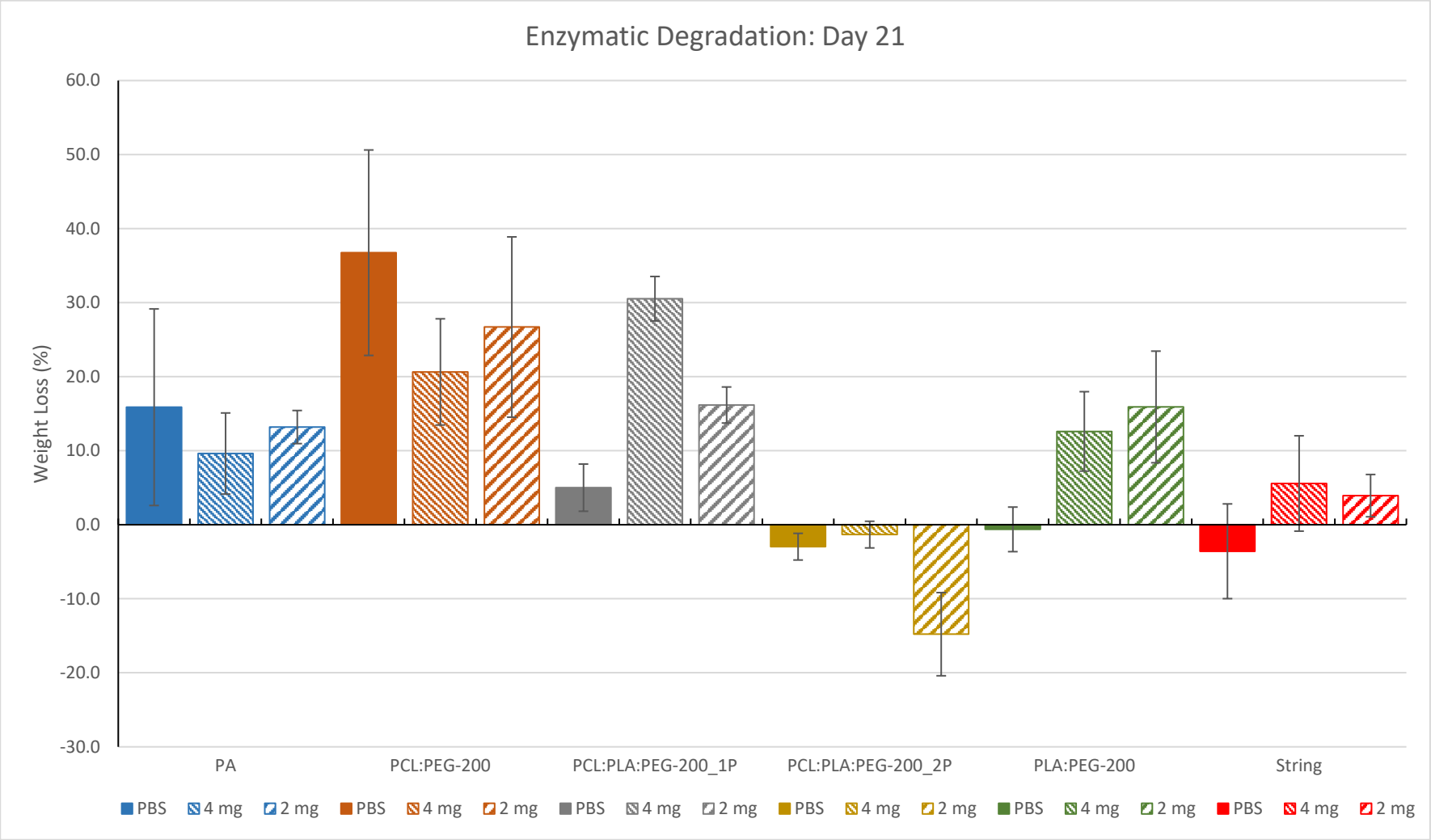

Figure 6: 7 Bar graph indicating the weight loss mean±SD (%) of samples after 21 days. Colours indicate the materials: Blue, Polyamide; Brown, 20% PEG-200 plasticised PCL; Grey, 1 pass 20% PEG-200 plasticised hybrid PCL:PLA 30:70WT%;Yellow, 2 pass 20% PEG-200 plasticised hybrid PCL:PLA 30:70WT%; Green, 10% PEG-200 plasticised PLA; Red, labelling strings. The solution types are indicated by pattern: solid, PBS; narrow stripe, 4 mg trypsin; thick stripe, 2 mg trypsin.

Table 6: 9 Day 21 LSMEANs Material Interactions Summary. Significant values are underlined and italicised. Factor of Significance 0.05. Rounded to 4 D.P.

		Solution	
Contrasts	**PBS Control (0 mg)**	**2 mg**	**4 mg**
1P-2P	0.8514	*0.0009*	*0.0006*
1P-PA	0.5202	0.9978	*0.0468*
1P-PCL	*0.0007*	0.6505	0.7068
1P-PLA	0.9612	1.0000	0.1232
1P-Strings	0.8070	0.4893	*0.0105*
2P-PA	0.0925	*0.0032*	0.6110
2P-PCL	*0.0001*	*0.0001*	*0.0322*
2P-PLA	0.9994	*0.0010*	0.3490
2P-Strings	1.0000	0.0964	0.9156
PA-PCL	*0.0468*	0.3834	0.6018
PA-PLA	0.1842	0.9987	0.9978
PA-Strings	0.0755	0.7575	0.9910
PCL-PLA	*0.0001*	0.6232	0.8492
PCL-Strings	*0.0001*	*0.0241*	0.2654
PLA-Strings	0.9979	0.5163	0.9058

Table 6: 10 Day 21 LSMEANs Material Interactions Summary. Significant values are underlined and italicised. Factor of Significance 0.05. Rounded to 4 D.P.

	Materials					
Contrasts	**1P**	**2P**	**PA**	**PCL**	**PLA**	**Strings**
0-2	0.2494	0.2137	0.9208	0.3205	0.0549	0.5235
0-4	*0.0020*	0.9695	0.6372	0.0624	0.1469	0.3897
2-4	0.1088	0.1390	0.8606	0.6553	0.8814	0.9707

Table 6: 11 Day 21 Type 3 ANOVA of Material Interactions. Significant values are underlined and italicised. Factor of Significance 0.05. Rounded to 4 D.P.

Interaction	**P-Value**
(Intercept)	0.3010
Material	*0.0000*
Solution Type	*0.0010*
Material*Solution Type	*0.0007*

6.3.4 Time Series Trends

A limited number of statistically significant interactions were identified across the time series dataset. This aimed to determine if degradation period had any effect on mean weight loss (tables 6: 12 and 13). Table 6: 12 provides contrasts between the degradation period, for each material and solution type. Table 6: 13 compares the overall effects across the datasets, in respect to the material tested.

Over the 21 day degradation period, the polyamide fishing line showed no trends (figure 6: 8). Statistically, there is no difference between any of the means across this data set, in response to variations in degradation period (table 6: 12). Neither the solution type, degradation period, nor a combined effect resulted in any statistically significant differences in mean (table 6: 13). A significant intercept point was identified (tables 6: 13). The significant intercept supports that the average values are not zero (no weight change).

Testing of the string controls displayed a fairly linear response in all three data sets (figure 6: 13). PBS appears to grant an increase in weight in all cases. The 2 mg solution type provides a more pronounced effect than 4 mg, until 21 days of degradation. Statistically, there is no difference between any of the means across this data set, in response to variations in degradation period (table 6: 12). There is no statistical support for any degradation time, or solution type related effects on weight loss, nor is there support for a cumulative effect between the two factors (table 6: 13). The lack of a significant intercept suggests that there is no statistically significant degradation of the string in these solutions (table 6: 13).

The 20% PEG-200 plasticised PCL 100WT% fibres all displayed the same trend across the time series: weight loss increases with respect to time (figure 6: 9). Of the three degradation media, the PBS control returned the largest weight loss over the period (figure 6: 9). Across the time series data, differences were observed between 7 and 21 days, in all three solution types (table 6: 12). Differences between 14 and 21 days were also noted; this only occurred in the PBS control and 2 mg trypsin solutions (table 6: 12). Statistically, the sole factor responsible for changes in the mean weight loss is the degradation period (table 6: 13). No significant intercept is present, suggesting the mean weight loss could be zero (table 6: 13).

Two trends are observed across the 1 pass variant PCL:PLA 30:70WT% 20% PEG-200 plasticised fibre datasets (figure 6: 10). The 4 mg solution type displays an increased weight loss with respect to time. Both the PBS control solution and 2 mg solution type display a slight decrease in weight loss over time. It is worth noting that the PBS control solution has the lowest weight loss (%) of the three solutions. Statistically, across the time series only one significant interaction was identified (table 6: 12). When a 4 mg trypsin solution was used as the degradation media, a significant difference in mean weight loss was observed between 7 and 21 day (table 6: 12). No other time series effects were detected. Overall, the 1 pass variant time series displayed significant responses to solution type, and a cumulative effect between solution type and degradation period (table 6: 13). However, the degradation period itself was not found to explain any variation in the means (table 6: 13). A significant intercept value was observed, suggesting that the mean weight loss cannot equal zero (table 6: 13).

All 2 pass variant PCL:PLA 30:70WT% 20% PEG-200 plasticised fibre datasets displayed a downwards trend in response to an increased degradation time (see figure 6: 11). It appears, based on figure 6: 11, that a PBS solution causes the greatest weight loss after 7 and 14 days. Both the PBS solution and 4 mg solution type produce a weight loss at 7 and 14 days, with a near 0 weight gain at 21 days. At all time points, a 2 mg solution type causes a weight gain, increasing with respect to degradation time. No statistically significant changes in mean weight loss were identified between the time points, when the solution type was accounted for (table 6: 12). Overall however, degradation time was found to be a contributing factor to mean weight loss (table 6: 13). A statistically significant intercept was present, suggesting the mean weight loss does not equal zero (table 6: 13).

All three solutions produced different trends across the 10% PEG-200 plasticised PLA 100WT% fibres time series (figure 6: 12). The PBS control solution peaked after 14 days, but dropped to 0 for 21. Solutions containing 4 mg of trypsin had a steady weight loss at 7 and 14 days, with an increased weight loss after 21 days. Solution types of 2 mg had a large increase in weight loss between 7 and 14 days, but appeared to plateau between 14 and 21 days. Statistically, no variations in weight loss were observed between the three time points (table 6: 12). No significant intercept is present, suggesting the mean weight loss could be zero (table 6: 13).

Table 6: 12 Overall Results: LSMEANs Time Dependent Effects Summary. Significant Factor 0.05. Significant values are underlined. Rounded to 4 D.P.

		Solution Type		
Material Type	*Contrasts*	**PBS Control (0 mg)**	**2 mg**	**4 mg**
	7-14	0.9976	0.9589	0.4850
1P	*7-21*	0.9340	0.3781	*0.0042*
	14-21	0.9080	0.5405	0.0931
	7-14	0.9857	0.3355	0.9840
2P	*7-21*	0.5583	0.1914	0.8359
	14-21	0.4594	0.9408	0.9158
	7-14	0.8672	0.7073	0.2311
PA	*7-21*	0.8384	0.9668	0.9472
	14-21	0.9982	0.8482	0.3807
	7-14	0.3188	0.9547	0.7918
PCL	*7-21*	*0.0001*	*0.0012*	*0.0276*
	14-21	*0.0037*	*0.0030*	0.1273
	7-14	0.4908	0.0922	0.9857
PLA	*7-21*	0.9357	0.0856	0.3704
	14-21	0.3003	0.9994	0.2891
	7-14	0.9408	0.8334	0.9888
Strings	*7-21*	0.9999	0.5822	0.9374
	14-21	0.9357	0.9080	0.9782

Table 6: 13 Overall Results: Type 3 ANOVA of Material Interactions. Significant Factor 0.05. Significant values are underlined. Rounded to 4 D.P.

Material	Coefficient	P Value
1 Pass Hybrid	Intercept	*0.0493*
	Solution type	*0.0006*
	Degradation Time	0.8431
	Solution type*Degradation Time	*0.0004*
2 Pass Hybrid	Intercept	*0.0436*
	Solution type	0.0609
	Degradation Time	*0.0100*
	Solution type*Degradation Time	0.0530
Polyamide	Intercept	*0.0337*
	Solution type	0.6328
	Degradation Time	0.8591
	Solution type*Degradation Time	0.6047
PCL	Intercept	0.5167
	Solution type	0.9526
	Degradation Time	*0.0000*
	Solution type*Degradation Time	0.6460
PLA	Intercept	0.7156
	Solution type	0.9482
	Degradation Time	0.2951
	Solution type*Degradation Time	0.1391
String	Intercept	0.5997
	Solution type	0.3109
	Degradation Time	0.9583
	Solution type*Degradation Time	0.9624

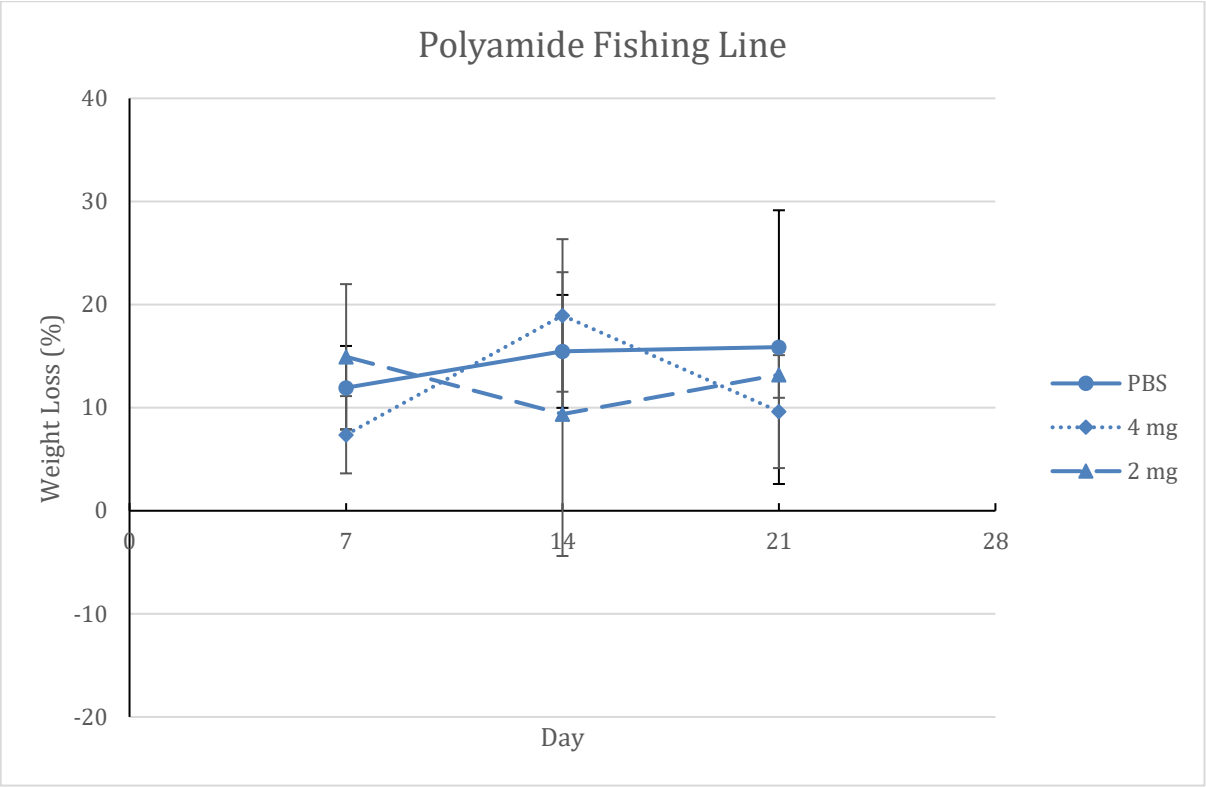

Figure 6: 8 Polyamide fishing line's time series graph. Solution types: PBS, solid; 4 mg, dotted; 2 mg, dashed.

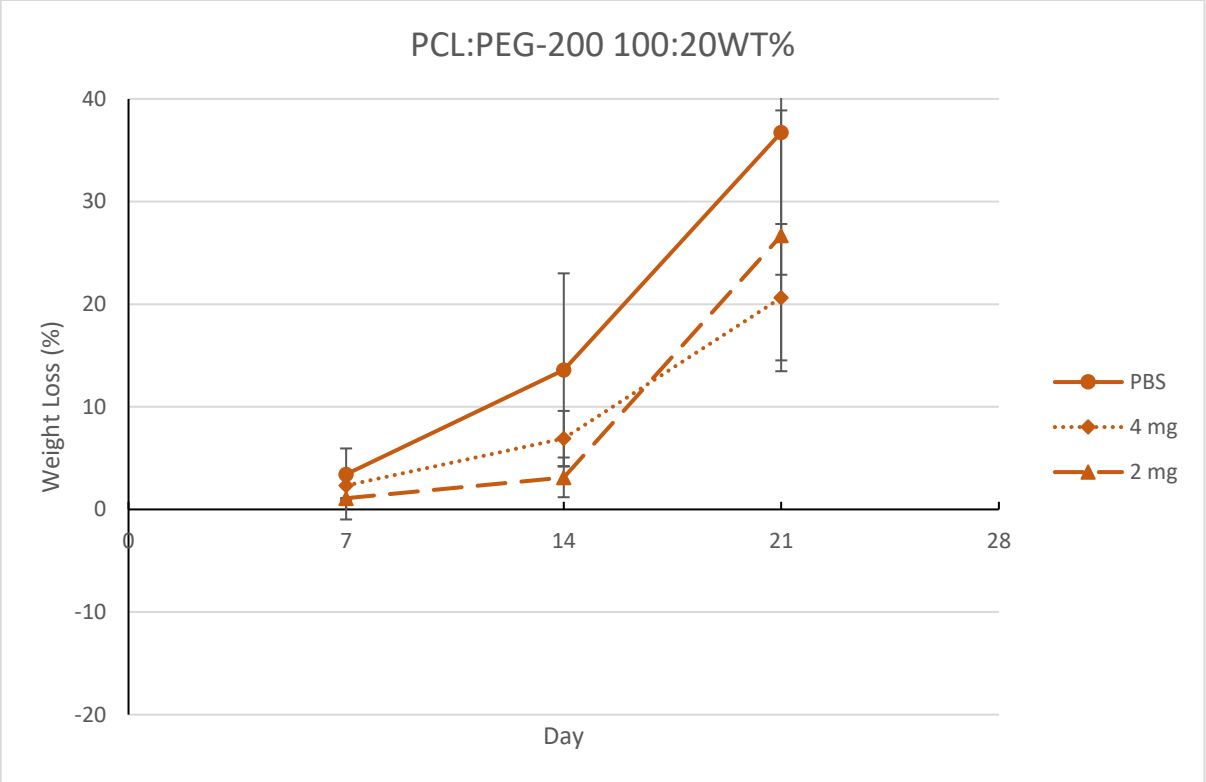

Figure 6: 9 PCL 100WT% plasticised with a 20% solution of PEG-200 time series graph. Solution types: PBS, solid; 4 mg, dotted; 2 mg, dashed.

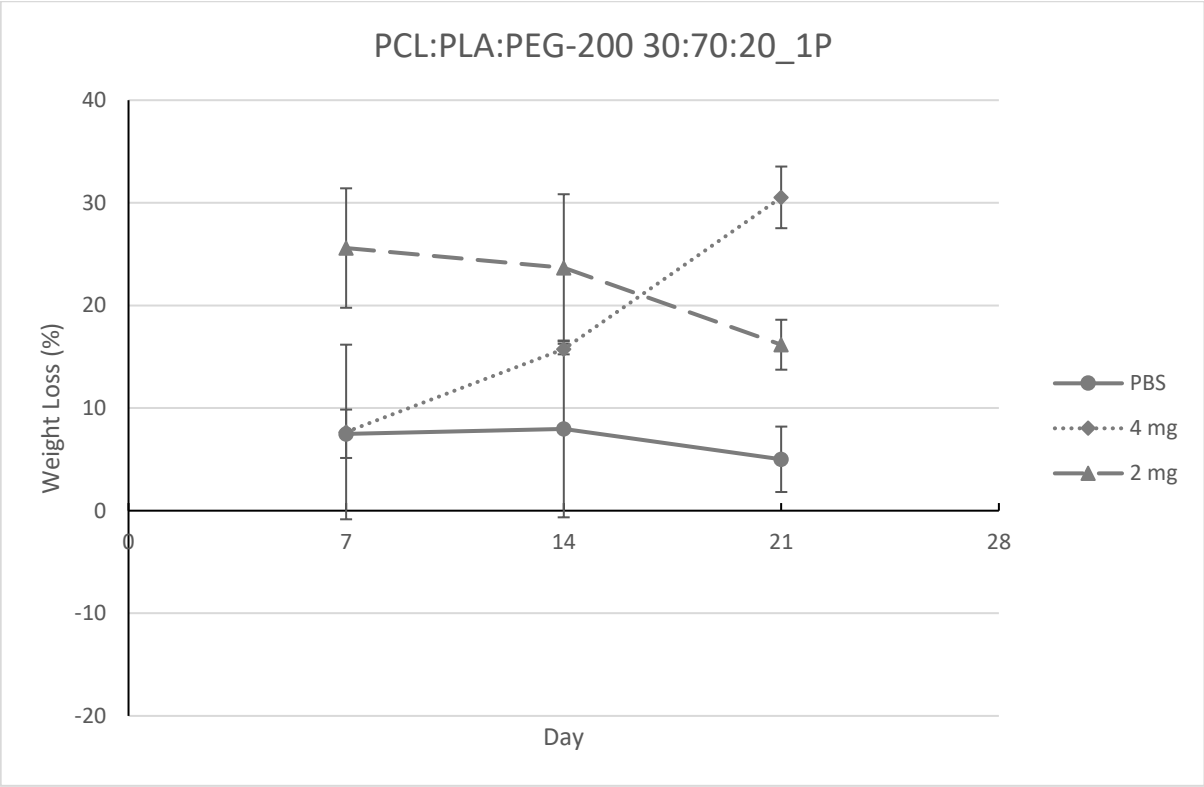

Figure 6: 10 PCL:PLA 30:70WT% 1 pass hybrid plasticised with a 20% PEG-200 solution time series graph. Solution types: PBS, solid; 4 mg, dotted; 2 mg, dashed.

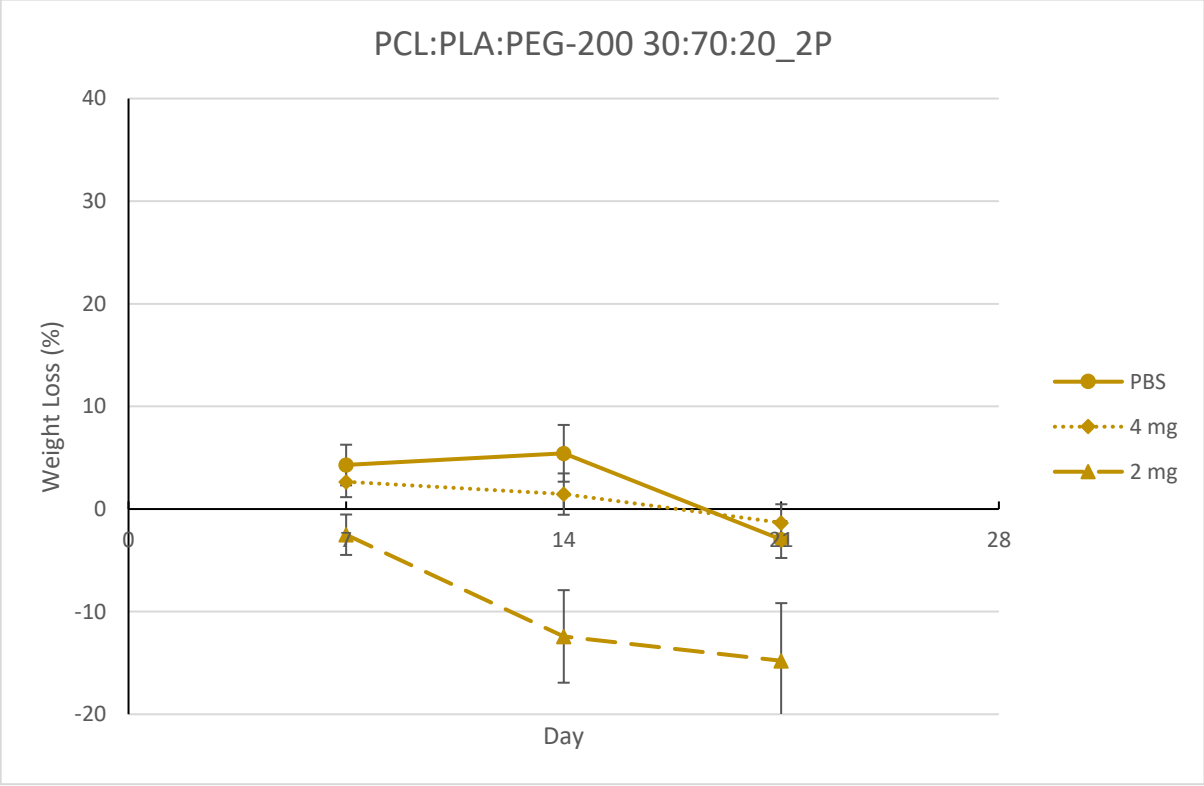

Figure 6: 11 PCL:PLA 30:70WT% 2 pass hybrid plasticised with a 20% PEG-200 solution time series graph. Solution types: PBS, solid; 4 mg, dotted; 2 mg, dashed.

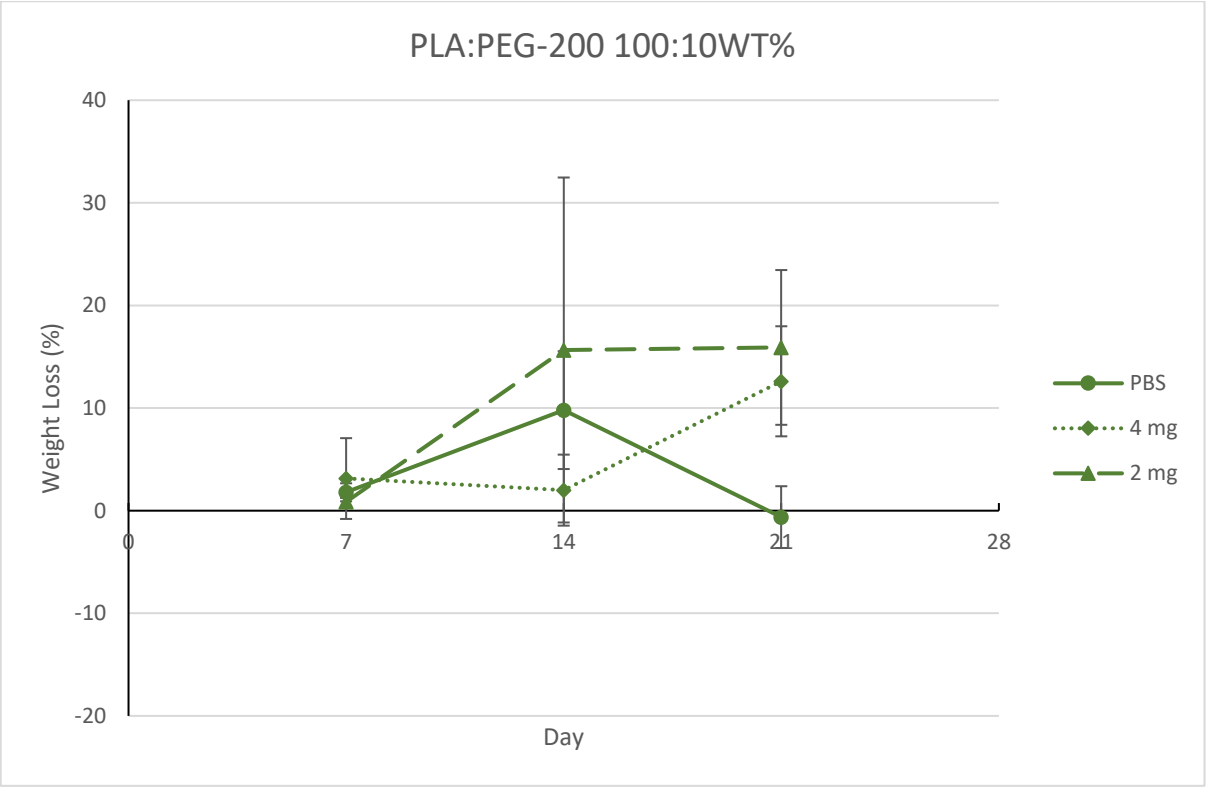

Figure 6: 12 PLA 100WT% plasticised with a 10% solution of PEG-200 time series graph. Solution types: PBS, solid; 4 mg, dotted; 2 mg, dashed.

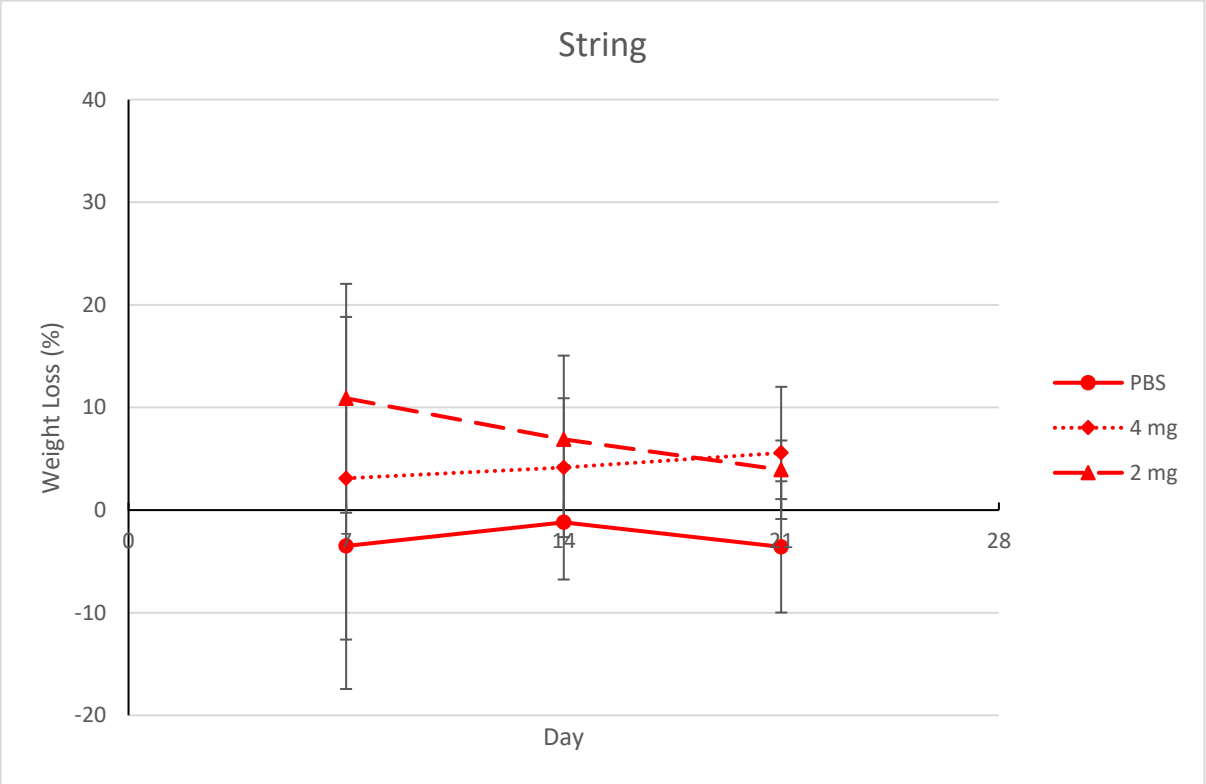

Figure 6: 13 Labelling String time series graph. Solution types: PBS, solid; 4 mg, dotted; 2 mg, dashed.

6.4 Discussion

Several aspects are discussed in this section. Firstly, the relationships between the materials at each time point are discussed. Secondly, the relationship between the individual materials across the time series are discussed. Finally, the suitability of the methods used will be analysed

6.4.1 Material Trends

The trypsin enzyme acts to degrade materials. To achieve degradation, intramolecular bonds are broken by the enzyme. All different materials contain different molecular compositions, with variations in bond presence. As such, each material is liable to degrade at a different rate so it is important to compare the two hybrid variants. Across the three time points, the 2 mg trypsin solutions produced statistically significant differences in mean between the 1 and 2 pass hybrid variants (tables 6: 3, 6 and 9). A 4 mg trypsin solution produced a difference in mean between 1 and 2 pass hybrid variants after 21 days (table 6: 9). When visualised (figures 6: 5 and 6), it is clear that a 2 pass hybrid variant shows significantly less weight loss.

At 2 mg of trypsin, the highest degradation rate is observed. It was observed that the 4 mg trypsin, and PBS control solution did not have a significant variation in degradation. This would suggest that the trypsin enzyme is essentially non-functional here. Trypsin enzymes can undergo self-autolysis, this could explain the result (Nord, Bier et al. 1956). It is reported that as trypsin concentration increases, so does the rate of self-autolysis (Nord, Bier et al. 1956). In the instance that this occurs, the trypsin enzymes will bind, and breakdown, other trypsin found in the solution. If no functional enzyme is targeting the fibres, the weight change should be roughly equivalent to the PBS control solution. However, it is unlikely that all of the trypsin enzyme would be tied up in self-autolysis; a low degradation rate of the fibre would be expected. That is, until a sufficient amount of trypsin had degraded, such that the majority of enzyme then targeted the fibres. In the case of 2 mg solution types, there is not enough ‘free enzyme’ to undergo sufficient self-autolysis to prevent a reaction.

After 21 days, unlike the previous time points (7, 14 days) the 4 mg solution type showed a significant effect on degradation when compared to PBS. However, the 2 mg solution type did not. The idea of trypsin self-autolysing was mentioned previously. After 21 days, it appears that the 4 mg solution type has stabilised, and acted on the fibres: 4 mg is now different to PBS. It is likely that the free trypsin enzymes have reduced in number enough to have a large proportion targeting the fibre, allowing degradation to occur. Previously, it was possible that too much free enzyme was present, encouraging self-autolysis, as opposed to fibre degradation.

No work has been carried out in this project on the amount of active enzyme in the solution. As such, there is no way to determine if trypsin is undergoing self-autolysis. However, future work could be carried out to study this effect: enzyme activity assays.

6.4.2 Time Series Trends

A number of trends have been identified across the individual time series. Firstly, trends were discussed in relation to a weight change. And secondly, trends were discussed in relation to the effects of the two factors (time and solution type) on the weight change.

6.4.4.1 Weight Change

One fibre type displayed a net weight gain across the time series: 2 pass hybrid fibre, in 2 mg of trypsin. This result was statistically significant. Other fibres also displayed a net weight increase; however, these lacked statistical support. This effect could be in response to material uptake from the solution, by the fibre. Trypsin enzyme act to cleave intramolecular bonds. When these bond break, spaces open in the molecular matrix of the fibre. If the spaces are large enough, other molecules can enter (water, trypsin) and become stuck internally in the fibre.

Across all data sets, only three fibres showed a statistically significant non-zero weight change (see table 6: 10). The polyamide blank, and two hybrid fibres, at 1 and 2 pass, showed a non-zero weight change; the remainder lack statistical evidence in support of a weight change. A likely reason for this is material crystallinity (Yang, Li et al. 2015). It has been identified that materials with a higher crystallinity exhibit a denser molecular matrix; this significantly reduces the ability of enzyme penetration and degradation (Yang, Li et al. 2015). Cross-linked PCL fibres have been investigated by Yang, Li et al. (2015), a higher crosslinking ratio equated to increased crystallinity. Work carried out on all crosslinked PCL materials displayed non-zero weight losses (Yang, Li et al. 2015). However, the PCL fibres used for this work did not display degradations over the degradation period.

Work done by Vieira, Vieira et al. (2011) suggests that PCL, PLA and PCL:PLA hybrids typically exhibit slow or no degradation in alkaline PBS solutions. The work carried out for this text demonstrated that in PBS buffered solution types, neither PCL nor PLA display a weight change. However, PCL:PLA hybrids did exhibit a statistically significant weight loss.

6.4.4.2 Effects of the Factors on Weight Change

Typically, within the literature there is support for a larger weight loss in respect to an increase in time (Vieira, Vieira et al. 2011, Yang, Li et al. 2015). However, it is important to note that degradation times can vary significantly between studies. A 5 day degradation was employed by (Yang, Li et al. 2015), whereas up to 30 weeks was used by (Vieira, Vieira et al. 2011). Three of the materials within this work displayed a significant difference in mean weight change, as a result of time (table 6: 10). PCL fibres, and the 2 pass hybrid variant display significant independent effects as a result of degradation time (table 6: 10). An interaction between solution type and degradation time was established in 1 pass hybrid fibres (table 6: 10). Given that PLA fibres lack any significant effects, it would appear likely that PCL is primarily responsible for degradation within the hybrid fibres.

Across all of the fibre types, only the hybrid variants exhibited any significant differences in average weight change, in respect to the solution type (tables 6: 9 and 10). In the case of the 1 pass variant, PBS and 2 mg solution types are different at 7 and 14 days of degradation; PBS and 4 mg solution types are equivalent. This is likely a result of the solution reaching optimal trypsin at 2 mg. As previously described a 4 mg solution type has a large amount of free enzyme, resulting in self-autolysis (Nord, Bier et al. 1956). After 21 days, the 1 pass hybrid exhibits an equivalent degradation between PBS buffer and 2 mg trypsin. In this instance, it appears that the trypsin may have become non-functional (Nord, Bier et al. 1956). At 7 days, all three solutions produced equal weight change in the 2 pass hybrid variant. This is a variation from the 1 pass hybrid. It would seem that the 2 pass variant is exhibiting a higher crystallinity than 1 pass. At both 14 and 21 days of degradation, the 2 pass variant displays a significant effect from 2 mg of trypsin, compared to PBS or 4 mg solution types.

6.4.3 Effectiveness of the Method

Overall, the methods were found to produce ambiguous results. Across the majority of samples, a high error was present. This was thought to be in response to the low sample size and inconsistency in fibre diameter. Within each set, a total of three samples was used at each time point. This results in a relatively high error, in response to variations in weight change. Further influencing this issue is that of sample diameter. Enzymes typically act on a material's surface, as such, a larger diameter should give a higher degradation rate (Yang, Li et al. 2015). However, in this scenario, the difference in diameter may only play a limited role in the observed changes in weight. A percentage value was obtained, based on the differences in initial and final weights. As the diameter changes, the initial weight will also change, meaning the dimeter could have a limited effect in producing error.

The method of desiccation could be revised in future work. There is a potential for PLA to uptake large amount of moisture, due to its hygroscopic nature (Jamshidian, Tehrany et al. 2010). In the event that the desiccation process is not able to remove the additional water from the materials, a reduction in weight decreases could be expected (Vieira, Vieira et al. 2011).

Future work would initially be centred on improving this method. It would be useful to reproduce the results, with minimal error. When an application is identified in the future, a number of modifications to the method can be carried out. The site of the potential application must be considered: the enzymes and conditions likely to present here should be accounted for.

6.5 Summary

Overall, three fibres types showed degradation from trypsin: the 1 and 2 pass hybrid variants and polyamide fishing line. PCL fibres displayed some evidence of degradation. 2 pass hybrid fibres degraded in 2 mg of trypsin displayed a weight gain. Both the PLA fibres and the strings showed no net weight loss. However, the overall method trialled here produced highly inconsistent results. The small (three) sample size resulted in large error rates on many of the samples. This method must be further refined prior to additional testing. Two factors should be considered here: firstly, the optimal number of samples; and lastly, if the diameter should

be standardised. Further trypsin digestions can be carried out after these factors are accounted for. If the method can produce consistent results, a more targeted experiment can proceed. An application must be determined for the materials prior to targeted degradation testing. The application will dictate the exact conditions and enzymes required.

Chapter 7 Overall Discussion

7.1 Introduction

The overall discussion will focus on the project aim: to investigate and fabricate biocompatible hybrid polymers that exhibit shape recovery properties. The four research objectives will be used to guide the overall discussion:

1. Investigation of biocompatible polymers and their fabrication techniques;
2. Investigation of shape memory polymers, their functionalities and processing methods;
3. Investigation of suitable polymer hybrid analyses methods; and
4. Provide a definition for the best materials properties in this work.

Within this project, the effects of both fibre quality and composition were determined to have significant effects on the mechanical, shape memory, and degradation properties. Based on the effects observed in response to fibre quality and composition, the suitability of the fabrication process can be questioned. Comparisons were made between the control fibres with the literary values; and between the hybrid fibres and the criteria defined for the best fibres. The best fibre criteria was defined, based on comparisons with the control PCL and PLA fibres. As a result, the suitability of the defined best fibre criteria must be critiqued. Four fibres were defined as the best, based on the criteria. The effect of using only four fibres must be discussed: it could either improve or hinder the ability to adequately complete the research objectives. Finally, the aim will be discussed. This project aimed to investigate and fabrication biocompatible hybrid polymers with shape that display shape memory properties. Did this project achieve the prescribed aim, and what were the main challenged in doing so? The limitations to this study will be identified and discussed. Future work to remedy these limitations will be identified and allow the research to be taken further.

7.2 Hybrid Polymer Processing and Properties

Overall, melt extrusion of polymer hybrids produced a large variety of fibre qualities. As mentioned in Chapter 3 (Fibre Processing) the initial, non-plasticised fibres produced were not homogeneous, yielding low quality fibres. As a result, the fibres were brittle, and displayed yellowing; both symptoms of degradation (Pospíšil, Horák et al. 1999). Non-plasticised fibres were found to have significantly reduced mechanical properties, over what was suggested in the literature (Monticelli, Calabrese et al. 2014, Zhao and Zhao 2016). Elongation was typically below 5% (table 4: 6), compared to literary values of 600% elongation minimum (Zhao and Zhao 2016). However, when the fibres were plasticised with either glycerol or PEG-200, the overall fibre quality was significantly improved (chapter 3). No fibres that underwent plasticisation display any signs of degradation: the fibres were not brittle, or displayed yellowing (Pospíšil, Horák et al. 1999). A correlation was identified between the overall increase in fibre quality, and the mechanical properties. As the fibre quality improved, the mechanical properties also increased. While the plasticised hybrid fibres displayed a significant increase in elongation at break, up to 420% (tables 4: 12 and 13), this did not match the proposed 600% minimum reported by Zhao and Zhao (2016). However, no literature was identified that used melt extrusion to produce single hybrid fibres that

subsequently underwent tensile testing; therefore, some degree of variation between the results obtained within this study, and literary values is to be expected, as different processes were employed.

The overall fibre quality did effect, to a degree, the shape recovery effect. All non-plasticised (low quality) fibres tested were unable to undergo shape recovery, regardless of soak time. However, when looking at the plasticised fibres (both glycerol and PEG-200), this result is inconsistent. Fibre quality is, on average, the same between the glycerol and PEG-200 plasticised fibre sets. This does not translate into an effect on shape recovery. Human physiological temperature recovery testing (table 5: 3) indicates that only one PEG-200 plasticised fibre does not recover, but seven glycerol fibres do not recover. Within this work, no link was found between slight variations in fibre qualities and shape recovery. In terms of mechanical properties, no correlation is identifiable. It is apparent that the plasticiser choice does effect the ability of the fibres to undergo shape recovery. No explanation has been identified for why PEG-200 produces better responses than glycerol. However, glycerol has previously been reported to not blend with PLA (Müller, Bere et al. 2016); this has the potential to be affect the overall fibre quality. DSC curves were used to establish this affect; distinct glass transition points were identified for both PLA and glycerol (Müller, Bere et al. 2016). As such, DSC methods could be carried out to identify the efficacy of glycerol plasticisation of PLA.

Degradation testing was found to experience a single effect in relation to all other tests/properties. During testing, it was noted that the fibres with larger diameters expressed an increased weight loss. However, the initial weight was also increased; therefore, the actual percentage weight change was not substantially different to the other fibres. Ultimately, this is to be expected. Enzymes function to degrade the outer surface of the materials (Yang, Li et al. 2015). As a result, if the surface area increases, so does degradation rate, assuming free enzyme is present (Puri 1984). Equation 2: 1 provides the formula for the surface area of a cylinder (all fibres were roughly cylindrical). All fibres used in the degradation testing had their length (h) standardised; however, the average diameter (therefore radius, r) was inconsistent between fibres.

7.3 The Best Fibres

The best fibres were defined by the criteria stipulated in table 2: 4. Based on the mechanical properties, a very limited number (five) of the hybrid polymer fibres were identified as matching the criteria (table 4: 24). This proved to be a suitable number for use in this work, as it informed the number of samples for use within the limitations of the degradation pilot study (table 4: 25). However, for a more detailed study, the mechanical properties provide a far too narrow selection. For the most part, the PCL:PLA ratio is constant among the best fibres (30:70WT%); and the plasticiser concentration is at 20% (both glycerol and PEG-200). Further, based solely on whether shape recovery effects are present, a large number of fibres are suitable. The ability of hybrid fibres to undergo shape recovery was a central point in this work. As such, there is a potential need to further analyse more fibres. Table 5: 3 shows that 34 (of 52) hybrid fibres were able to undergo shape recovery. This would suggest that only selecting five fibres as the best, and only testing two for degradation, based on their mechanical properties is too few.

There is potential to relax the tensile property requirements. However, this change would be application dependent. Currently, the lack of a defined application means that only a limited weighting can be placed on the tensile properties. Within this work, no weighting was placed on the tensile (or yield) strength of the materials; rather, the ability to elongate was considered. The lack of a defined application also impacted the desired degradation properties. Currently, a pilot study was carried out to determine the profiles, and if the method was suitable. However, this degradation study potentially bears no relevance to the actual usage sites of the materials. Future work must be done to further characterise the fibres with both enzymes and conditions relevant to the proposed applications. Further work must be done to determine if degradation is beneficial or detrimental to the application. Most materials do degrade over time; therefore, the duration required in the application and rates of degradation must be identified.

Overall, the criteria for the best fibres (table 2: 4) were too narrow for an in depth analysis. However, they were suitable for this work. The majority of this work aimed to provide novel hybrid materials that have appropriate tensile properties, and exhibited shape recovery. The materials and methods should be further refined, to ensure the optimal fibres can be produced for a particular application.

7.4 Achieving the Research Aim

The aim of this work was to investigate and fabricate biocompatible hybrid polymers with shape memory properties. There are several key parts to this aim, firstly, production of polymer hybrids, biocompatibility, and finally, presence of shape recovery. This work has thus far demonstrated that polymer hybrids can be fabricated from PCL and PLA blends. Further, shape recovery properties have been identified in almost all polymer hybrids. However, only an initial pilot study has been carried out into biocompatibility, with further refinement required. Ultimately, both *in vivo* and human clinic trials would be required with the preferred hybrid polymers – this will prove biocompatibility, if present (Mihai, Florescu et al. 2011). However, prior to this, the materials will need to be refined and tested further in response to application criteria.

7.5 Limitations

Several limitations were present within this study. The melt extrusion and manual drawing processing method produced fibres with a larger than desired variation in diameter. Ideally, a minimal variation in diameter should be achieved. However, the only option available to draw the fibres was a manual draw. In the event that the fibres could have been mechanically drawn, there would be less variation in the diameters. A further limitation was the number of repeats used in the analysis. This appeared to limit statistical power to a degree. If more samples had been used, the statistical predictions may have been more accurate. Further, the samples used for mechanical testing may not have been representative. Only three different samples were mechanically tested from each batch of fibres. This means that approximately 120 mm (3 times 40 mm gauge length) out of several meters of fibre was tested. While the

fibres were randomly selected, a larger number of test specimens could have improved this study.

Further limitations centred on access to resources, and time. A number of further experiments would ideally have been done; but they could not due to time constraints. Thermal properties of the hybrid fibres should have been identified through DSC methods. The results from DSC analysis would have identified the glass transition points of the materials; and, by proxy, if the plasticisers had been incorporated correctly into the blends. SEM and TEM studies should have been carried out to characterise the morphology and associated micro level homogeneity of the hybrid fibres.

The lack of a defined application proved to be a limitation in this work. The criteria defined in table 2: 4 were not tailored towards a specific application. As such, the best fibres discussed within this work are not necessarily suitable for all biomedical applications. This was most evident during degradation testing. No defined objectives could be defined within the *in vitro* degradation study. Rather, a degradation profile was identified. However, the profile is essentially meaningless without an application. The *in vitro* degradation pilot study demonstrated two additional limitations: sample size and enzyme choice. By only using three samples for each measure, a large amount of variation in weight loss was achieved for most fibres. This suggests that more samples were required. Trypsin enzymes undergo self-autolysis; this was not accounted for (Nord, Bier et al. 1956). Based on the obtained results, it is difficult to determine the effect of the trypsin enzyme: very few fibre types displayed solution dependent changes. This could suggest that the enzyme was essentially non-functional, and the PBS buffer was acting solely to degrade the materials. Alternatively, the trypsin enzyme was not able to effect the materials. Further analysis could be carried out to identify the extent of trypsin's self-autolysis within the solutions.

The material choice also poses an application dependent limitation. There is a distinct possibility that PCL and PLA will not be suitable for some applications. As such, this could considerably limit the scope of future research into applications. There is little use in testing materials for applications that they are known to be unsuitable for.

7.6 Future Work

The primary objective for future work is to determine biomedical applications for this material. Based on the potential applications, a number of further methods would be employed. Initially, the material would be further refined. Mechanical drawing of the fibres would be carried out to ensure industrial scale repeatability. If the materials were not suitable for industrial production, alterations to the process would be required. An expansion on the trypsin digestion pilot study can be carried out. Several additional processes will be required. Initially, a larger sample size will be employed – likely five or more hybrid fibres. This should significantly increase the studies reliability. Enzyme activity assays can be carried out to quantify the self-autolysis of trypsin. Nord, Bier et al. (1956) reported that a 0.1 mg/mL trypsin solution lost approximately 40% of its activity after just 7 hours of incubation. It must be noted that the reported decrease is for a 0.1 M borate buffer solution with pH 8.5, and 25°C temperature (Nord, Bier et al. 1956). While these differ to the conditions used in this study (PBS solution, pH 7.4, 37.5°C) it would be useful to quantify the effect of self-autolysis.

A more in depth degradation study will be required. Based on the application, the samples may require a longer than 21 day period of activity. In this event, the samples must be proven safe for this period. Finally, further characterisation methods will be employed. Primarily, DSC, TEM and SEM studies will be used to demonstrate how effective the plasticisation process was.

Based on the application for this material, a number of further tests will be required. Assuming the material is used to be used in humans for some purpose, *in vitro* and *in vivo* testing will be required. Initially, the materials will be tested against biologically relevant cell lines, such as human fibroblasts (skin) cells. If that proved successful, further work could be carried out in animal models (mice, sheep). With the potential to progress to human clinical trials.

A potential alternate route to take is that of thermal contraction. The tested materials, when at or exceeding 60°C, curled. This has the potential to be useful in biomedical applications. If the material is able to undergo recovery at temperatures below 60°C following contraction, this allows for a number of applications. Essentially, a small mass of material could be first contacted, but expand once implanted in a human. However, no work on this phenomenon has been carried out here. A number of future experiments would be required, primarily centred around how the materials recover following thermal contraction.

A variety of factors require more investigation in shape recovery. However, several of these are application dependent. Based on the aim of this project, a biocompatible material is desired. This means a temperature of approximately 37.5°C is useful for shape recovery (Vieira, Vieira et al. 2011, Pinho, Rodrigues et al. 2016). This desired application precludes the use of temperature outside of a 30 – 45°C range. However, one interesting factor identified was the ability of the fibres to undergo thermal contraction. This phenomenon was observed at temperatures exceeding 60°C, therefore not suitable for human use. The use of thermal contraction has the potential to be beneficial to other applications. There is significant potential for medical applications. If the fibre could be forced to undergo thermal contraction at a higher temperature than the human body, but recovered to the original shape on application of a 37.5°C temperature. This provides scope for future work. Further, it is possible that PCL 100WT% fibres could exhibit shape recovery if they undergo thermal transitioning. However, PCL has a glass transition of -60°C (Middleton and Tipton 2000); again, this is not suitable for human use. Further investigations into the potential shape recovery of PCL 100WT% fibres could be carried out, with other applications in mind.

Further work could be carried out on quantifying the reduction in glass transition temperatures in the hybrid fibres. This has the potential to explain some of the results observed here. It has been reported in published literature that thermal shape recovery has at least some degree of dependency on the glass transition temperature of the polymer (Behl and Lendlein 2007).

Chapter 8 Conclusions

A number of findings were identified within the separate aspects of this study. The initial, and arguably most important result of this work was that PCL:PLA hybrid biomaterials (fibre) could be produced through melt extrusion processes. During fibre processing, it was evident that PCL:PLA fibres could be extruded without the addition of any plasticisers. However, these fibres were inadequately blended, as a result, the extruded fibres were of a low quality. The fibres had yellow tinges and were brittle, both potential indicators of thermal degradation (Pospíšil, Horák et al. 1999). Due to the brittleness, the fibres could not successfully undergo mechanical testing, such as tensile testing and elongation. Typically, the non-plasticised hybrid fibres produced low tensile properties, when compared to those reported by Zhao and Zhao (2016), using similar PCL and PLA hybrid ratios. The addition of either glycerol or PEG-200 as plasticisers were found to improve the overall quality of the PCL:PLA hybrid fibres, when compared with the non-plasticised hybrid variants. Regardless of plasticiser type and concentration, a significant improvement was observed in tensile properties. Tensile testing was found to be successful only when fibre mounts were used. Without the use of a mount, the fibres were found to slip from the grip negating the results. Within the scope of this study, higher PLA content fibres produced higher elongation at break and Young's modulus values, and overall higher quality fibres. Plasticised PCL:PLA 30:70WT% fibres were consistently identified as the most appropriate as per the criteria identified in table 2: 4. Further, the use of PEG-200 as a plasticiser was found to produce tensile properties that were more desirable than glycerol plasticised fibres (table 4: 24). More PEG-200 plasticised fibres had desirable mechanical properties (table 4: 24) and exhibited shape recovery (table 5: 3).

Overall, the method for shape recovery testing was successful. Two distinct methods were employed; *in vitro* shape recovery testing was carried out at human physiological temperature, 37.5°C (Pinho, Rodrigues et al. 2016). Overall, this testing demonstrated that most PCL:PLA hybrid fibres did display shape recovery. Fibres that did not undergo shape recovery were thought to have low homogeneity – PCL fibres did not display shape recovery. A second test using a range of temperatures between 30 – 90°C, using solely the best fibres identified in table 4: 25. During the shape recovery testing of the best fibres, an unexpected result was identified: thermal contraction. That is, when the tested fibres were exposed to temperature in excess of 50°C (PLA 100WT% 10% PEG-200), or 60°C (PCL:PLA 30:70WT% 20% PEG-200 plasticised 1 and 2 pass), they curled and did not return to their original conformations (table 5: 4). This phenomenon has the potential to be useful in a variety of (not established) applications. Further work is required on thermal contraction to provide an insight into what the potential uses of these materials are.

The *in vitro* trypsin digestion pilot study proved to be informative in regards to the method used, but unsuccessful in obtaining suitable results. The error was identified to be too great in the samples, producing inconsistent results. Three samples were used at each point, meaning large variations in weight loss were more apparent. An increase in sample number could act to mitigate this effect. A number of results were observed during *in vitro* trypsin degradation. PCL 100WT% fibres plasticised with 20% PEG-200 were the only set to, in all solutions, display a weight loss. All solutions appeared to cause a weight gain in the 2 pass variant of PCL:PLA 30:70WT% hybrid fibres, plasticised with 20% PEG-200. Two solutions, PBS control and 2 mg trypsin, appeared to cause a weight increase in 1 pass variant of PCL:PLA 30:70WT% hybrid fibres, plasticised with 20% PEG-200; however, a weight loss was seen in the same fibre type, in solutions of 4 mg trypsin. The remaining fibre types, PLA 100WT%,

10% PEG-200 plasticised, string controls, and PA controls, displayed no weight changes. However, the high error rate identified meant that these results lack accuracy.

Overall, the best hybrid fibre was found to be PCL:PLA 30:70WT% plasticised with 20% PEG-200. In terms of mechanical and shape recovery properties, the 1 and 2 pass variants were similar. However, *in vitro* digestion with trypsin enzymes yielded different results, based on whether the 1 or 2 pass variant was used. At this stage, the study outcomes demonstrated that the hybrid biomaterials have the potential to be applied in biomedical applications. Without a particular application in mind, it cannot be determined if a presence or absence of degradation is beneficial. Both variants of PCL:PLA 30:70WT% PEG-200 20% plasticised fibres exhibited shape recovery.

References

Ajili, S. H., N. G. Ebrahimi and M. T. Khorasani (2003). "Study on thermoplastic polyurethane/polypropylene (TPU/PP) blend as a blood bag material." Journal of Applied Polymer Science **89**(9): 2496-2501.

Almany, L. and D. Seliktar (2005). "Biosynthetic hydrogel scaffolds made from fibrinogen and polyethylene glycol for 3D cell cultures." Biomaterials **26**(15): 2467-2477.

Ameli, A., Y. Kazemi, S. Wang, C. B. Park and P. Pötschke (2017). "Process-Microstructure-Electrical Conductivity Relationships in Injection-Molded Polypropylene/Carbon Nanotube Nanocomposite Foams." Composites Part A: Applied Science and Manufacturing.

Attia, U. M., S. Marson and J. R. Alcock (2009). "Micro-injection moulding of polymer microfluidic devices." Microfluidics and Nanofluidics **7**(1): 1-28.

Balakrishnan, B., D. S. Kumar, Y. Yoshida and A. Jayakrishnan (2005). "Chemical modification of poly(vinyl chloride) resin using poly(ethylene glycol) to improve blood compatibility." Biomaterials **26**(17): 3495-3502.

Bardsley, K., I. Wimpenny, R. Wechsler, Y. Shachaf, Y. Yang and A. J. El Haj (2016). "Defining a turnover index for the correlation of biomaterial degradation and cell based extracellular matrix synthesis using fluorescent tagging techniques." Acta Biomater **45**: 133-142.

Behl, M. and A. Lendlein (2007). "Shape-memory polymers." Materials Today **10**(4): 20-28.

Bélard, L., F. Poncin-Epaillard, P. Dole and L. Avérous (2013). "Plasma-polymer coatings onto different biodegradable polyesters surfaces." European Polymer Journal **49**(4): 882-892.

Byun, Y., Y. T. Kim and S. Whiteside (2010). "Characterization of an antioxidant polylactic acid (PLA) film prepared with α-tocopherol, BHT and polyethylene glycol using film cast extruder." Journal of Food Engineering **100**(2): 239-244.

Cadek, M., J. N. Coleman, V. Barron, K. Hedicke and W. J. Blau (2002). "Morphological and mechanical properties of carbon-nanotube-reinforced semicrystalline and amorphous polymer composites." Applied Physics Letters **81**(27): 5123-5125.

Cai, Q., G. Shi, J. Bei and S. Wang (2003). "Enzymatic degradation behavior and mechanism of Poly(lactide-co-glycolide) foams by trypsin." Biomaterials **24**(4): 629-638.

Cao, N., X. M. Yang and Y. H. Fu (2009). "Effects of various plasticizers on mechanical and water vapor barrier properties of gelatin films." Food Hydrocolloids **23**(3): 729-735.

Carlson, D., L. Nie, R. Narayan and P. Dubois (1999). "Maleation of polylactide (PLA) by reactive extrusion." Journal of Applied Polymer Science **72**(4): 477-485.

Catanzano, O., S. Acierno, P. Russo, M. Cervasio, M. Del Basso De Caro, A. Bolognese, G. Sammartino, L. Califano, G. Marenzi, A. Calignano, D. Acierno and F. Quaglia (2014). "Melt-spun bioactive sutures containing nanohybrids for local delivery of anti-inflammatory drugs." Mater Sci Eng C Mater Biol Appl **43**: 300-309.

Chabrier, F., C. H. Lloyd and S. N. Scrimgeour (1999). "Measurement at low strain rates of the elastic properties of dental polymeric materials." Dental Materials **15**(1): 33-38.

Chatani, S., C. J. Kloxin and C. N. Bowman (2014). "The power of light in polymer science: photochemical processes to manipulate polymer formation, structure, and properties." Polym. Chem. **5**(7): 2187-2201.

Chavalitpanya, K. and S. Phattanarudee (2013). "Poly(Lactic Acid)/Polycaprolactone Blends Compatibilized with Block Copolymer." Energy Procedia **34**: 542-548.

Chen, L., C.-y. Sheng, Y.-x. Duan and J.-m. Zhang (2011). "Morphology, Microstructure and Properties of PEG-plasticized PVC." Polymer-Plastics Technology and Engineering **50**(4): 412-417.
Chen, L., Z. Xie, J. Hu, X. Chen and X. Jing (2006). "Enantiomeric PLA–PEG block copolymers and their stereocomplex micelles used as rifampin delivery." Journal of Nanoparticle Research **9**(5): 777-785.
Chen, R.-y., W. Zou, C.-r. Wu, S.-k. Jia, Z. Huang, G.-z. Zhang, Z.-t. Yang and J.-p. Qu (2014). "Poly(lactic acid)/poly(butylene succinate)/calcium sulfate whiskers biodegradable blends prepared by vane extruder: Analysis of mechanical properties, morphology, and crystallization behavior." Polymer Testing **34**: 1-9.
Chen, Y.-T., A.-C. Yeh, M.-Y. Li and S.-M. Kuo (2017). "Effects of processing routes on room temperature tensile strength and elongation for Inconel 718." Materials & Design **119**: 235-243.
Chinn, R. E., K. H. Kate and S. V. Atre (2016). "Powder injection molding of silicon carbide: processing issues." Metal Powder Report **71**(6): 460-464.
Cho, J. W., J. W. Kim, Y. C. Jung and N. S. Goo (2005). "Electroactive Shape-Memory Polyurethane Composites Incorporating Carbon Nanotubes." Macromolecular Rapid Communications **26**(5): 412-416.
Chung, D. D. L. (2017). "Processing-structure-property relationships of continuous carbon fiber polymer-matrix composites." Materials Science and Engineering: R: Reports **113**: 1-29.
Cipolatti, E. P., S. Moreno-Pérez, L. T. d. A. Souza, A. Valério, J. M. Guisán, P. H. H. d. Araújo, C. Sayer, J. L. Ninow, D. d. Oliveira and B. C. Pessela (2015). "Synthesis and modification of polyurethane for immobilization of Thermomyces lanuginosus (TLL) lipase for ethanolysis of fish oil in solvent free system." Journal of Molecular Catalysis B: Enzymatic **122**: 163-169.
Corden, T. J., I. A. Jones, C. D. Rudd, P. Christian, S. Downes and K. E. McDougall (2000). "Physical and biocompatibility properties of poly-ε-caprolactone produced using in situ polymerisation: a novel manufacturing technique for long-fibre composite materials." Biomaterials **21**(7): 713-724.
Costa, P. F., A. M. Puga, L. Díaz-Gomez, A. Concheiro, D. H. Busch and C. Alvarez-Lorenzo (2015). "Additive manufacturing of scaffolds with dexamethasone controlled release for enhanced bone regeneration." International Journal of Pharmaceutics **496**(2): 541-550.
Dan-asabe, B. (2016). "Thermo-mechanical characterization of banana particulate reinforced PVC composite as piping material." Journal of King Saud University - Engineering Sciences.
De Focatiis, D. S. A. (2012). "Tooling for near net-shape compression moulding of polymer specimens." Polymer Testing **31**(4): 550-556.
Douglas, P., G. Andrews, D. Jones and G. Walker (2010). "Analysis of in vitro drug dissolution from PCL melt extrusion." Chemical Engineering Journal **164**(2-3): 359-370.
El-Hadi, A. M. (2014). "The effect of additives interaction on the miscibility and crystal structure of two immiscible biodegradable polymers." Polímeros Ciência e Tecnologia **24**(1): 9-16.
Eslami-Farsani, R., S. M. Reza Khalili, Z. Hedayatnasab and N. Soleimani (2014). "Influence of thermal conditions on the tensile properties of basalt fiber reinforced polypropylene–clay nanocomposites." Materials & Design **53**: 540-549.
European Committee for Standization (1997). EN ISO 291:1997 Plastics - Standard Atmospheres for Conditioning and Testing. EN ISO 291:1997. Berlin, Germany, Beuth Verlag GambH. **EN ISO 291**.
Frketic, J., T. Dickens and S. Ramakrishnan (2017). "Automated manufacturing and processing of fiber-reinforced polymer (FRP) composites: An additive review of

contemporary and modern techniques for advanced materials manufacturing." Additive Manufacturing **14**: 69-86.
Gardner, G. D., W. J. Dunn and L. Taloumis (2003). "Wear comparison of thermoplastic materials used for orthodontic retainers." American Journal of Orthodontics and Dentofacial Orthopedics **124**(3): 294-297.
Garni, M., S. Thamboo, C. A. Schoenenberger and C. G. Palivan (2017). "Biopores/membrane proteins in synthetic polymer membranes." Biochim Biophys Acta **1859**(4): 619-638.
Ghosh, A., M. A. Ali, L. Selvanesan and G. J. Dias (2010). "Structure-function characteristics of the biomaterials based on milk-derived proteins." International Journal of Biological Macromolecules **46**(4): 404-411.
Ghosh, A., M. A. Ali and R. Walls (2010). "Modification of microstructural morphology and physical performance of chitosan films." International Journal of Biological Macromolecules **46**(2): 179-186.
Giboz, J., T. Copponnex and P. Mélé (2007). "Microinjection molding of thermoplastic polymers: a review." Journal of Micromechanics and Microengineering **17**(6): R96-R109.
Gómez-del Río, T. and J. Rodríguez (2010). "Compression yielding of polypropylenes above glass transition temperature." European Polymer Journal **46**(6): 1244-1250.
Goodship, V., I. Brzeski, B. M. Wood, R. Cherrington, K. Makenji, N. Reynolds and G. J. Gibbons (2014). "Gas-assisted compression moulding of recycled GMT: Effect of gas injection parameters." Journal of Materials Processing Technology **214**(3): 515-523.
Grenade, C., M. C. De Pauw-Gillet, C. Pirard, V. Bertrand, C. Charlier, A. Vanheusden and A. Mainjot (2017). "Biocompatibility of polymer-infiltrated-ceramic-network (PICN) materials with Human Gingival Keratinocytes (HGKs)." Dent Mater.
Gu, J., Z. Lv, Y. Wu, Y. Guo, L. Tian, H. Qiu, W. Li and Q. Zhang (2017). "Dielectric thermally conductive boron nitride/polyimide composites with outstanding thermal stabilities via in-situ polymerization-electrospinning-hot press method." Composites Part A: Applied Science and Manufacturing **94**: 209-216.
Guttman, C. M., E. A. DiMarzio and J. D. Hoffman (1981). "Modelling the amorphous phase and the fold surface of a semicrystalline polymer—the Gambler's Ruin method." Polymer **22**(11): 1466-1479.
Hamm, J., K. Sullivan, A. J. Clippinger, J. Strickland, S. Bell, B. Bhhatarai, B. Blaauboer, W. Casey, D. Dorman, A. Forsby, N. Garcia-Reyero, S. Gehen, R. Graepel, J. Hotchkiss, A. Lowit, J. Matheson, E. Reaves, L. Scarano, C. Sprankle, J. Tunkel, D. Wilson, M. Xia, H. Zhu and D. Allen (2017). "Alternative approaches for identifying acute systemic toxicity: Moving from research to regulatory testing." Toxicol In Vitro.
Han, X. J., Z. Q. Dong, M. M. Fan, Y. Liu, J. H. li, Y. F. Wang, Q. J. Yuan, B. J. Li and S. Zhang (2012). "pH-induced shape-memory polymers." Macromol Rapid Commun **33**(12): 1055-1060.
Hassouna, F., J.-M. Raquez, F. Addiego, P. Dubois, V. Toniazzo and D. Ruch (2011). "New approach on the development of plasticized polylactide (PLA): Grafting of poly(ethylene glycol) (PEG) via reactive extrusion." European Polymer Journal **47**(11): 2134-2144.
Hassouna, F., J.-M. Raquez, F. Addiego, V. Toniazzo, P. Dubois and D. Ruch (2012). "New development on plasticized poly(lactide): Chemical grafting of citrate on PLA by reactive extrusion." European Polymer Journal **48**(2): 404-415.
Huang, J. and S. R. Turner (2017). "Recent advances in alternating copolymers: The synthesis, modification, and applications of precision polymers." Polymer.
Huo, J., R. Rojas, J. Bohlin, J. Hilborn and E. K. Gamstedt (2014). "Parametric elastic analysis of coupled helical coils for tubular implant applications: experimental characterization and numerical analysis." J Mech Behav Biomed Mater **29**: 462-469.

Ilankeeran, P., P. Mohite and S. Kamle (2012). "Axial Testing of Single Fibres." Modern Mechanical Engineering **2**(4): 151-156.
International Organization for Standardization (2005). ISO 139:2005 Textiles - Standard Atmospheres for Testing. ISO 139:2005. Arusha, Tanzania. **ISO 139**.
Jamshidian, M., E. A. Tehrany, M. Imran, M. Jacquot and S. Desobry (2010). "Poly-Lactic Acid: Production, Applications, Nanocomposites, and Release Studies." Comprehensive Reviews in Food Science and Food Safety **9**(5): 552-571.
Jayaraman, K. and R. Halliwell (2009). "Harakeke (phormium tenax) fibre–waste plastics blend composites processed by screwless extrusion." Composites Part B: Engineering **40**(7): 645-649.
Jia, S., J. Qu, C. Wu, W. Liu, R. Chen, S. Zhai, Z. Huang and F. Chen (2013). "Novel dynamic elongational flow procedure for reinforcing strong, tough, thermally stable polypropylene/thermoplastic polyurethane blends." Langmuir **29**(44): 13509-13517.
Jiang, N., S. Jiang, Y. Hou, S. Yan, G. Zhang and Z. Gan (2010). "Influence of chemical structure on enzymatic degradation of single crystals of PCL-b-PEO amphiphilic block copolymer." Polymer **51**(11): 2426-2434.
Jung, J., Z. Deng, J. Simonsen, R. M. Bastías and Y. Zhao (2016). "Development and preliminary field validation of water-resistant cellulose nanofiber based coatings with high surface adhesion and elasticity for reducing cherry rain-cracking." Scientia Horticulturae **200**: 161-169.
Khankrua, R., S. Pivsa-Art, H. Hiroyuki and S. Suttiruengwong (2014). "Effect of chain extenders on thermal and mechanical properties of poly(lactic acid) at high processing temperatures: Potential application in PLA/Polyamide 6 blend." Polymer Degradation and Stability **108**: 232-240.
Kobayashi, Y., S. Okajima and H. Kosuda (1967). "Change of orientation by thermal contraction of polyacrylonitrile fiber." Journal of Applied Polymer Science **11**(12): 2525-2531.
Koleske, J. V. and R. D. Lundberg (1969). "Lactone polymers. I. Glass transition temperature of poly-ε-caprolactone by means on compatible polymer mixtures." Journal of Polymer Science Part A-2: Polymer Physics **7**(5): 795-807.
Lei, M., K. Yu, H. Lu and H. J. Qi (2017). "Influence of structural relaxation on thermomechanical and shape memory performances of amorphous polymers." Polymer **109**: 216-228.
Lendlein, A. and S. Kelch (2002). "Shape-Memory Polymers." Angewandte Chemie International Edition **41**(12): 2034-2057.
Lendlein, A. and R. Langer (2002). "Biodegradable, Elastic Shape-Memory Polymers for Potential Biomedical Applications." Science **296**(5573): 1673-1676.
Li, X., Y. Zhang, H. Li, H. Chen, Y. Ding and W. Yang (2014). "Effect of oriented fiber membrane fabricated via needleless melt electrospinning on water filtration efficiency." Desalination **344**: 266-273.
Liang, J. Z., C. Y. Chen, S. Y. Zou, C. P. Tsui, C. Y. Tang and S. D. Zhang (2015). "Melt flow behavior of polypropylene composites filled with multi-walled carbon nanotubes during extrusion." Polymer Testing **45**: 41-46.
Lim, H. A., T. Raku and Y. Tokiwa (2005). "Hydrolysis of polyesters by serine proteases." Biotechnol Lett **27**(7): 459-464.
Lladó, J. and B. Sánchez (2008). "Influence of injection parameters on the formation of blush in injection moulding of PVC." Journal of Materials Processing Technology **204**(1-3): 1-7.
López, A., J. Aisa, A. Martinez and D. Mercado (2016). "Injection moulding parameters influence on weight quality of complex parts by means of DOE application: Case study." Measurement **90**: 349-356.

Lu, H., Y. Liu, J. Gou, J. Leng and S. Du (2010). "Electrical properties and shape-memory behavior of self-assembled carbon nanofiber nanopaper incorporated with shape-memory polymer." Smart Materials and Structures **19**(7): 075021.
Luzi, F., E. Fortunati, D. Puglia, R. Petrucci, J. M. Kenny and L. Torre (2015). "Study of disintegrability in compost and enzymatic degradation of PLA and PLA nanocomposites reinforced with cellulose nanocrystals extracted from Posidonia Oceanica." Polymer Degradation and Stability **121**: 105-115.
Malinowski, R. (2016). "Mechanical properties of PLA/PCL blends crosslinked by electron beam and TAIC additive." Chemical Physics Letters **662**: 91-96.
Mallakpour, S., A. Abdolmaleki and H. Tabebordbar (2016). "Production of PVC/α-MnO2-KH550 nanocomposite films: Morphology, thermal, mechanical and Pb (II) adsorption properties." European Polymer Journal **78**: 141-152.
Mallakpour, S. and N. Nouruzi (2016). "Effect of modified ZnO nanoparticles with biosafe molecule on the morphology and physiochemical properties of novel polycaprolactone nanocomposites." Polymer **89**: 94-101.
Martin, O. and L. Avérous (2001). "Poly(lactic acid): plasticization and properties of biodegradable multiphase systems." Polymer **42**(14): 6209-6219.
Mekonnen, T., P. Mussone, H. Khalil and D. Bressler (2013). "Progress in bio-based plastics and plasticizing modifications." Journal of Materials Chemistry A **1**(43): 13379.
Meng, H. and G. Li (2013). "A review of stimuli-responsive shape memory polymer composites." Polymer **54**(9): 2199-2221.
Meng, Q. and J. Hu (2009). "A review of shape memory polymer composites and blends." Composites Part A: Applied Science and Manufacturing **40**(11): 1661-1672.
Mercado, S. A., C. Orellana-Tavra, A. Chen and N. K. Slater (2016). "The intracellular fate of an amphipathic pH-responsive polymer: Key characteristics towards drug delivery." Mater Sci Eng C Mater Biol Appl **69**: 1051-1057.
Middleton, J. C. and A. J. Tipton (2000). "Synthetic biodegradable polymers as orthopedic devices." Biomaterials **21**(23): 2335-2346.
Mihai, R., I. P. Florescu, V. Coroiu, A. Oancea and M. Lungu (2011). "In vitro biocompatibility testing of some synthetic polymers used for the achievement of nervous conduits." Journal of Medicine and Life **4**(3): 250-255.
Mittal, G., D. K. Sahana, V. Bhardwaj and M. N. Ravi Kumar (2007). "Estradiol loaded PLGA nanoparticles for oral administration: effect of polymer molecular weight and copolymer composition on release behavior in vitro and in vivo." J Control Release **119**(1): 77-85.
Monticelli, O., M. Calabrese, L. Gardella, A. Fina and E. Gioffredi (2014). "Silsesquioxanes: Novel compatibilizing agents for tuning the microstructure and properties of PLA/PCL immiscible blends." European Polymer Journal **58**: 69-78.
Moody, H. R., C. P. Brown, J. C. Bowden, R. W. Crawford, D. L. S. McElwain and A. O. Oloyede (2006). "In vitro degradation of articular cartilage: does trypsin treatment produce consistent results?" Journal of Anatomy **209**(2): 259-267.
Moon, J., J. Choi and M. Cho (2016). "Programmed shape-dependence of shape memory effect of oriented polystyrene: A molecular dynamics study." Polymer **102**: 1-9.
Moon, S., F. Cui and I. J. Rao (2015). "Constitutive modeling of the mechanics associated with triple shape memory polymers." International Journal of Engineering Science **96**: 86-110.
Mosanenzadeh, S. G., S. Khalid, Y. Cui and H. E. Naguib (2015). "High thermally conductive PLA based composites with tailored hybrid network of hexagonal boron nitride and graphene nanoplatelets." Polymer Composites: n/a-n/a.
Müller, P., J. Bere, E. Fekete, J. Móczó, B. Nagy, M. Kállay, B. Gyarmati and B. Pukánszky (2016). "Interactions, structure and properties in PLA/plasticized starch blends." Polymer **103**: 9-18.

Nord, F. F., M. Bier and L. Terminiello (1956). "On the mechanism of enzyme action. LXI. The self digestion of trypsin, calcium-trypsin and acetyltrypsin." Archives of Biochemistry and Biophysics **65**(1): 120-131.
Ostafinska, A., I. Fortelny, M. Nevoralova, J. Hodan, J. Kredatusova and M. Slouf (2015). "Synergistic effects in mechanical properties of PLA/PCL blends with optimized composition, processing, and morphology." RSC Adv. **5**(120): 98971-98982.
Pan, Y.-T., C. Trempont and D.-Y. Wang (2016). "Hierarchical nanoporous silica doped with tin as novel multifunctional hybrid material to flexible poly(vinyl chloride) with greatly improved flame retardancy and mechanical properties." Chemical Engineering Journal **295**: 451-460.
Peet, M. J., H. S. Hasan and H. K. D. H. Bhadeshia (2011). "Prediction of thermal conductivity of steel." International Journal of Heat and Mass Transfer **54**(11-12): 2602-2608.
Pinho, D., R. O. Rodrigues, V. Faustino, T. Yaginuma, J. Exposto and R. Lima (2016). "Red blood cells radial dispersion in blood flowing through microchannels: The role of temperature." J Biomech **49**(11): 2293-2298.
Pinto, V. C., T. Ramos, A. S. F. Alves, J. Xavier, P. J. Tavares, P. M. G. P. Moreira and R. M. Guedes (2017). "Dispersion and failure analysis of PLA, PLA/GNP and PLA/CNT-COOH biodegradable nanocomposites by SEM and DIC inspection." Engineering Failure Analysis **71**: 63-71.
Pospíšil, J., Z. Horák, Z. Kruliš, S. Nešpůrek and S.-i. Kuroda (1999). "Degradation and aging of polymer blends I. Thermomechanical and thermal degradation." Polymer Degradation and Stability **65**(3): 405-414.
Preis, M., J. Breitkreutz and N. Sandler (2015). "Perspective: Concepts of printing technologies for oral film formulations." International Journal of Pharmaceutics **494**(2): 578-584.
Prud'homme, R. E. (2016). "Crystallization and morphology of ultrathin films of homopolymers and polymer blends." Progress in Polymer Science **54-55**: 214-231.
Puri, V. P. (1984). "Effect of crystallinity and degree of polymerization of cellulose on enzymatic saccharification." Biotechnology and Bioengineering **26**(10): 1219-1222.
Raja, M., S. H. Ryu and A. M. Shanmugharaj (2013). "Thermal, mechanical and electroactive shape memory properties of polyurethane (PU)/poly (lactic acid) (PLA)/CNT nanocomposites." European Polymer Journal **49**(11): 3492-3500.
Riaz Ahmed, K. B., A. M. Nagy, R. P. Brown, Q. Zhang, S. G. Malghan and P. L. Goering (2017). "Silver nanoparticles: Significance of physicochemical properties and assay interference on the interpretation of in vitro cytotoxicity studies." Toxicol In Vitro **38**: 179-192.
Robey, P. G. and J. D. Termine (1985). "Human bone cells in vitro." Calcified Tissue International **37**(5): 453-460.
Sarode, A. L., H. Sandhu, N. Shah, W. Malick and H. Zia (2013). "Hot melt extrusion (HME) for amorphous solid dispersions: predictive tools for processing and impact of drug-polymer interactions on supersaturation." Eur J Pharm Sci **48**(3): 371-384.
Sastra, H. Y., J. P. Siregar, S. M. Sapuan and M. M. Hamdan (2006). "Tensile Properties ofArenga pinnataFiber-Reinforced Epoxy Composites." Polymer-Plastics Technology and Engineering **45**(1): 149-155.
Schotzko, T., M. Reuter and W. Lang (2015). "Sensor integration in rubber gaskets for structural health monitoring made by compression molding." Polymer Testing **48**: 31-36.
Sedlak, M. (2016). "A novel approach to controlled self-assembly of pH-responsive thermosensitive homopolymer polyelectrolytes into stable nanoparticles." Adv Colloid Interface Sci **232**: 57-69.

Shi, Y., F. Chen, J. Yang and M. Zhong (2010). "Crystallinity and thermal stability of LDH/polypropylene nanocomposites." Applied Clay Science **50**(1): 87-91.
Sionkowska, A. (2011). "Current research on the blends of natural and synthetic polymers as new biomaterials: Review." Progress in Polymer Science **36**(9): 1254-1276.
Sterzyński, T., J. Tomaszewska, K. Piszczek and K. Skórczewska (2010). "The influence of carbon nanotubes on the PVC glass transition temperature." Composites Science and Technology **70**(6): 966-969.
Suplicz, A., F. Szabo and J. G. Kovacs (2013). "Injection molding of ceramic filled polypropylene: The effect of thermal conductivity and cooling rate on crystallinity." Thermochimica Acta **574**: 145-150.
Treece, M. A. and J. P. Oberhauser (2007). "Processing of polypropylene–clay nanocomposites: Single-screw extrusion with in-line supercritical carbon dioxide feed versus twin-screw extrusion." Journal of Applied Polymer Science **103**(2): 884-892.
Urquijo, J., G. Guerrica-Echevarría and J. I. Eguiazábal (2015). "Melt processed PLA/PCL blends: Effect of processing method on phase structure, morphology, and mechanical properties." Journal of Applied Polymer Science **132**(41): n/a-n/a.
Vieira, A. C., J. C. Vieira, J. M. Ferra, F. D. Magalhaes, R. M. Guedes and A. T. Marques (2011). "Mechanical study of PLA-PCL fibers during in vitro degradation." J Mech Behav Biomed Mater **4**(3): 451-460.
Vieira, M. G. A., M. A. da Silva, L. O. dos Santos and M. M. Beppu (2011). "Natural-based plasticizers and biopolymer films: A review." European Polymer Journal **47**(3): 254-263.
Wan, Y., X. Lu, S. Dalai and J. Zhang (2009). "Thermophysical properties of polycaprolactone/chitosan blend membranes." Thermochimica Acta **487**(1–2): 33-38.
Wan, Y., H. Wu, X. Cao and S. Dalai (2008). "Compressive mechanical properties and biodegradability of porous poly(caprolactone)/chitosan scaffolds." Polymer Degradation and Stability **93**(10): 1736-1741.
Wang, H., C. Q. Wang, J. G. Fu and G. H. Gu (2014). "Flotability and flotation separation of polymer materials modulated by wetting agents." Waste Manag **34**(2): 309-315.
Wang, J., D. Langhe, M. Ponting, G. E. Wnek, L. T. J. Korley and E. Baer (2014). "Manufacturing of polymer continuous nanofibers using a novel co-extrusion and multiplication technique." Polymer **55**(2): 673-685.
Wei, W., N. Wu, J. Xu, Q. Chen, Q. Qian, Y. Luo, X. Liu, L. Xiao and B. Huang (2014). "Preparation and characterization of PVC-based carbon nanofibers with barrel-like graphite granules by electrospinning." Materials Letters **126**: 48-51.
Wu, D. and M. Hakkarainen (2015). "Recycling PLA to multifunctional oligomeric compatibilizers for PLA/starch composites." European Polymer Journal **64**: 126-137.
Wu, D., Y. Zhang, L. Yuan, M. Zhang and W. Zhou (2010). "Viscoelastic interfacial properties of compatibilized poly(ε-caprolactone)/polylactide blend." Journal of Polymer Science Part B: Polymer Physics **48**(7): 756-765.
Xie, T. (2011). "Recent advances in polymer shape memory." Polymer **52**(22): 4985-5000.
Yang, L., J. Li, Y. Jin, M. Li and Z. Gu (2015). "In vitro enzymatic degradation of the cross-linked poly(ε-caprolactone) implants." Polymer Degradation and Stability **112**: 10-19.
Yao, M., H. Deng, F. Mai, K. Wang, Q. Zhang, F. Chen and Q. Fu (2011). "Modification of poly(lactic acid)/poly(propylene carbonate) blends through melt compounding with maleic anhydride." Express Polymer Letters **5**(11): 937-949.
Yeong, W. Y., N. Sudarmadji, H. Y. Yu, C. K. Chua, K. F. Leong, S. S. Venkatraman, Y. C. Boey and L. P. Tan (2010). "Porous polycaprolactone scaffold for cardiac tissue engineering fabricated by selective laser sintering." Acta Biomater **6**(6): 2028-2034.

Yu, X., S. Zhou, X. Zheng, T. Guo, Y. Xiao and B. Song (2009). "A biodegradable shape-memory nanocomposite with excellent magnetism sensitivity." Nanotechnology **20**(23): 235702.
Yuan, H., X. Liu, L. Ma, Z. Yang, H. Wang, J. Wang and S. Yang (2017). "Application of two-dimensional MoS2 nanosheets in the property improvement of polyimide matrix: Mechanical and thermal aspects." Composites Part A: Applied Science and Manufacturing **95**: 220-228.
Zhang, L., G. Zhao and G. Wang (2017). "Formation mechanism of porous structure in plastic parts injected by microcellular injection molding technology with variable mold temperature." Applied Thermal Engineering **114**: 484-497.
Zhang, Z., S. Chen, J. Zhang, B. Li and X. Jin (2010). "Influence of chlorinated polyethylene on poly (vinyl chloride)/poly (α-methylstyrene-acrylonitrile) blends: Mechanical properties, morphology and thermal properties." Polymer Testing **29**(8): 995-1001.
Zhao, H. and G. Zhao (2016). "Mechanical and thermal properties of conventional and microcellular injection molded poly (lactic acid)/poly (epsilon-caprolactone) blends." J Mech Behav Biomed Mater **53**: 59-67.
Zhao, H. B. and G. Q. Zhao (2016). "Mechanical and thermal properties of conventional and microcellular injection molded poly (lactic acid)/poly (epsilon-caprolactone) blends." Journal of the Mechanical Behavior of Biomedical Materials **53**: 59-67.